UNIVERSITY OF SOUTHAMPTON

On Lepton Flavour Violation in Realistic Supergravity Models

by

Jonathan Geoffrey Hayes

A thesis submitted for the degree of

Doctor of Philosophy

School of Physics and Astronomy

September 2005

Dedicated to my parents, Nicola, and the rest of my family.

UNIVERSITY OF SOUTHAMPTON

ABSTRACT

FACULTY OF SCIENCE

SCHOOL OF PHYSICS AND ASTRONOMY

Doctor of Philosophy

ON LEPTON FLAVOUR VIOLATION IN REALISTIC SUPERGRAVITY MODELS

Jonathan Geoffrey Hayes

We study the phenomenological consequences of a string inspired effective supergravity model arising from intersecting D-branes supplemented by an additional $U(1)$ family symmetry, detailing the scientific progress leading up to the advent of this model and giving reasons as to why one should consider it. Realistic effective supergravity models have a variety of sources of lepton flavour violation (LFV) which can drastically affect the predictions relative to the usual scenarios in the literature based on minimal supergravity and the supersymmetric see-saw mechanism. We catalogue the additional sources of LFV which occur in this model including the effect of D-terms arising from the Abelian $U(1)$ family symmetry, non-aligned trilinear contributions from scalar F-terms, as well as non-minimal supergravity contributions and the effect of different Yukawa textures. In order to quantify these effects, we calculate the branching ratios for $\mu \to e\gamma$ and $\tau \to \mu\gamma$ for a range of benchmark points designed to isolate the different contributions. In such theories the magnitude of the D-terms is predicted, and we find that the D-term contributions are generally dangerously large, but in certain cases such contributions can lead to a dramatic suppression of LFV rates. In the class of string models considered here, we find the surprising result that the D-terms can sometimes restore universality in effective non-minimal supergravity models.

Contents

List of Figures

List of Tables

Preface

The work described in this thesis was carried out in collaboration with Prof. S. F. King and Dr. I. N. R. Peddie.

Chapters 3 and 4 contain our original work which appears in the following reference: J. G. Hayes, S. F. King, and I. N. R. Peddie, [arXiv:hep-ph/0509218].

No claims to originality are made for the content of the introductory Chapters 1 and 2 which were compiled using a variety of other sources.

Acknowledgements

Firstly, I would like to thank my supervisor Steve for his advice, encouragement, trust and, above all, patience. I would also like to thank my collaborator Iain for his invaluable assistance and helpful discussions.

I have thoroughly enjoyed my time at Southampton, and everyone in the group deserves credit for creating and maintaining a friendly and stimulating working environment. Special mention should go to the other two Jons, Oli, Martin, and Phil for their interest, their informative discussions, and for tolerating the chatter and distractions I freely gave.

Finally, I would like to thank Nicola and my family for always supporting and encouraging me, for nodding and smiling, and for providing me with places to escape to.

Chapter 1

General Introduction

1.1 Preliminaries

1.1.1 Motivation

The work in this thesis concerns the analysis of models with lepton flavour violating (LFV) processes, which are predicted to be so abundant in Nature but have not, as yet, been observed in experiment. Thus the inconsistency between predictions from theories and observations of experiments has not yet been fully explained by physics. Thus we need to create models that predict smaller rates of LFV in order to be consistent with observations. The models considered here augment the Minimal Supersymmetric Standard Model (MSSM) with a 'family' symmetry. This is a spontaneously broken gauge symmetry that relates the three generations of matter and breaks to a vacuum expectation value (VEV) at a high energy scale, resulting in D-terms that contribute to the flavour violation. The success of these models is that they can, in principle, naturally explain the hierarchy of quark and lepton masses, the relative smallness of the quark mixings and largeness of the neutrino mixings. These models would not be of such scientific interest if they could not be tested phenomenologically. The models

herein were studied with several goals in mind:

- to identify the origin of the quark and lepton mass hierarchy;
- to understand the relative sizes of the mixing between generations for quarks and neutrinos;
- to make predictions that can realistically be tested at experimental collaborations such as the LHC [http://lhc-new-homepage.web.cern.ch/lhc-new-homepage/] and the ILC [http://www.interactions.org/linearcollider/]. Such predictions may, in principle, result in the models presented here being accepted as agreeing with empirical findings, or being ruled out. Either way will, however, allow theorists to study only that which is consistent with experiment. Examples of such constraints are:
  - the mass spectra of supersymmetric particles;
  - the bounds on flavour changing neutral current decays, such as $\mu \to e\gamma$;
  - the level of fine-tuning necessary for the models to fit with the data[1].

One would not, in general, expect to find the Standard Model (SM) fermion mass spectrum and mixings within models that extend the MSSM, yet the entire fermion sector of the SM can be described here without the need for fine tuning. This gives us a strong motivation for studying the models considered herein. In particular, we shall be exploring large contributions to LFV processes that arise from the D-terms of this family symmetry.

[1]This last point would not necessarily rule out the models, fine tuning just serves to de-emphasize a model in favour of a more 'natural' one. The greater the amount of fine tuning, the less likely it is that the models will be investigated in the future.

1.1.2 Thesis structure

This subsection details the way in which this thesis is organised.

Chapter 1 reviews the Standard Model and the motivations for its extension. Low energy $\mathcal{N} = 1$ supersymmetry and the Minimal Supersymmetric Standard Model are focused on in particular. The see-saw mechanism for explaining neutrino masses, and the Froggatt-Nielsen mechanism, which can explain the Yukawa couplings are also considered. These two mechanisms both work at extremely high energy scales, but can be indirectly detected at low energies.

Chapter 2 introduces supergravity, the framework in which we can study models at extremely high energies. Aspects of string theory that are relevant to model building are considered, concentrating on brane-world set-ups in type I string theory. The Pati-Salam model is discussed before placing this model within the framework discussed at the beginning of this chapter, to detail a string Pati-Salam set-up coming from a type I brane scenario.

Chapter 3 details the particular model that is considered in this thesis. There is a discussion of anomalies and how to obtain the charge structure for the $U(1)_F$ family symmetry, followed by a brief introduction to the differences between the two models considered here. A full derivation of the D-terms is given, followed by the specific operator textures that are used for both models, including the varying values of particular Yukawa elements.

Chapter 4 considers the sources of lepton flavour violation that can arise within these Pati-Salam-based models. A discussion of the soft supersymmetry breaking masses is given, including the effect that the D-terms have. The numerical procedure is outlined before the results are given. The results are presented for five different benchmark points that highlight the different contributions to LFV in both models discussed, with

the varying Yukawa elements turned on and off.

Chapter 5 presents the overall conclusions to this thesis, which is followed by a number of appendices.

1.2 The Standard Model

The Standard Model[2] (SM) of particle physics combines the strong and electroweak forces within the framework of a renormalisable gauge quantum field theory. The gauge group of the Standard Model is $G_{\rm SM} = SU(3)_c \otimes SU(2)_L \otimes U(1)_Y$. There are three generations of elementary fermions, where each generation contains a family of quarks and leptons. Each member of a generation has a corresponding member in both of the other two generations, which is identical in every way except mass and mixing to the other generations. The SM is a quantum field theory (QFT), thus every fundamental particle (as observed experimentally) corresponds to a field in the QFT. Table 1.1 lists the gauge quantum numbers of these fields under the gauge group $G_{\rm SM}$.

The gauge symmetry forbids gauge boson and fermion (Dirac) mass terms in the Lagrangian[3] since left- and right-handed fields transform in different representations of $SU(2)_L$. We cannot simply add gauge boson mass terms which explicitly break the gauge symmetry, as this would make the theory non-unitary. We can, however, construct a gauge invariant Yukawa interaction term by adding a fundamental Higgs scalar doublet ϕ to the spectrum of the Standard Model,

$$-\mathcal{L}_{\rm Yukawa} = \overline{Q}_{iL}(-i\tau_2\phi^*)u_{jR}Y^u_{ij} + \overline{Q}_{iL}\ \phi\ d_{jR}Y^d_{ij} + \overline{L}_{iL}\ \phi\ e_{jR}Y^e_{ij} + \text{h.c.}\ . \qquad (1.1)$$

[2]There are many excellent introductions to the SM, such as [1, 2].

[3]Note that neutrinos are massless in the SM since there are no right-handed neutrinos with which to form Dirac masses, $m_D \sim \nu_L^\dagger \nu_R + \text{h.c.}$. Also the $SU(2)_L \otimes U(1)_Y$ gauge symmetry is violated by Majorana mass terms, which are forbidden by conservation of lepton number.

Field	Spin	$SU(3)_c$	$SU(2)_L$	$U(1)_Y$
Left-handed quarks, $Q_{iL} \equiv (u_{iL}, d_{iL})$	1/2	**3**	**2**	1/6
Right-handed up quarks u_{iR}	1/2	**3**	**1**	2/3
Right-handed down quarks d_{iR}	1/2	**3**	**1**	$-1/3$
Left-handed leptons $L_{iL} \equiv (\nu_{iL}, e_{iL})$	1/2	**1**	**2**	$-1/2$
Right-handed electrons e_{iR}	1/2	**1**	**1**	-1
Higgs boson, $\phi \equiv (\phi^+, \phi^0)$	0	**1**	**2**	1/2
Gluons, g^α, $(\alpha = 1 - 8)$	1	**8**	**1**	0
Weak bosons, W^a, $(a = 1 - 3)$	1	**1**	**3**	0
Hypercharge boson, B	1	**1**	**1**	0

Table 1.1: $G_{\rm SM}$ gauge group representations of the Standard Model fields. Note that left-handed (right-handed) fields transform as fundamental (trivial) representations of $SU(2)_L$. The fermion index i is a generation index, so $(u_1, u_2, u_3) = (u, c, t)$ etc.

$i, j = (1, 2, 3)$ are family indices as before, thus the $Y_{ij}^{u,d,e}$ are 3×3 Yukawa matrices in generation space. Note that the gauge indices have been suppressed. The Yukawa interaction terms in the SM couple the scalar Higgs field to quarks and leptons. Indeed most of the free parameters in the Standard Model are Yukawa coupling constants. In order to generate Dirac mass terms from the Yukawa interactions in Eq. (1.1), we deploy the Higgs mechanism, which makes use of spontaneous electroweak symmetry breaking (EWSB). The electroweak gauge symmetry is broken down to electromagnetism via the potential of the Higgs scalar developing a non-trivial vacuum expectation value (VEV). Thus

$$SU(2)_L \otimes U(1)_Y \rightarrow U(1)_{\text{em}} \ . \tag{1.2}$$

To show how the gauge invariant masses for all the SM fermions and gauge bosons are generated by this EWSB, we need to consider the Lagrangian for the complex Higgs doublet:

$$\mathcal{L}_{\text{Higgs}} = (D^\mu \phi)^\dagger (D_\mu \phi) - \left[m_\phi^2 \phi^\dagger \phi + \lambda (\phi^\dagger \phi)^2 \right] \ , \tag{1.3}$$

where the electroweak covariant derivative is given by

$$D_\mu \phi = \left(\partial_\mu - i g' Y B_\mu - i g W_\mu^a T^a \right) \phi \ , \tag{1.4}$$

where g' and g are the $U(1)_Y$ and $SU(2)_L$ gauge couplings respectively, Y is the hypercharge of $U(1)_Y$ as detailed in Table 1.1, and T^a are the four generators of $SU(2) \otimes U(1)_Y$.

To keep $\mathcal{L}_{\text{Higgs}}$ gauge invariant, the Higgs scalars must belong to $SU(2) \otimes U(1)$ multiplets. The simplest construction is to arrange four fields in an isospin doublet with weak hypercharge $Y = 1/2$:

$$\phi = \begin{pmatrix} \phi^+ \\ \phi^0 \end{pmatrix} \quad \text{with} \quad \begin{aligned} \phi^+ &\equiv (\phi_1 + i\phi_2)/\sqrt{2} \ , \\ \phi^0 &\equiv (\phi_3 + i\phi_4)/\sqrt{2} \ . \end{aligned} \tag{1.5}$$

If $m_\phi^2 = +|\mu|^2$ and $\lambda > 0$, then this behaves as a standard scalar field coupled to two gauge fields, where $|\mu|^2 > 0$. But if $m_\phi^2 = -|\mu|^2$, then there can no longer be a minimum of the potential at $\phi = 0$. Instead, the Higgs potential develops a minimum at $\langle \phi^\dagger \phi \rangle = -m_\phi^2/2\lambda$.

We can use the gauge freedom to make a global $SU(2)_L$ rotation $\phi \to \phi' = e^{i\alpha_a \tau_a/2}\phi$, such that the real VEV is located in the lower, neutral component of the Higgs doublet, so we can write this minimum as

$$\phi_0 = \frac{1}{\sqrt{2}} \begin{pmatrix} 0 \\ v \end{pmatrix} , \tag{1.6}$$

where

$$v = \sqrt{\frac{-m_\phi^2}{\lambda}} . \tag{1.7}$$

In order to generate masses for the gauge bosons we need to expand around this vacuum, and we write the Higgs VEV as

$$\phi(x) = \frac{1}{\sqrt{2}} \begin{pmatrix} 0 \\ v + h(x) \end{pmatrix} , \tag{1.8}$$

where $h(x)$ is the degree of freedom associated with the physical Higgs field.

Any choice of $\phi(x)$ which breaks a symmetry operation will inevitably generate a mass for the corresponding gauge boson. However, if the vacuum is left invariant by some subgroup of gauge transformations, then the gauge bosons associated with this subgroup will remain massless. Table 1.1 shows the choice of $\phi(x)$ with $Y = 1/2$ and $\mathbf{T}$ as a doublet, therefore $T^3 = -1/2$, which will break both $SU(2)_L$ and $U(1)_Y$ gauge symmetries. But since $\phi(x)$ is neutral, the $U(1)_{\text{em}}$ symmetry with generator

$$Q = T^3 + Y \tag{1.9}$$

remains unbroken. That is

$$Q\phi(x) = 0 , \tag{1.10}$$

so that

$$\phi(x) \to \phi'(x) = e^{i\alpha(x)Q}\phi(x) = \phi(x) \tag{1.11}$$

for any value of $\alpha(x)$. The vacuum is thus invariant under $U(1)_{\rm em}$ transformations, and the photon will remain massless. Out of the four $SU(2)_L \otimes U(1)_Y$ generators $\mathbf{T}$, Y, only the combination Q obeys relation (1.10). The other three break the symmetry and generate massive gauge bosons. Thus the remaining three degrees of freedom from the original complex Higgs scalar doublet, shown in Eq. (1.5), have been 'eaten' by the gauge fields associated with the broken electroweak generators. If we substitute Eq. (1.8) into the Higgs-sector Lagrangian, Eq. (1.3), we can see these gauge boson mass terms generated by the non-derivative terms in the covariant derivative of Eq. (1.4) that multiply the VEV:

$$\Delta\mathcal{L}_{\rm Higgs} = \frac{1}{2}\frac{v^2}{4}\left[g^2(W^1_\mu W^{1\,\mu} + W^2_\mu W^{2\,\mu}) + (-gW^3_\mu + g'B_\mu)(-gW^{3\,\mu} + g'B^\mu)\right] . \tag{1.12}$$

We form linear combinations of W^i and B to give us the physical states. The charged mass eigenstates have definite electric charge since electromagnetism survives as a gauge symmetry, and are formed by W^1 and W^2:

$$W^\pm_\mu = \frac{1}{\sqrt{2}}(W^1_\mu \mp iW^2_\mu) , \tag{1.13}$$

with masses $M_W = gv/2$. EWSB mixes the electrically neutral W^3 and B states, such that the mass eigenstates are given by

$$\begin{pmatrix} Z^0_\mu \\ A_\mu \end{pmatrix} = \begin{pmatrix} \cos\theta_W & -\sin\theta_W \\ \sin\theta_W & \cos\theta_W \end{pmatrix} \begin{pmatrix} W^3_\mu \\ B_\mu \end{pmatrix} , \tag{1.14}$$

where $\tan\theta_W = g'/g$ is the weak mixing angle. The neutral weak Z^0 boson $Z^0_\mu = \frac{1}{\sqrt{g^2+g'^2}}(gW^3_\mu - g'B_\mu)$ gains a mass of $M_Z = \frac{v}{2}\sqrt{g^2+g'^2}$, and the linear combination

$A_\mu = \frac{1}{\sqrt{g^2+g'^2}}(g'W_\mu^3 + gB_\mu)$ is the massless electromagnetic photon. The electromagnetic charge e is related to the $SU(2)_L$ and $U(1)_Y$ couplings via

$$e = g' \cos\theta_W \ . \tag{1.15}$$

Now that we have masses for the gauge bosons of the SM, we must consider generating mass terms for the fermions. Substituting the Higgs VEV into the Yukawa Lagrangian, Eq. (1.1), generates the masses and mixings for the quarks and charged leptons. The fermion[4] mass matrices are

$$m_{ij}^{u,d,e} = \frac{v}{\sqrt{2}} Y_{ij}^{u,d,e} \ . \tag{1.16}$$

As these mass matrices are not, in general, diagonal, fermions from different generations can mix together. We can extract the physical masses by making a unitary transformation on the weak eigenstates $(u_{iL}, d_{iL}, u_{iR}, d_{iR})$ that will diagonalise the mass matrices in order to get the mass eigenstates. Perturbative calculations make particular use of this, as it is much easier to have diagonal propagators and non-diagonal vertices than the other way around. We highlight this unitary transformation below:

$$\begin{aligned} u_{iL} \to u'_{iL} = (V_L^u)_{ij} u_{jL} \ , \quad u_{iR} \to u'_{iR} = (V_R^u)_{ij} u_{jR} \ , \\ d_{iL} \to d'_{iL} = (V_L^d)_{ij} d_{jL} \ , \quad d_{iR} \to d'_{iR} = (V_R^d)_{ij} d_{jR} \ , \end{aligned} \tag{1.17}$$

where $V_{L,R}^{u,d}$ are unitary and diagonalise the quark mass matrices:

$$m_{\text{diag}}^{u,d} = V_L^{u,d} m^{u,d} V_R^{u,d\dagger} \ . \tag{1.18}$$

The absence of a right-handed neutrino field in the SM means that we can simultaneously diagonalise the charged lepton mass matrices and their couplings to the electroweak bosons, and diagonalise the neutrino couplings to the electroweak bosons. Thus we need not make a distinction for the leptons.

[4]We note that there are no neutrino mass terms in the Standard Model as there is no right-handed neutrino field with which to form a Yukawa coupling.

The combination $V_{CKM} = V_L^u V_L^{d\dagger}$ is the unitary Cabibbo-Kobayashi-Maskawa (CKM) mixing matrix [3]. The standard parameterisation involves three physical mixing angles and a single phase that can lead to CP violation. The CKM matrix elements are observable in weak charged current processes, and V_{CKM} is found to be highly diagonal.

1.2.1 Successes of the Standard Model

Since its inception, the Standard Model has been subjected to rigorous testing at a multitude of high energy accelerators, as illustrated by the plethora of high precision data regularly collated and published by the Particle Data Group [4]. This includes measurements of the Z^0 boson decay width, which constrain the number of active (non-sterile) neutrinos with mass $m_\nu \leq M_Z/2$ to be three. Furthermore, chiral anomalies, where quantum corrections break symmetries of the classical theory, are exactly cancelled only within each complete generation of quarks and leptons[5]. Considering these two points together leads us to conclude that there must only be three complete generations of matter in the SM.

The quark model of mesons and baryons invokes approximate flavour symmetries to successfully predict the light hadronic spectra of bound quark states. The unitarity of the CKM matrix provides a method for suppressing rare flavour changing processes. This is the Glashow-Illiopoulos-Maiani (GIM) mechanism [5] that was used to predict the charm quark prior to its experimental discovery.

The Higgs mechanism gives us an explanation of how the electroweak bosons gain mass, and consequently why the range of the electroweak force is so short. It has been

[5]This statement strongly constrains any new matter that we may supplement the SM with, which makes extending the SM more difficult. We will return to this point when we discuss supersymmetry and the MSSM; a method of extending the SM.

possible to perform many perturbative calculations of physical observables, since the majority of couplings in the SM are so small. The computations compare very well with empirical findings. The evolution of Renormalisation Group Equations (RGEs) is one such calculation, which allows us to understand the variation of physical parameters with energy scale. The infra-red behaviour of the Quantum Chromodynamics (QCD) gauge group $SU(3)_c$ is one such example, which leads to our understanding of the confinement of quarks inside hadrons. Here, quarks always bind together to form $SU(3)_c$ singlet states of three quarks (a baryon) or a quark-antiquark pair (a meson).

1.2.2 Unanswered questions in the Standard Model

Whilst the Standard Model has been very successful over the past few decades, there is an ever-increasing amount of observational and theoretical data that tends to suggest some form of physics exists beyond the Standard Model. One immediately obvious drawback is that the SM does not incorporate gravity, which leads us to believe that the SM is a low energy effective theory. Quantum gravity effects are anticipated to appear around the Planck scale $M_{\rm Pl} \sim 10^{19}$ GeV, but this leaves a vast 'energy desert' above the electroweak scale where 'new physics' can appear. The question now is *"what lies beyond the Standard Model"?* Any realistic theory must reduce to an effective theory at low energies that replicates the successes of the SM, whilst eliminating at least one of the problems that lies within it. This section details the main issues that the Standard Model does not successfully deal with.

- **Neutrino masses**

The recent experimental confirmation of massive neutrinos is the clearest indicator of the necessity of physics beyond the Standard Model.

The discrepancy between the Standard Solar Model (SSM) of neutrinos and the measurements of solar neutrinos when they reach the earth has long been known. The SSM predicted that electron neutrinos would be generated by fusion reactions in the sun. These solar neutrinos travel out from the sun, thus some have a path which intersects with the orbit of the Earth, such that Earth-based experiments can measure them. The first neutrino astrophysics experiments in the 1960's successfully measured the flux of the solar neutrinos, but found that the number reaching the Earth was about a third of that predicted by the SSM. This discrepancy could be explained by electron neutrinos oscillating into muon and tau neutrinos, which would be undetectable by the experiments of the time. Any oscillation would, however, require the neutrinos to be massive, which would go against the Standard Model of particle physics. The inconsistency between the SSM prediction and the observed neutrino flux had no solid conclusion, as one could not distinguish between the two possible outcomes: the SSM prediction being incorrect without oscillation; and the SSM prediction being correct with massive neutrinos oscillating into each other.

More recent observations at the super-Kamiokande laboratory [6] have shown a deficit of atmospheric muon neutrinos reaching the surface after being generated in the upper atmosphere. The production of atmospheric neutrinos involves a decay chain of $\pi^- \rightarrow \mu^- + \overline{\nu}_\mu$ followed by $\mu^- \rightarrow e^- + \overline{\nu}_e + \nu_\mu$. Thus the predicted rate, without neutrino oscillations, suggests that there should be twice the number of atmospheric muon neutrinos compared to electron neutrinos.

When the Sudbury Neutrino Observatory (SNO) reported their results [7], the issue of the solar neutrino observations was rapidly settled. SNO separately measured the total flux of all three neutrino species and the individual flux of electron neutrinos. Their findings demonstrated that the SSM prediction of neutrino flux was indeed

correct, thus neutrino oscillation must occur.

If one combines the results from various experiments, it is possible to extract the differences between the squared masses of the three neutrinos and two of the three leptonic mixing angles in the PMNS matrix[6]. These mass differences are incompatible with zero, indicating that at least two of the neutrinos must have mass.

There are no right-handed neutrino states in the SM with which to form Dirac neutrino masses, and gauge-invariance prevents a renormalisable Majorana neutrino mass, thus the advent of neutrino masses is inconsistent with the Standard Model. To overcome this problem, we look towards a deeper theory in which to embed the SM; one in which masses and couplings are predicted *a priori*.

- **The fermion hierarchy**

The fermion masses and mixing angles in the SM come from 27 input parameters in the Yukawa coupling matrices. This is a completely *ad hoc* procedure, requiring a different coupling for each massive fermion. The SM has no way of explaining how the top quark is six orders of magnitude heavier than the electron, other than the fact that the top quark Yukawa is six orders of magnitude larger than the electron Yukawa. The three generations of massive fermions seem to form a hierarchy, with the members of each successive generation having masses larger than their counterparts in the previous generation. This is indicative of some 'organising principle', but the only explanation offered by the SM is one of coincidence. Again, we are pointed towards physics beyond the Standard Model.

- **The gauge hierarchy problem**

[6]The PMNS matrix is the leptonic equivalent of the CKM matrix.

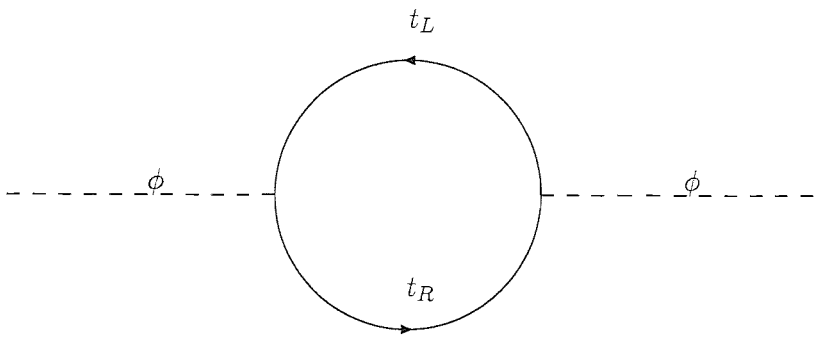

Figure 1.1: The dominant correction to the Standard Model Higgs (mass)^2 comes from the one-loop top quark bubble diagram.

Another inadequacy of the Standard Model is its failure to explain why the electroweak scale is so much lower than the Planck scale. There are two parts to this problem with the gauge hierarchy: why the electroweak symmetry breaks at an energy scale of order 100 GeV; and how one can stabilise the hierarchy between these two scales without resorting to unnatural fine-tuning.

For the first part, there is no reason to expect the Higgs mass parameter m_ϕ^2 to be driven negative at this particular energy scale. The fact that it is has to be put in by hand to make the SM work. Prior to this EWSB, fermions and gauge bosons are massless since mass terms explicitly violate gauge-invariance. However there is no symmetry that protects the Higgs boson mass from receiving large radiative corrections of order Λ_{UV}, the cutoff scale. Figure 1.1 shows the leading contribution to the Higgs mass renormalisation, δm_ϕ^2, from the top quark bubble diagram. The dominant term is

$$\delta m_\phi^2 = \frac{|\lambda_t|^2}{16\pi^2}\left[-2\Lambda_{UV}^2 + 6m_t^2 \ln\left(\frac{\Lambda_{UV}}{m_t}\right) + \cdots\right] . \tag{1.19}$$

As the Higgs is a scalar, the finite part of the renormalisation is sensitive to the largest mass in the theory that couples directly or indirectly to the Higgs boson. We also have a problem with the naturalness of this model. If there is nothing beyond the SM, then the ultraviolet cutoff Λ_{UV}, must be associated with the Planck scale $M_{\rm Pl}$, where quantum gravity effects start to become large. Then the Higgs boson mass correction would involve Planck-scale particles in virtual loops that would push the Higgs mass towards $M_{\rm Pl}$. As EWSB occurs at the weak scale $\mathcal{O}(M_W)$, we need a renormalised Higgs mass of $\mathcal{O}(100\ \text{GeV})$ if $\lambda \sim 1$ in the Higgs VEV of Eq. (1.7). The tree level mass must therefore be set to $\mathcal{O}(\Lambda_{UV}^2)$ in order to cancel the leading quadratic divergence in the one-loop diagram of Figure 1.1. Thus

$$m^2_{\phi\ \text{physical}} = (m^2_\phi)_0 + \delta m^2_\phi = \Lambda^2_{UV} - \Lambda^2_{UV} + \mathcal{O}(100\ \text{GeV})^2\ . \tag{1.20}$$

This process does, however, involve fine-tuning the tree level mass such that the two contributions to the physical mass cancel down to a number 20 orders of magnitude smaller. This would be an incredible coincidence, and yet the Standard Model affords no other explanation.

- **Problems with gauge unification**

Parameters within the Standard Model vary with energy scale. $G_{\rm SM}$, the gauge group of the SM, contains three independent gauge coupling constants, and the observed values of these couplings are larger for the larger components of the gauge group. If one could imagine that these couplings met at some very high energy scale, then by running down the energy scale one would see the $SU(3)_c$ and $SU(2)_L$ couplings increase at smaller energies due to their asymptotically free renormalisation group equations, whilst the $U(1)_Y$ coupling would decrease, resulting in the divergent values observed at low energy scales. This led to the prediction that $G_{\rm SM}$ was embedded in some larger

symmetry group, such as $SU(5)$ or $SO(10)$, which is spontaneously broken at a very high energy scale. Such models are known as Grand Unified Theories (GUTs). Each generation of matter forms a complete representation of the 'Grand Unified' group. Neutrino masses must be another prediction to come out of a suitable GUT, and indeed there are many groups that could contain $G_{\rm SM}$ as a subgroup, most of which require the necessary right-handed neutrino field with which to form neutrino masses.

Calculations running the gauge couplings up from the observed low energy scale to a high energy, in order to find the point at which the $G_{\rm SM}$ couplings unify, found that they actually did not all meet at a single point, as would be required for a GUT.

There are many well motivated solutions to these problems, including supersymmetry, string theory, family symmetries, and the see-saw mechanism, which subsequent sections will review.

1.3 Supersymmetry

Supersymmetry (SUSY) is an essential ingredient in superstring models, which offer the only consistent framework for combining all four fundamental forces together in a single theory. It is a symmetry that transforms between fermions and bosons, and is not an internal symmetry of the Poincaré group, unlike gauge symmetries.

This section highlights the important features of phenomenologically viable low energy supersymmetric models, and there are many excellent reviews that provide further technical details on SUSY formalism, [8, 9, 10, 11]. The next subsection details the *superfield* formalism, which is useful in constructing supersymmetric actions and thus defining the Minimal Supersymmetric Standard Model (MSSM), which is the minimal consistent supersymmetric extension of the SM. This section on supersymmetry concludes with a discussion of the benefits and unresolved problems of the MSSM.

1.3.1 Superfield basics

A generator of supersymmetry is an operator that commutes with the Hamiltonian and converts bosonic states into fermionic states. The generators of SUSY are fermionic, and satisfy the anti-commutation relation

$$\left\{Q_\alpha, \overline{Q}_{\dot{\beta}}\right\} = 2\sigma^\mu_{\alpha\dot{\beta}} P_\mu \ . \tag{1.21}$$

Thus supersymmetry extends the ordinary Poincaré spacetime to 'superspace' by non-trivially combining spacetime symmetries with internal symmetries of the Poincaré group. This is the super-algebra. The SUSY generators commute with the momentum operator P_μ, so

$$[Q_\alpha, P_\mu] = \left[\overline{Q}_{\dot{\alpha}}, P_\mu\right] = 0 \ . \tag{1.22}$$

We now introduce Weyl spinors containing Grassman variables $\theta_\alpha, \overline{\theta}_{\dot{\alpha}}$, which correspond to the SUSY charge operators $Q_\alpha, \overline{Q}_{\dot{\alpha}}$, in the same way that x_μ is the coordinate corresponding to the momentum operator P_μ. The properties of these anti-commuting Grassman variables will be of great help to us in the following formalism.

Since $\theta, \overline{\theta}$ are Grassman coordinates, the Taylor series in $\theta, \overline{\theta}$ terminates, and can be written exactly in terms of component fields. We can write a superfield $S(x, \theta, \overline{\theta})$ as a function of all three coordinate types. The 'chiral' superfield $\Phi(y, \theta)$, will be of use here:

$$\Phi(y, \theta) = \phi(y) + \sqrt{2}\theta\psi(y) + \theta\theta F(y) \ , \tag{1.23}$$

where $y^\mu = x^\mu + i\theta\sigma^\mu\overline{\theta}$.

An advantageous property of chiral superfields is that the product of two chiral superfields is itself a chiral superfield. Also of use to us is the 'vector' superfield, which is the most general real superfield, so $V(y) = V^\dagger(y)$.

Auxiliary fields appear in both types of superfield; F for chiral superfields, and D for vector superfields. Under SUSY transformations, both F and D change only by a derivative term, so they leave the action invariant, which leads to a convenient way of constructing supersymmetric actions. We obtain a supersymmetric action by extracting the F term from a mass dimension 3 chiral superfield, and the D term from a vector superfield of mass dimension 2. Thus there are two ways of constructing SUSY invariant actions:

$$\int d^4x \left[\int d^2\theta \; \Phi(y,\theta) + \int d^2\overline{\theta} \; \Phi^\dagger(y^\dagger,\overline{\theta}) \right] \tag{1.24}$$

for any chiral superfield Φ; and

$$\int d^4x \; d^4\theta \; V(x,\theta,\overline{\theta}) \tag{1.25}$$

for any vector superfield V. Both are needed to generate an interesting theory.

We will define the 'superpotential' W, as a chiral superfield of mass dimension 3. In order to satisfy this constraint, the superpotential must be a holomorphic polynomial of chiral superfields. This will contain the interactions. We then define the 'Kähler' potential K, as a vector superfield of mass dimension 2.

It is convenient to work in terms of these chiral (and vector) superfields which unite scalars with fermions (fermions with vector bosons) within a single field. We consider the simplest case of a chiral fermion and its scalar partner field, thus $K = \Phi\Phi^\dagger$. The superfield can be expanded in superspace notation into component fields[7],

$$\begin{aligned} \Phi(x_\mu,\theta,\overline{\theta}) \;\; &= \;\; \phi(x) + \sqrt{2}(\theta\psi_\phi(x)) + (\theta\theta)F_\phi(x) + i(\theta\sigma^\mu\overline{\theta})\partial_\mu\phi(x) \\ &\quad -\frac{i}{\sqrt{2}}(\theta\theta)\partial_\mu\psi_\phi(x)\sigma^\mu\overline{\theta} - \frac{1}{4}(\theta\theta)(\overline{\theta\theta})\Box\phi(x) \; , \end{aligned} \tag{1.26}$$

where ϕ is a complex scalar (e.g. squark, slepton, or Higgs boson), ψ is a left-handed

[7]We will consistently suppress the spinorial indices on ψ and θ. For technical details about spinor algebra, see [9, 11], for example.

2-component Weyl fermion (e.g. quark, lepton, or Higgsino), and $\sigma^\mu \equiv (1_2, \sigma^i)$ with σ^i as the Pauli matrices.

Notice that we have included the complex scalar auxiliary field F that will allow us to close the SUSY algebra off-shell and help us keep track of the number of degrees of freedom. F is, however, a non-dynamical field which can be eliminated using its classical equation of motion:

$$\frac{\delta \mathcal{L}}{\delta F} = \partial_\mu \frac{\delta \mathcal{L}}{\delta \partial_\mu F} \ , \tag{1.27}$$

and similarly solving the Euler-Lagrange equation for F^* leads to the solutions

$$-F = m\phi^* + g\phi^*\phi^* \qquad -F^* = m\phi + g\phi\phi \ . \tag{1.28}$$

The conjugate superfield $\Phi^\dagger$ expansion is found by simply taking the hermitian conjugate of Eq. (1.26) where the Weyl fermion is right-handed. We will refer to Φ ($\Phi^\dagger$) as a left (right) superfield since it involves left-handed (right-handed) Weyl spinors.

In order to extract the SUSY-invariant part of the Kähler potential (which is a vector superfield), we need to extract the auxiliary field D. The definition of a vector superfield includes a term

$$V = C(x) + ... + (\theta\theta)(\overline{\theta\theta})(D(x) - \frac{1}{2}\Box C(x)) \ , \tag{1.29}$$

which means that in order to extract the auxiliary D term, we must add $\frac{1}{2}\Box$ operating on the θ-independent term. So

$$K|_{\theta\theta\overline{\theta\theta}} + \frac{1}{2}\Box \ K|_{\text{no } \theta} = -\frac{1}{4}\Box\phi^*\phi - \frac{1}{4}\phi^*\Box\phi + F_\phi^*(x)F_\phi(x) + \frac{1}{2}\partial^\mu\phi^*\partial_\mu\phi + \frac{1}{2}\Box(\phi^*\phi) \ , \tag{1.30}$$

which, with the other terms from $K = \Phi\Phi\dagger$ using Eq. (1.26), contributes to the action in the following way

$$\begin{aligned} S_K \ = \ & \int d^4x \Big[\partial^\mu\phi^*\partial_\mu\phi + \frac{i}{2}\Big\{ \Big(\Big[\partial_\mu\psi_\phi^\dagger(x)\Big] \sigma^\mu \psi_\phi(x) \Big) \\ & - \psi_\phi^\dagger(x)\sigma^\mu\partial_\mu\psi_\phi(x) \Big\} + F_\phi^*(x)F_\phi(x) \Big] \ . \end{aligned} \tag{1.31}$$

The Kähler potential has thus generated the kinetic terms for the scalar field ϕ and fermionic field ψ_ϕ, with an auxiliary field F_ϕ, which is non-propagating mass dimension 2 scalar field. It is not an accident that these kinetic terms are canonically normalised, as we wrote down a canonically normalised Kähler potential. If we had chosen to work with a non-canonical Kähler potential, then in order to canonically normalise it we would have had to rescale the fields within it[8].

We now consider the superpotential,

$$W = \frac{1}{2}m\Phi^2 + \frac{1}{3}g\Phi^3 \ , \tag{1.32}$$

which gives the following contribution to the action,

$$\begin{aligned} S_W \ &= \ \int d^4x \Big[m\big(\psi_\phi(x)\psi_\phi(x)\big) + mF_\phi(x)\phi(x) \\ &\qquad + g\phi(x)\big(\psi_\phi(x)\psi_\phi(x)\big) + g|\phi(x)\phi(x)|^2 \Big] \ . \end{aligned} \tag{1.33}$$

We obtain the full action of the theory by adding the separate contributions from the Kähler potential, the superpotential, and the hermitian conjugate of the superpotential, thus

$$S = S_K + S_W + S_{W^*} \ . \tag{1.34}$$

Substituting the Euler-Lagrange solutions for the auxiliary field F, Eqs. (1.28), into the full action of the theory yields

$$\begin{aligned} S \ &= \ \int d^4x \Big[\partial^\mu\phi^*(x)\partial_\mu\phi(x) + \frac{i}{2}\Big\{ \Big(\Big[\partial_\mu\psi_\phi^\dagger(x)\Big]\sigma^\mu\psi_\phi(x)\Big) - \Big(\psi_\phi^\dagger(x)\sigma^\mu\partial_\mu\psi_\phi(x)\Big)\Big\} \\ &\qquad - m\Big[(\psi_\phi(x)\psi_\phi(x)) + \Big(\psi_\phi^\dagger(x)\psi_\phi^\dagger(x)\Big)\Big] - \big|m\phi + g\phi^2\big|^2 \Big] \ . \end{aligned} \tag{1.35}$$

[8]Note that in an effective field theory, the act of at least one scalar field gaining a VEV could cause the effective Kähler potential K_{eff}, to become non-canonical. In this situation, a previously canonical Kähler potential would become non-canonical, and the fields within the effective theory would have to be rescaled. This shift would need to be applied consistently throughout the theory.

This is a theory of a self-coupling complex scalar coupled to a fermion with an identical (Majorana) mass term. It does not involve gauge fields or chiral superfields that transform non-trivially under any gauge symmetry. It is possible to construct the gauge sector of a supersymmetric gauge field theory by using the superfield formalism if one first constructs superfields which contain field strength tensors. The non-gauge sector can, however, be constructed in the way outlined above, providing each term in the superpotential is a gauge singlet. The next subsection defines the Minimal Supersymmetric Standard Model (MSSM).

1.3.2 The Minimal Supersymmetric Standard Model

The minimal supersymmetric extension to the Standard Model details the minimal supersymmetric particle content that supplements the SM in order to form a more complete theory, evading some of the downfalls of the Standard Model, such as the gauge hierarchy problem. By embedding the SM within a supersymmetric theory, one hopes to tie the masses of the Standard Model to the energy scale at which supersymmetry is broken, and thus give reason to why these particles do not have masses of $\mathcal{O}(M_{\rm Pl})$. This would occur if the supermultiplet of a chiral representation of the gauge group contained the scalar fields along with the fermions, as supersymmetry would then require vanishing bare masses for the scalars as well as the fermions.

The MSSM uses the minimal gauge group necessary to include the extra supersymmetric partners, and this transpires to be the same gauge group as that of the SM, $G_{\rm MSSM} = G_{\rm SM} = SU(3)_c \otimes SU(2)_L \otimes U(1)_Y$. The fermionic partners to the Higgs fields can, however, contribute to chiral anomalies, since they have hypercharge 1/2. Thus the minimal field content is not found just by promoting all the SM fields to superfields. The arising anomalies are cancelled by introducing a new Higgs doublet with

hypercharge $-1/2$. This transpires to be necessary in order to generate the up-type fermion masses, due to the holomorphy of the superpotential.

The standard tilde notation is used throughout this work, so for every field in the SM, there exists a partner field in the MSSM which is indicated by the tilde on top of the letter denoting the field. We prefix an 's' to the supersymmetric field if it is a scalar, and use the suffix 'ino' if the new field is fermionic. There are no new vector fields introduced. We shall refer to the supersymmetric partner field of a SM field as its 'superpartner', and the particles corresponding to the new fields as 'sparticles'. With this information, we can now name the squark as the new sparticle corresponding to the superpartner field of the quark, and the superpartner of the Higgs is named the Higgsino. Table 1.2 details the MSSM fields and their gauge representations.

The superpotential of the MSSM is

$$W = Q_i H_u \overline{U}_j Y^u_{ij} + Q_i H_d \overline{D}_j Y^d_{ij} + L_i H_d \overline{E}_j Y^e_{ij} + \mu H_u H_d \ . \tag{1.36}$$

To ensure gauge invariance, the Kähler potential must be modified slightly. To be consistent with supersymmetry and gauge invariance, we introduce a set of superfields which contain the gauge fields g^μ_α, W^μ_a, and B^μ, and their gaugino superpartners. We then need to ensure that the gauge and gaugino fields have kinetic terms.

SUSY cannot be an exact symmetry in Nature, as we have not yet observed any light scalar fields that could be superpartners to the charged leptons. We do not, however, know the mechanism(s) by which supersymmetry is broken, although many models have been proposed. The allowed parameter space is not yet strongly constrained enough to indicate which of these models could be correct, so we must wait for the observation of sparticles at high energy accelerators such as the LHC. Thus, as SUSY is broken in Nature, we must break SUSY in the MSSM. We do this by introducing a set of terms

Superfield	Spin 0	Spin-1/2	Spin-1	$SU(3)_c$	$SU(2)_L$	$U(1)_Y$
Q_{iL}	$\widetilde{q}_{iL}$	q_{iL}	–	$\mathbf{3}$	$\mathbf{2}$	$1/6$
$\overline{U}_{iR}$	$\widetilde{\overline{u}}_{iR}$	$\overline{u}_{iR}$	–	$\overline{\mathbf{3}}$	$\mathbf{1}$	$-2/3$
$\overline{D}_{iR}$	$\widetilde{\overline{d}}_{iR}$	$\overline{d}_{iR}$	–	$\overline{\mathbf{3}}$	$\mathbf{1}$	$1/3$
L_{iL}	$\widetilde{l}_{iL}$	l_{iL}	–	$\mathbf{1}$	$\mathbf{2}$	$-1/2$
$\overline{E}_{iR}$	$\widetilde{\overline{e}}_{iR}$	$\overline{e}_{iR}$	–	$\mathbf{1}$	$\mathbf{1}$	1
H_u	h_u	$\widetilde{H}_u$	–	$\mathbf{1}$	$\mathbf{2}$	$1/2$
H_d	h_d	$\widetilde{H}_d$	–	$\mathbf{1}$	$\mathbf{2}$	$-1/2$
G^α	–	$\widetilde{g}^\alpha$	g^α	$\mathbf{8}$	$\mathbf{1}$	0
W^a	–	$\widetilde{W}^a$	W^a	$\mathbf{1}$	$\mathbf{3}$	0
B	–	$\widetilde{B}$	B	$\mathbf{1}$	$\mathbf{1}$	0

Table 1.2: The $G_{\rm SM}$ representations of the field content of the MSSM. We have taken the CP-conjugate of the right-handed singlet fields so that they transform as left-handed fields. As before, $i = 1-3$, $\alpha = 1-8$, $a = 1-3$.

which explicitly break the supersymmetry in the Lagrangian, but do so 'softly'[9]. We define

$$\begin{aligned} -\mathcal{L}_{\text{soft}} &= \frac{1}{2}\left(M_3\widetilde{g}\widetilde{g} + M_2\widetilde{W}\widetilde{W} + M_1\widetilde{B}\widetilde{B}\right) + h.c. \\ &+\widetilde{\overline{u}}_{iR}\widetilde{q}_{jL}h_u\widetilde{A}^u_{ij} - \widetilde{\overline{d}}_{iR}\widetilde{q}_{jL}h_d\widetilde{A}^d_{ij} - \widetilde{\overline{e}}_{iR}\widetilde{l}_{jL}h_d\widetilde{A}^e_{ij} + h.c. \\ &+\widetilde{q}^\dagger_{iL}m^2_{QL}\widetilde{q}_{jL} + \widetilde{\overline{u}}^\dagger_{iR}m^2_{UR}\widetilde{\overline{u}}_{jR} + \widetilde{\overline{d}}^\dagger_{iR}m^2_{DR}\widetilde{\overline{d}}_{jR} + \widetilde{l}^\dagger_{iL}m^2_{LL}l_{jL} + \widetilde{\overline{e}}^\dagger_{iR}m^2_{ER}\widetilde{\overline{e}}_{jR} \\ &+m^2_{h_u}h^\dagger_u h_u + m^2_{h_d}h^\dagger_d h_d - (B\mu h_u h_d + h.c.)\ , \end{aligned} \tag{1.37}$$

where the M_i are gaugino masses, the $\widetilde{A}^f_{ij}$ are trilinear scalar interactions, and the m^2_{ij} are scalar mass terms. The trilinears and sfermion masses are 3×3 matrices in generation space.

The SUSY breaking parameters are generated from some underlying theory, e.g. supergravity or string theory, which we shall touch upon in Chapter 2. These parameters can have complex entries, although the mass matrices must be hermitian, so after phase redefinitions, the MSSM is left with an additional 105 free independent masses, phases and mixing angles that cannot be rotated away.

Using this soft Lagrangian and the superpotential, we can write down the full MSSM Lagrangian $\mathcal{L}_{\text{MSSM}}$. We can then calculate the physical mass spectra of the superpartners by diagonalising the mass terms in $\mathcal{L}_{\text{MSSM}}$. The two complex Higgs scalars contain 8 real degrees of freedom, of which 3 Goldstone modes are eaten by the $W^\pm, Z^0$ bosons, which consequently gain mass. The remaining 5 physical degrees of freedom comprise the physical Higgs sector of the MSSM:

- $H^\pm$ - a charged Higgs boson pair,

[9]Soft breaking preserves the 'nice' features of the symmetry. The terms in $\mathcal{L}_{\text{soft}}$ must not re-introduce quadratic divergences [12] and spoil the solution to the hierarchy problem.

- H^0, h^0 - two CP-even neutral Higgs bosons,

- A^0 - a CP-odd Higgs boson.

Electroweak symmetry is broken when the neutral components of the two Higgs scalar doublets acquire VEVs,

$$\langle H_u \rangle = \frac{1}{\sqrt{2}} \begin{pmatrix} 0 \\ v_u \end{pmatrix} \quad , \quad \langle H_d \rangle = \frac{1}{\sqrt{2}} \begin{pmatrix} v_d \\ 0 \end{pmatrix} \ . \tag{1.38}$$

We know that $v_u^2 + v_d^2 \approx (246\text{GeV})^2$ from measurements of the Fermi constant G_F. We do not, however, know the ratio between the VEVs, as given by $\tan\beta = v_u/v_d$, and look to experiment for constraints on parameter space.

After EWSB, fields with identical quantum numbers, i.e. in the same representation under $SU(3)_c \otimes U(1)_\text{em}$, can mix. This results in the (observable) mass eigenstates being linear combinations of the (unbroken) gauge eigenstates. Thus the charged Higgsinos and charged gauginos mix to form chargino states:

$$\widetilde{h}_u^+ \ , \ \widetilde{h}_d^- \ , \ \widetilde{W}^1 \ , \ \widetilde{W}^2 \rightarrow \widetilde{\chi}_1^\pm \ , \ \widetilde{\chi}_2^\pm \ , \tag{1.39}$$

and the neutral Higgsinos and neutral gauginos mix into neutralino states:

$$\widetilde{h}_u^0 \ , \ \widetilde{h}_d^0 \ , \ \widetilde{W}^3 \ , \ \widetilde{B} \rightarrow \widetilde{\chi}_1^0 \ , \ \widetilde{\chi}_2^0 \ , \ \widetilde{\chi}_3^0 \ , \ \widetilde{\chi}_4^0 \ , \tag{1.40}$$

where the lightest neutralino $\widetilde{\chi}_1^0$ is often called the lightest supersymmetric partner (LSP).

1.3.3 Successes of the MSSM

Supersymmetry offers solutions to many of the problems in the SM, and this is a strong theoretical motivation for pursuing supersymmetric extensions of the SM.

- **The hierarchy problem**

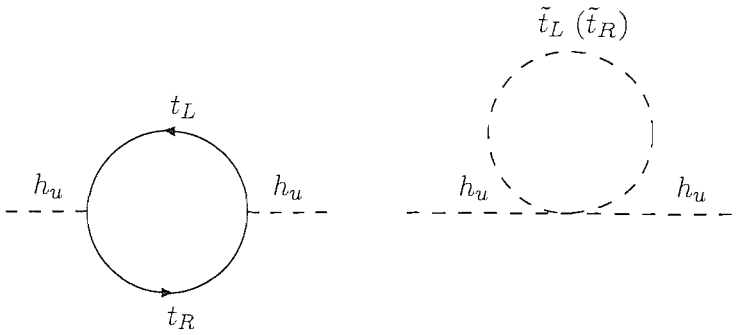

Figure 1.2: The dominant corrections to the MSSM Higgs (mass)^2 comes from both the top quark bubble and the one-loop top squark diagram.

Figure 1.1 showed that the Higgs scalars are not protected in the SM from acquiring quadratically divergent radiative corrections from virtual loops of Planck-scale particles. One benefit of SUSY is that it acts to stabilise the hierarchy between the electroweak and Planck scales by contributing sparticle loops for every particle loop, see Figure 1.2. Thus the corrections to the Higgs self-energy now have superpartners in the loops, which exactly cancel the original quadratic divergence (compare Eq. (1.41) below with Eq. (1.19)). So with softly broken SUSY there is an extra correction due to the parameters in $\mathcal{L}_{\text{soft}}$, and the correction to the Higgs (mass)^2 from the supersymmetric particles is

$$\delta m_{h_u}^2 = -\frac{6|\lambda_t|^2}{16\pi^2} m_{\tilde{t}}^2 \ln\left(\frac{\Lambda_{UV}}{m_{\tilde{t}}}\right) + \cdots , \tag{1.41}$$

where $m_{\tilde{t}}^2$ contains both stop masses via a linear combination such as $m_{\tilde{t}}^2 = \frac{1}{2}(m_{\tilde{t}_L}^2 + m_{\tilde{t}_L}^2)$ for instance.

In the limit that SUSY is preserved, $m_{\tilde{t}_L} = m_{\tilde{t}_R} = m_t$, the Higgs mass would be one-loop finite. The supersymmetric cancellation stabilises the hierarchy and avoids the problem of fine-tuning, provided that SUSY is broken around the TeV scale, such that the soft parameters are $\mathcal{O}$(TeV).

Within the hierarchy problem, we must also understand why the electroweak breaking scale is so far below the Planck scale. This is addressed in the MSSM by the process known as radiative electroweak symmetry breaking.

- **Radiative electroweak symmetry breaking**

Supersymmetry can also provide an explanation for why the Higgs mass becomes tachyonic. In the SM, we had to insert by hand the fact that the Higgs mass is driven negative at some energy around the electroweak scale, in order to trigger EWSB. In supergravity models with universal soft parameters at the Grand Unified Theory (GUT) scale, we find that $m_{h_u}^2$ receives large radiative corrections from top and stop loops that do not exactly cancel. In the MSSM, the renormalisation group equations (RGEs) for $m_{h_u}^2$ are such that if the top quark Yukawa is $\mathcal{O}(1)$, then RG running down to low energies can automatically drive $m_{h_u}^2$ negative close to the electroweak scale, which causes EWSB [13]. This helps to explain why the electroweak scale is much lower than the Planck scale.

- **Gauge coupling unification**

We have already mentioned that we do not obtain gauge coupling unification in the SM. The additional TeV scale sparticles in the MSSM carry gauge quantum numbers, and will consequently change the RGEs. This will change the predictions for the evolution of the three gauge couplings to high energy scales. The MSSM RGEs for the gauge couplings are smaller in magnitude, leading to approximate unification at a higher scale. We use the SM RGEs up to the scale at which the sparticle fields enter, whereupon we switch to the MSSM RGEs. By changing the scale at which we switch to the MSSM RGEs, we can control the gradient of the lines depicting the size of the gauge couplings. As the lines approach each other, two of them will always meet, so

by changing the scale at which we turn on the MSSM RGEs we can deviate the lines so that all three meet at a single point. The appropriate energy at which to switch RGEs is on the TeV scale, which yields approximate gauge coupling unification at a scale $M_X \approx 2 \times 10^{16}$ GeV. This is consistent with the desired scale necessary for supersymmetry breaking in order to solve the hierarchy problem above.

Many string-inspired models have some amount of unification close to the Planck scale, so this is promising for both SUSY GUTs and string phenomenology.

1.3.4 Unanswered questions in the MSSM

Our understanding of low energy SUSY is not complete since there are many unanswered questions.

- **Free parameters**

One of the main concerns is the huge number of arbitrary parameters in the MSSM. There are 124 masses, phases, and mixing angles (excluding neutrino masses) compared to the 19 free parameters of the SM. There are currently no strong direct constraints on most of the free MSSM parameters, other than limits due to rare decays, which can be ameliorated by increasing the scale of all the soft parameters. At the moment there isn't an accepted standard model for SUSY breaking, or even a consensus on how SUSY breaking is transmitted to the visible sector. With the advent of sparticle data, it may be possible to probe these questions. At present though, the sheer number of parameters means that it is very difficult to make general predictions using the MSSM.

- **The SUSY flavour problem**

Despite the multitude of free parameters in $\mathcal{L}_{\text{soft}}$, experimental constraints on rare flavour violating decays, amongst other things, are indicative of some organising struc-

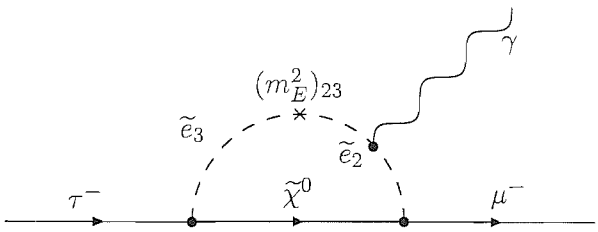

Figure 1.3: Feynman diagram contributing to the process $\tau \to \mu\gamma$ at one-loop in the MSSM.

ture. The branching ratios of lepton flavour violating processes, such as $\tau \to \mu\gamma$, are strongly constrained to very small values by experimental limits. A typical Feynman graph contributing to $\tau \to \mu\gamma$ is shown in Figure 1.3. To see how these flavour violating decays are generated, we move to the basis where the Yukawa matrices are flavour diagonal and see that the couplings of charged leptons to neutralinos and charginos are flavour diagonal. The contributions to these flavour violating decays then come from the off-diagonal elements in the slepton mass matrices m_L^2, m_E^2, and are suppressed by larger diagonal elements.

This highlights the SUSY flavour problem. As we must not violate the strong experimental limits on $\mathrm{BR}(\tau \to \mu\gamma)$, for example, we need to generate very small flavour violation. Thus we know that the slepton mass matrices must be *nearly* diagonal in the basis where the Yukawa matrices are diagonal. We do not, however, expect the soft couplings to originate from the same (unknown) physics as the Yukawa couplings, so we must explain one of two questions about the slepton mass matrices; why they are aligned to the Yukawa matrices, or why they are so close to the identity. The quark sector throws up similar questions, where we need alignment or universality in the squark mass matrices to avoid predicting rates for processes such as $b \to s\gamma$ that are far too large, and violate experimental limits.

- **Neutrino masses**

Like the Standard Model, the MSSM (assuming R-parity) predicts massless neutrinos, as it does not have any right-handed neutrino fields. This is obviously a problem for the MSSM, as neutrino oscillations have been observed [6, 14], which demonstrates that at least two neutrinos must have non-zero mass. There is no current standard model for generating neutrino masses, so an extended MSSM that incorporates massive neutrinos is not yet a viable option.

1.4 Low energy indications of high energy physics

In the context of supersymmetry, it transpires that it is possible to consistently have fields with mass terms close to the Planck scale, which can then be integrated out of the effective field theory (the MSSM or one of its extensions). We cannot do this within the bounds of the SM, as radiative corrections to the Higgs mass would be of the order of the new energy scale. However, in a supersymmetric theory, the supersymmetry protects the Higgs mass, so the large scale involved does not become a technical problem.

Some circumstances do, in fact, make it possible to see the low energy effects of such high energy physics.

1.4.1 Neutrinos and the see-saw mechanism

One can consider the see-saw mechanism [15] as a rather general way in which to create left-handed neutrino field Majorana mass terms that are naturally of the correct order. Right-handed neutrino field(s) are introduced with masses just below the SUSY GUT scale of approximately 2.2×10^{16} GeV. Yukawa terms are also allowed, but gauge invariance forbids left-handed Majorana terms. Assuming that there are three[10] right-

[10]This fits in with phenomenology, and is a requirement of most GUTs and string-inspired models.

handed neutrino singlet fields $\overline{N}_i$, the see-saw part of the full superpotential is

$$W_{\text{see-saw}} = L_i H_u \overline{N}_j Y^{\nu}_{ij} + \frac{1}{2}\overline{N}_i \overline{N}_j \left(M_{RR}\right)_{ij} \ . \tag{1.42}$$

Here, Y^{ν} is the matrix of neutrino couplings, M_{RR} is the right-handed neutrino Majorana mass matrix, and L and H_u denote the left-handed lepton and up-type Higgs doublets respectively. Then when we break $SU(2)_L \otimes U(1)_Y \rightarrow U(1)_{\text{em}}$ and integrate out the right-handed neutrino fields, a tree level left-handed Majorana mass matrix will be generated, despite the fact that gauge invariance forbids it. This results in the following term in the effective Lagrangian

$$\Delta\mathcal{L}_{\text{eff}} = -\nu_i \nu_j \left\langle h_u \right\rangle^2 \left(Y^{\nu} \cdot M^{-1}_{RR} \cdot Y^{\nu\,\dagger}\right)_{ij} \ . \tag{1.43}$$

At energies much below the mass scale of the right-handed neutrinos, this leads to an effective Majorana mass matrix for the left-handed neutrinos:

$$m_{LL} = Y^{\nu} \cdot M^{-1}_{RR} Y^{\nu\,\dagger} \left\langle h_u \right\rangle^2 \ . \tag{1.44}$$

Providing the right-handed masses are just below the GUT scale, we can produce Majorana masses of the correct order if we set the Dirac-Yukawa mass term to be of the order of the up-type quark mass terms. As there is no symmetry within the MSSM that protects the right-handed neutrino fields from gaining a mass, they are naturally expected to attain masses around the high energy scale. GUTs and string-inspired theories, however, often do contain protective symmetries for the right-handed neutrinos, and the neutrino singlets are expected to acquire masses close to the energy scale at which this symmetry is broken[11]. So if we consider a string-inspired GUT, then the see-saw mechanism will automatically generate neutrino masses of the required order.

[11] Thus in unified theories, we expect right-handed neutrinos to gain masses just below the unification scale $M_X \approx 10^{16}$ GeV.

The see-saw mechanism can also naturally predict neutrino angles [16], which means that neutrino measurements can act as a window into very high energy physics. If the see-saw mechanism is correct, then observations may show that there is an energy scale for SUSY theories that is very close to the GUT scale.

1.4.2 The Froggatt-Nielsen mechanism

The way in which we use the see-saw mechanism to understand the neutrino masses and mixings can give us insight into the hierarchical form of the Yukawa matrices. We follow the idea of Froggatt and Nielsen [17], assuming that there is a high energy theory for which the MSSM is the appropriate low energy effective theory. We introduce a new $U(1)_F$ gauge symmetry into the full theory, where the subscript F indicates that there is a 'family' dependent charge which can split the generations. The Higgs fields are also allowed to carry charges under the new family symmetry. We also introduce a new superfield $\Phi_{\rm FN}$, associated with this symmetry, which has charge -1 under $U(1)_F$. There are also messenger fields χ in the full theory.

When $\Phi_{\rm FN}$ gets a VEV, Yukawa interactions are generated as effective operators in the MSSM. As an example, we look at a (non-renormalisable) term in the effective superpotential

$$\mathcal{O}^u_{ij} = a^u_{ij} Q_i \overline{U}_j H_u \left(\frac{\Phi_{\rm FN}}{M_\chi}\right)^{x_{q_i}+x_{u_j}+x_{h_u}} , \tag{1.45}$$

where M_χ is the mass associated with the messenger field, a^u_{ij} is a coupling that we expect to be of $\mathcal{O}(1)$, and the x_f are the $U(1)_F$ charges for the fields f. In the SM and the MSSM, when the Higgs develops a VEV we get a Dirac mass term. Similarly to this, $\Phi_{\rm FN}$ developing a VEV leads to a Yukawa interaction. In this situation, defining $\epsilon = \langle\phi_{\rm FN}\rangle/M_\chi$, we can read off

$$Y^u_{ij} = a^u_{ij}\, \epsilon^{x_{q_i}+x_{u_j}+x_{h_u}} . \tag{1.46}$$

By imposing non-universal $U(1)_F$ family charges, we can begin to explain the hierarchical nature of the Yukawa matrices and the small quark mixing angles. By doing this, it is possible to understand the Yukawa matrices in terms of $\mathcal{O}(1)$ parameters, within the context of a symmetry that is broken at a very high energy scale.

This procedure can be very useful when combined with the idea of a GUT. In order to be consistent with the larger multiplets of Grand Unification, we must impose the constraint that the charges of some, if not all, of the fields are universal. Considering a Pati-Salam[12] unified theory enhanced with a $U(1)_F$, we demand that $x_{q_i} = x_{l_i}$, and $x_{u_i} = x_{d_i} = x_{e_i} = x_{n_i}$. This is of great use for model-building, as there will only be a small number of symmetries that can be consistent with a unified group such as Pati-Salam or $SO(10)$, and also give the correct SM particle spectrum.

Supersymmetry is thus a very powerful framework, and offers many solutions to SM problems. However, we still need to consider *how* to embed the MSSM within a deeper theory such as superstring theory. This is explored in the next chapter.

[12]We shall explore this in greater depth in Chapter 2.

Chapter 2

Introduction to Supergravity, Strings and the Pati-Salam Model

2.1 Preamble

The aim of this chapter is to introduce two formalisms to aid in our understanding of high energy particle physics. 'High energy' refers to scales approaching the Planck scale, at which it is believed that gravitation becomes comparable in strength to the gauge interactions, and quantum gravitational effects must be considered. The two formalisms are those of string theory and unification, which we shall tie together in the context of describing a string-inspired Pati-Salam model.

First of all though, we must build upon our knowledge of supersymmetry from Chapter 1.

2.2 Supergravity basics

Using conventional supergravity (SUGRA) formalism, we will describe the 4-dimensional effective theory that describes the low energy limit of string models, and show how to generate soft SUSY breaking terms using SUGRA. Supergravity (localised supersymmetry) is defined in terms of a Kähler function G, of generic chiral superfields $\phi = h, C_a$,

$$G(\phi, \overline{\phi}) = \frac{K(\phi, \overline{\phi})}{\tilde{M}_{\rm Pl}^2} + \ln\left(\frac{W(\phi)}{\tilde{M}_{\rm Pl}^3}\right) + \ln\left(\frac{W^*(\overline{\phi})}{\tilde{M}_{\rm Pl}^3}\right) . \tag{2.1}$$

We have included powers of the reduced Planck mass $\tilde{M}_{\rm Pl} = M_{\rm Pl}/\sqrt{8\pi}$, that appear in the Kähler function to obtain the correct mass dimensions, although it is often the convention to adopt natural units and set $\tilde{M}_{\rm Pl} = 1$. The chiral superfields include the hidden sector closed strings $h = S, T_i$, and open string matter states $C_a = C_j^{5_i}, C^{5_i 5_j}, C^{5_i 9}, C_i^9$.

The closed string states are the dilaton S, and the *untwisted* moduli[1] T_i. The superscript numbers on the C_a indicate the 'brane(s)' on which the ends of the open strings reside. If the open string state has both ends on the same brane, then the subscript on the C specifies which pair of compactified extra dimensions the string is free to vibrate in. Dp-branes are extended solitonic objects upon which the ends of the open strings are constrained to lie. We will cover the concept of branes in more detail in Section 2.3.1.

The Kähler potential $K(\phi, \overline{\phi})$ is a real function of chiral superfields, and may be expanded in powers of the matter states C_a [18], including non-perturbative contributions,

$$K = \overline{K}(h, \overline{h}) + \tilde{K}_{\overline{a}b}(h, \overline{h})\overline{C}_{\overline{a}}C_b + \left[\frac{1}{2}Z_{ab}(h, \overline{h})C_aC_b + h.c.\right] + \ldots , \tag{2.2}$$

where $\tilde{K}_{\overline{a}b}$ is the (generally non-diagonal) matter metric known as the Kähler metric.

[1] We shall not consider the hidden sector Y_k twisted moduli within the scope of this thesis.

$\overline{C}_{\overline{a}}$ are the matter states for the conjugated superfield. The non-zero bilinear term Z_{ab} can generate the μ-term through the Giudice-Masiero mechanism [19], subject to gauge invariance. $W(\phi)$ is the superpotential, a holomorphic function of chiral superfields that can also be expanded:

$$W = \hat{W}(h) + \frac{1}{2}\mu_{ab}(h)C_aC_b + \frac{1}{6}Y_{abc}C_aC_bC_c + \dots . \tag{2.3}$$

Note that this includes a trilinear Yukawa term that will generate fermion masses, and also a bilinear μ-term. The Kähler potential and superpotential do, however, receive non-perturbative corrections that are often difficult to predict. All parameters here are generally functions of the hidden sector fields, and once these fields gain (large) VEVs, the parameters will play the role of various couplings in the observable sector.

2.2.1 Soft terms from supergravity

We know that SUSY is broken in Nature, but we lack a canonical model of SUSY breaking. If SUSY is broken, then the auxiliary fields $F_\phi \neq 0$ for some ϕ. To help overcome this and the non-perturbative problems, we use Goldstino[2] angles to parameterise our ignorance. To control the relative contributions to SUSY breaking from the various F-term[3] VEVs, we introduce a matrix P that canonically normalises the Kähler metric, $P^\dagger K_{\overline{J}I}P = 1$.[4] We also define a column vector Θ which has unit length and satisfies $\Theta^\dagger\Theta = 1$. As long as we meet these constraints, we have complete freedom over the parameterisation of Θ.

To obtain the soft SUSY breaking terms, we must fix the gravitino mass $m_{3/2}$ and

[2]After SUSY breaking, the supersymmetric partner of the Goldstone boson, the Goldstino, is eaten by the massless gravitino through the super-Higgs mechanism.

[3]At present we shall ignore the D-term contributions arising from the gauge sector.

[4]The subscripts on the Kähler potential K_I mean $\partial_I K$, whereas the subscripts on the F-terms just label the fields. $I, J \equiv \phi_I, \phi_J \in \{h, C_a\}$.

the VEVs of the hidden sector fields, while sending the Planck mass to infinity. The fermion Yukawa couplings are then rescaled as

$$Y'_{abc} = \frac{\hat{W}^*}{|\hat{W}|}\, e^{\overline{K}/2}\, Y_{abc} \ . \tag{2.4}$$

Using Eqs. (2.2) and (2.3), we can write down the *un-normalised* soft masses and trilinears that appear in the soft SUGRA potential [18].

$$V_{\text{soft}} = m^2_{\overline{a}b}\overline{C}_{\overline{a}}C_b + \left(\frac{1}{6}A_{abc}Y_{abc}C_aC_bC_c + h.c.\right) + \ldots \ , \tag{2.5}$$

where the generally non-diagonal Kähler metrics lead to the non-canonically normalised soft masses

$$m^2_{\overline{a}b} = \left(m^2_{3/2} + V_0\right)\tilde{K}_{\overline{a}b} - F_{\overline{I}}\left(\partial_{\overline{I}}\partial_J\tilde{K}_{\overline{a}b} - \partial_{\overline{I}}\tilde{K}_{\overline{a}c}\left(\tilde{K}^{-1}\right)^{c\overline{d}}\partial_J\tilde{K}_{\overline{d}b}\right)F_J \ , \tag{2.6}$$

and trilinears

$$\begin{aligned} A_{abc}Y_{abc} \ = \ & \frac{\hat{W}^*}{|\hat{W}|}\, e^{\overline{K}/2}\, F_I\Big[\overline{K}_I Y_{abc} + \partial_I Y_{abc} - \Big(\left(\tilde{K}^{-1}\right)^{d\overline{e}}\partial_I\tilde{K}_{\overline{e}a}Y_{dbc} \\ & + (a \leftrightarrow b) + (a \leftrightarrow c)\Big)\Big] \ . \end{aligned} \tag{2.7}$$

Here, V_0 is the vacuum energy and the subscripts I, J run over the fields h, C_a, although the hidden sector parts of the Kähler potential and metrics are independent of the matter fields by definition. Note that the non-diagonal Kähler metric for the matter states will generate a mass matrix between different fields. We transform to the canonically normalised Kähler metric using the matrix $\tilde{P}$ where $\tilde{P}^\dagger\tilde{K}_{\overline{a}b}\tilde{P} = 1$, such that the physical canonically normalised masses m^2_a are related to the previous non-canonical mass matrix $m^2_{\overline{a}b}$ by the relation

$$m^2_a = \tilde{P}^\dagger m^2_{\overline{a}b}\tilde{P} \ . \tag{2.8}$$

If the Kähler metric is diagonal and *non*-canonical $\tilde{K}_a = \tilde{K}_{\overline{a}b}\delta_{\overline{a}b}$, then the canonically normalised scalar square masses are given by

$$m^2_a = m^2_{3/2} - F_{\overline{J}}F_I\partial_{\overline{J}}\partial_I\left(\ln\tilde{K}_a\right) \ , \tag{2.9}$$

as in [20] where $I, J = h, C_a$. Note that we have chosen the vacuum energy, or rather the cosmological constant V_0, to be vanishingly small as in [20] so it does not contribute to Eq. (2.9). The soft gaugino mass associated with the gauge group G_α is

$$M_\alpha = \frac{1}{2\Re f_\alpha} F_I \partial_I f_\alpha \ , \tag{2.10}$$

where $I = h$ only here. α tells us which D-brane we are considering, and hence which gauge group. f_α is the 'gauge kinetic function'. In type I string models without twisted moduli, the gauge kinetic functions take the form $f_9 = S$; $f_{5_i} = T_i$.

Assuming that the terms $\partial_{C_a} Y_{abc} \neq 0$, the canonically normalised SUSY breaking trilinear term is

$$A_{abc} = F_I \left[\overline{K}_I + \partial_I \ln Y_{abc} - \partial_I \ln \left(\tilde{K}_a \tilde{K}_b \tilde{K}_c \right) \right] \ , \tag{2.11}$$

where $I, J = h, C_a$ again. If the Yukawa hierarchy is taken to be generated by a Froggatt-Nielsen field ϕ, such that $Y \propto \phi^p$,[5] and for small ϕ we expect $F_\phi \propto m_{3/2}\phi$ as in [21], thus $F_\phi \partial_\phi \ln Y \propto m_{3/2}$. So even though these fields are expected to have heavily sub-dominant F-terms, they contribute to the trilinears on an equal footing to the moduli.

For the models considered within this thesis, we use a Kähler potential that does not include twisted moduli [22]

$$\begin{aligned} K \ = \ & -\ln\left(S + \overline{S} - \left|C_1^{5_1}\right|^2 - \left|C_2^{5_2}\right|^2 \right) - \ln\left(T_1 + \overline{T}_1 - \left|C_1^{9}\right|^2 - \left|C_3^{5_3}\right|^2 \right) \\ & - \ln\left(T_2 - \overline{T}_2 - \left|C_2^{9}\right|^2 - \left|C_3^{5_1}\right|^2 \right) - \ln\left(T_3 - \overline{T}_3 - \left|C_3^{9}\right|^2 - \left|C_2^{5_1}\right|^2 - \left|C_1^{5_1}\right|^2 \right) \\ & + \frac{\left|C^{5_1 5_2}\right|^2}{\left(S + \overline{S}\right)^{1/2} \left(T_3 + \overline{T}_3\right)^{1/2}} + \frac{\left|C^{95_1}\right|^2}{\left(T_2 + \overline{T}_2\right)^{1/2} \left(T_3 + \overline{T}_3\right)^{1/2}} \\ & + \frac{\left|C^{95_2}\right|^2}{\left(T_1 + \overline{T}_1\right)^{1/2} \left(T_3 + \overline{T}_3\right)^{1/2}} \ . \end{aligned} \tag{2.12}$$

[5] p is a number representing the charge on the Froggatt-Nielsen field, such as the $U(1)_F$ charge.

2.3 Strings and phenomenology

Having laid down the basic foundations of supergravity in the last section, we now aim to review the current status of string phenomenology. We shall bypass the more technical details, but there are many excellent introductory texts [9, 23, 24] that should be consulted for further details.

String theories are so attractive as they offer the only *consistent* framework for unifying the four fundamental forces[6] of Nature. All fields within a quantum field theory (QFT) are represented within a string theory as different vibrational modes of microscopic strings. So fermions, scalars, gauge bosons, and gravitons would all be viewed as different resonant frequencies of these fundamental strings. These fundamental objects are one-dimensional, and of length $1/M_*$, where M_* is the string scale. Strings can either be 'open' or 'closed' so that their ends are either free or have joined together to form a loop. The latter can be thought of as the bound state of two open strings. Closed strings posses a spin-2 massless excitation which acts like a mediator of gravitational interactions would, and is thus said to represent the graviton.

The most promising models arise from 'superstring' theories, which use supersymmetric strings and lead to a supersymmetric spectrum of particles. String phenomenology is the area of research aimed at trying to embed the SM or the MSSM within a string theory in such a way as to generate a realistic matter spectrum at low energies. This study is hindered by a plethora of problems, including the multitude of vacua within most string theories, the vast array of experimental constraints that any successful model must be consistent with, and the difficulty of performing detailed calculations within string theory.

[6]These are electromagnetism, the strong and weak nuclear forces, and gravity.

2.3.1 String dualities and M-theory

Since the arrival of string theory in the scientific arena, its progress has been characterised by sudden surges in knowledge after key breakthroughs. These revolutions are followed by longer slack periods of little progress. The first of these revolutions occurred in 1984 when Green and Schwarz [25] constructed the first 10-dimensional anomaly free type I string theory. The theory involved both open and closed strings, with the gauge group $SO(32)$. This was followed by the construction of two 10d heterotic closed string theories, that combined bosonic strings in 26 dimensions with the 10d supersymmetric Green-Schwarz theory to give a gauge group of $SO(32)$ or $E_8 \times E_8$ [26]. Both type I and heterotic string theories exhibit $\mathcal{N} = 1$ spacetime supersymmetry and contain large gauge groups that can easily accommodate the gauge group of the MSSM; both $SO(32)$ and E_8 can break to $SU(3) \otimes SU(2) \otimes U(1)$. Type II string theories, which possess $\mathcal{N} = 2$ SUSY in 10d, were later developed, yielding further candidates to deliver the MSSM at low energies. These models seem to be less promising though, as $\mathcal{N} = 2$ SUSY automatically preserves parity, which is in direct conflict with the parity-violating weak interaction of the Standard Model. Thus a method by which to break $\mathcal{N} = 2$ to $\mathcal{N} = 1$ must be incorporated into the type II string theories, otherwise the correct phenomenology will not be generated at low energies. There were then five different theories, all of which predicted extraneous exotic matter states not found within the MSSM. Also, the extra dimensions had to be compactified in order to meld with the low energy physics of the four spacetime dimensions in which we live.

The second string revolution occurred in 1995, with the discovery of the strong/weak coupling duality [27]. This is a duality between the physics of the strong (weak) coupling phase of the type I string theory with the weak (strong) coupling phase of the heterotic $SO(32)$ theory. There exist a number of dualities that link the five separate string

theories, as shown in Figure 2.1. The idea of these dualities led to the proposal that each of the five theories were in fact different perturbative limits of one all encompassing theory – 11-dimensional 'M-theory'.

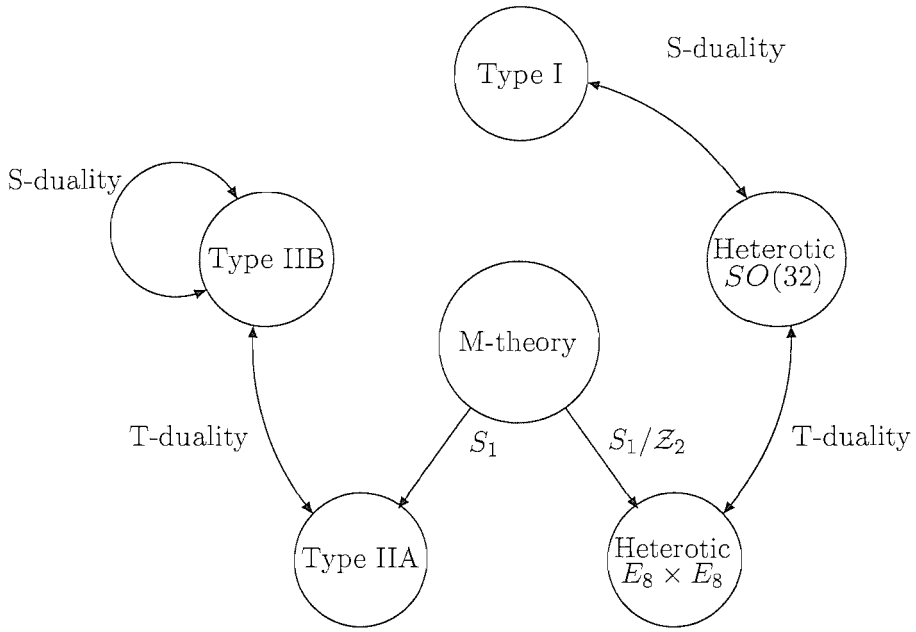

Figure 2.1: The web of string dualities. The dualities linking the five string theories are shown as double headed arrows. The compactifications leading from M-theory to a 10d string theory are denoted by a radial arrow.

Another important development was the discovery of extended solitonic objects called Dirichlet-branes (D-branes) [28, 29, 30], that exist within the vacua of type I and II string theories. A Dp-brane is a $(p+1)$-dimensional sub-manifold of the full 10d spacetime. It is the hyper-surface upon which the ends of open strings are constrained to lie. The open strings subsequently obtain Neumann boundary conditions within the 'world-volume' of the brane, and Dirichlet boundary conditions in the $(9-p)$ spatial coordinates transverse to the Dp-brane. Open strings attached to a Dp-brane

have Kaluza-Klein 'winding' states along the compact dimensions, with Neumann and Dirichlet boundary conditions as appropriate. With Neumann boundary conditions the end of the string is free to move about, but no momentum flows out. With Dirichlet boundary conditions the endpoint is fixed to move only on some manifold – the D-brane.

A stack of N coincident D-branes results in a $U(N)$ symmetry group under which the open strings transform. When viewed from the perspective of the string 'world-sheet',[7] this symmetry group behaves as a global symmetry, but when viewed from the target-space perspective, it behaves as a gauge symmetry group. Open strings carry Chan-Paton gauge quantum numbers for the gauge groups of the branes to which they are attached. Closed strings are identified with gravity fields, and these are free to move throughout the 'bulk' without necessarily being attached to a brane. This natural way of generating small gauge groups makes the study of D-branes very interesting, and type I and II string theories that incorporate D-branes can lead to models that provide less exotic matter to contend with. The discovery of the dualities between the different string theories meant that the less accessible corners of M-theory space could be reached by performing equivalent calculations in another string limit, then transforming back to the more difficult region.

2.3.2 Aspects of type I strings

This section aims to review some aspects of type I string theory necessary to construct models that contain the MSSM, or one of its simple extensions, as their low energy limit. This can include string-inspired GUTs at energies close to the string scale. [22] contains a more complete discussion on how to build these models.

10d $SO(32)$ type I string theory can be understood as an 'orientifold' [31, 32, 33, 34,

[7] The surface swept out by the string.

35] of 10d type IIB string theory. An orientifold, or Z_2 projection, is a mirror symmetry – a parity operation Ω on the IIB string world-sheet that transforms left- and right-moving vibrations into one another. It projects out states that are not invariant under Ω and breaks $\mathcal{N} = 2$ SUSY down to $\mathcal{N} = 1$. Thus by orientifolding a 10d type IIB string theory, where the closed strings are oriented, we have been left with an unoriented type I closed string theory in 10 dimensions. The process of orientifolding does, however, lead to an inconsistency, as 'tadpole'[8] anomalies arise in the string amplitudes. By adding in states that are 'twisted' with respect to Ω, we find that we cancel these divergences and restore the consistency of the theory. These twisted states are simply type I open strings whose ends are attached to D-branes, such that there is a net Ramond-Ramond charge of zero[9]. We find that requiring 32 D9-branes in the vacuum, where their world-volumes fill the entire 10d spacetime, causes the attached open strings to give rise to massless 10d gauge fields that transform in the adjoint representation of $SO(32)$. This leads to a consistent 10-dimensional, $\mathcal{N} = 1$ target-space string theory with open and closed strings.

We then run into the problem of 'compactification'. We have a theory in 10 dimensions, but somehow we need to get to our observable 4 dimensions. We do this by compactifying the 6 extra spatial dimensions on a six-torus $T^6 \equiv T_1^2 \times T_2^2 \times T_3^2$, where each pair of compactified dimensions is wrapped around a symmetric two-torus T_i^2 of radius R_i and volume $v_i = (2\pi R_i)^2$. The spacetime coordinates are labelled x_i, where $x_0 - x_3$ span the usual 4d Minkowski spacetime, and the remaining $x_4 - x_9$ are the extra dimensions. It is convenient to pair up these six compact dimensions so that they

[8]So named due to the shape of the Feynman diagram – a loop with one leg.

[9]Both orientifold planes and D-branes carry Ramond-Ramond charges, so to cancel a tadpole anomaly we must add in the correct number and type of D-branes to produce a net Ramond-Ramond charge of zero, thereby quashing the tadpole divergence.

behave as a triad of complex numbers, z_i:

$$z_1 = (x_4, x_5) \quad , \quad z_2 = (x_6, x_7) \quad , \quad z_3 = (x_8, x_9) \ , \tag{2.13}$$

where z_i spans the two-torus T_i^2. This set-up of complex, compact dimensions is shown in Figure 2.2. We will consider type IIB 4d orientifolds obtained by this compactification onto a six-torus [36, 37, 38, 39, 40, 41, 42, 43, 44].

The SUSY generators must be in the fundamental spinor representation of the Poincaré group – $SO(9,1)$ for a 10d theory, and $SO(3,1)$ for a 4d theory. The extra degrees of freedom do not vanish here. The fermionic SUSY generators become 'split' by compactification, leading to an extended supersymmetry in the lower dimensional theory. Thus $\mathcal{N} = 1$ SUSY in 10d is equivalent to $\mathcal{N} = 4$ SUSY[10] in 4d, so compactification is required to break three of the 4d supersymmetries in order to leave us with the $\mathcal{N} = 1$, 4d theory that we desire.

By imposing an orientifold group $\{\Omega \times G\}$, we 'twist' the theory, resulting in an $\mathcal{N} = 1$, 4d theory with fixed points that are invariant under the action of the orientifold group[11]. Here, Ω is the world-sheet parity and $G = \prod_{i=1}^{n} Z_i$ is a discrete Abelian group. There is, however, only a finite subset of type IIB orientifolds that can lead to $\mathcal{N} = 1$ in 4d, and these have already been classified in the context of toroidal heterotic compactifications [45]. As mentioned above, the act of orientifolding leads to tadpole divergences, and these are cancelled by introducing Dp-branes into the vacuum, where in order to preserve the $\mathcal{N} = 1$ SUSY, p must equal 5 and/or 9. The string constructions can thus contain D9-branes and D5_i-branes, where the latter span Minkowski space-

[10]The number of supersymmetries can be counted by considering the spectrum, as the number of supersymmetries must be equal to the number of gravitinos. Only one graviton can exist, but there will be $\mathcal{N}$ SUSY generators Q_α that will generate $\mathcal{N}$ gravitinos when acting upon the graviton state.

[11]A trivial example of a fixed point is the origin of a compact space.

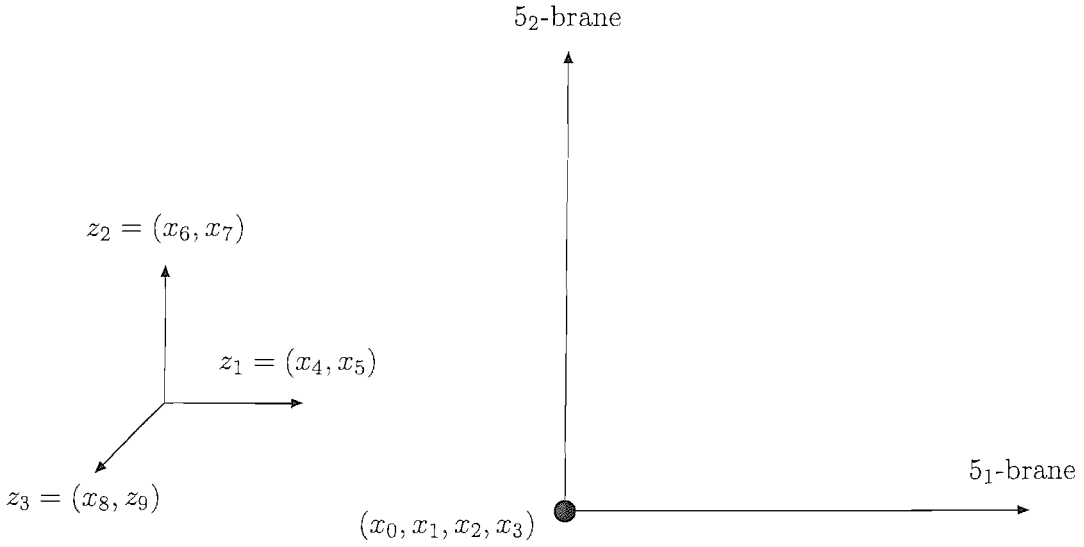

Figure 2.2: We represent the six-dimensional compact space using a complex coordinate system (*left*), where $D5_i$-branes are shown as straight lines along the z_i directions. A $D5_1$-brane and a $D5_2$ brane will overlap in Minkowski space (which is the origin of the coordinate system) but extend out into the "perpendicular" compact dimensions (*right*).

time and the two-torus T_i^2.[12] The gauge structure and massless spectrum are strongly constrained by the tadpole cancellation conditions[13], as these project out states that are not invariant under the orientifold group [22, 41, 42, 46].

We are not restricted to using just the world-sheet parity operation Ω; we are free to use other Z_2 parity operators to orientifold the type IIB theory. Other choices lead to vacua where D3-branes and/or D7-branes are required in order to cancel the tadpole anomalies. We use *T-duality* transformations to switch from this scenario to the one above involving D5$_i$-branes and/or D9-branes:

$$R_i \leftrightarrow \frac{1}{M_*^2 R_i} \quad , \quad \lambda_I \leftrightarrow \frac{\lambda_I}{M_*^2 R_i} \ , \tag{2.14}$$

where R_i is the radius of compactification of the two-torus T_i, M_* is the string scale, and λ_I is the 10d dilaton that controls the type I string coupling. So T-dualising a pair of compact dimensions will interchange Neumann and Dirichlet boundary conditions, thus Dp-branes will become D$(p \pm 2)$-branes.

Heterotic string models have a string scale that is fixed close to the Planck scale, independent of the compactification radii, by the relation $M_* = \sqrt{\alpha_{\rm GUT}/8}\, M_{\rm Pl}$, with $\alpha_{\rm GUT} \approx 1/24$. The fundamental string scale of type I models can, however, take a range of values, which makes these models phenomenologically more appealing. By dimensionally reducing the effective 10d Lagrangian, we can extract expressions for the Planck mass and D-brane gauge couplings in terms of the compactification scales

[12] Instead of just the subscript i, one sometimes uses the subscript 5_i for clarity, thus $R_i \equiv R_{5_i}$, and similarly for gauge couplings associated with the D5$_i$-branes.

[13] The tadpole cancellation conditions can be modified by the presence of a background $B_{\mu\nu}$ field or non-trivial Wilson lines, which reduce the rank of the gauge group since fewer D-branes are required to cancel the tadpoles.

$M_i = 1/R_i$ and the string scale M_* [22, 46].

$$G_N = \frac{1}{M_{\rm Pl}^2} = \frac{\lambda_I^2 M_1^2 M_2^2 M_3^2}{8 M_*^8} , \tag{2.15}$$

$$\alpha_{5_i} = \frac{\lambda_I M_i^2}{2 M_*^2} , \tag{2.16}$$

$$\alpha_9 = \frac{\lambda_I M_1^2 M_2^2 M_3^2}{2 M_*^6} , \tag{2.17}$$

where $\alpha_{5_i(9)} = g_{5_i(9)}^2/4\pi$ and $\lambda_I \leq \mathcal{O}(1)$ to remain perturbative. This explicit dependence of type I models on the size and shape of the compactification manifold gives the string scale its freedom of 1 TeV $\lesssim M_* \lesssim M_{\rm Pl}$. Of particular interest is the exciting possibility of large extra dimensions that type I string theory offers. These could yield quantum gravity effects that might, in principle, be accessible to the next generation of accelerators.

We now consider the open and closed string states that arise in generic constructions involving stacks of coincident D9-branes and up to three types of D5_i-branes, ($i = 1, 2, 3$). Recall that a D9-brane fills the entire 10d spacetime ($x_0 - x_9$), while a D5_i-brane spans the Minkowski spacetime ($x_0 - x_3$), plus the two extra compact dimensions that wrap around the two-torus T_i^2. We represent the 6d compact space on the six-torus T^6 using a complex 3d coordinate system z_i, where each of the complex coordinates corresponds to a pair of compact dimensions, as detailed in Eq. (2.13). Therefore, in this system a stack of coincident D5_i-branes is represented by a single line along the i^{th} coordinate. This is depicted in Figure 2.2 where we have two separate stacks of D5_i-branes that overlap at the origin (the intersection, ($x_0 - x_3$)), but have world-volumes that extend along different pairs of compact dimensions.

Closed string chiral singlets and charged open string states are the two types of massless $\mathcal{N} = 1$ chiral fields that arise in type I string models:

- **Closed string chiral singlets**

The scalar excitations of closed string states gives rise to chiral singlets. These include a complex 4d dilaton S and untwisted moduli fields T_i, $(i = 1, 2, 3)$, that are allowed to move freely throughout the entire 10d spacetime.[14] The sizes of the compactified dimensions are parameterised by the VEVs of the untwisted moduli, where the radius of compactification for the i^{th} two-torus T_i^2 is given by [22]

$$R_i = \frac{\sqrt{T_i + \overline{T_i}}}{2M_*} \,. \tag{2.18}$$

In models of type I string theory, the gauge coupling corresponding to a stack of D-branes is related to either the dilaton or the untwisted moduli – S for the D9-branes and T_i for the D5$_i$-branes. Using an orientifold to compactify the 10d theory leads to fixed point singularities of the orientifold group. Closed string states that have been trapped at these fixed points are known as *twisted* moduli fields Y_k, and they parameterise the size of the fixed point singularities. Twisted states can contribute to SUSY breaking and modify the brane gauge coupling relations.

- **Charged open string states**

Chiral matter, Higgs fields, and gauge bosons arise as open strings attached to D-branes. Open strings have two ends which can be localised on either the *same* brane (denoted by $C_j^{5_i}$ or C_j^9 for example), or *different* branes (denoted by $C^{5_i 5_j}$ or C^{95_i} for example). Notice that the former carry an additional index that details the winding direction and can constrain the form of the renormalisable superpotential. The latter are also known as intersection states, as they span the intersection between the two branes to which they are attached, and carry charges under the gauge groups of both D-branes.

[14] Do not confuse the two-torus T_i^2 with the untwisted moduli T_i.

The most general set-ups involving three types of $D5_i$-brane and a D9-brane are governed by string selection rules that constrain the allowed combinations of open string states that can appear in the renormalisable superpotential [22].

$$\begin{aligned} W &= g_9 \left(C_1^9 C_2^9 C_3^9 + C_1^9 C^{95_1} C^{95_1} + C_2^9 C^{95_2} C^{95_2} \right) \\ &\quad + g_{5_1} \left(C_1^{5_1} C_2^{5_1} C_3^{5_1} + C_3^{5_1} C^{5_1 5_2} C^{5_1 5_2} + C_1^{5_1} C^{95_1} C^{95_1} \right) \\ &\quad + g_{5_2} \left(C_1^{5_2} C_2^{5_2} C_3^{5_2} + C_3^{5_2} C^{5_1 5_2} C^{5_1 5_2} + C_2^{5_2} C^{95_2} C^{95_2} \right) \\ &\quad + g_{5_3} C^{5_1 5_2} C^{95_1} C^{95_2} \ , \end{aligned} \tag{2.19}$$

where the Yukawa coupling constants associated with fields arising from the D9-brane and each $D5_i$-brane are given by [22]

$$g_{5_i}^2 = \frac{4\pi}{\Re T_i} \quad , \quad g_9^2 = \frac{4\pi}{\Re S} \ . \tag{2.20}$$

We shall now use the information presented thus far to outline a particular model upon which the work in this thesis is based.

2.4 The Pati-Salam model

The aim of this section is to detail the properties of the supersymmetric Pati-Salam model [47] that arises in type I string constructions, amongst others.

The next step above electroweak theory is a unified theory, which unifies the left-handed quarks and leptons into left-handed 'doublets' above the scale of electroweak symmetry breaking. The first such model proposed was the non-supersymmetric Pati-Salam model [48], which attempts to embed the SM in a larger gauge group. It considers lepton flavour as the 'fourth colour' of quarks under a larger colour gauge group $SU(4)_c$, which undergoes spontaneous symmetry breaking at some very high energy scale. Thus leptons and quarks are united within the same multiplets of this gauge

group, as required, and right-handed neutrino fields arise naturally. So this model predicts neutrino masses and we can form a full right-handed representation without an *ad hoc* introduction of right-handed neutrino fields. The gauge group of the Pati-Salam model is

$$G_{\rm PS} = SU(4)_c \otimes SU(2)_L \otimes SU(2)_R \ . \tag{2.21}$$

Under $G_{\rm PS}$, the left-handed matter F transforms non-trivially under $SU(4)_c$ and $SU(2)_L$, whilst the right-handed matter $\overline{F}$ transforms non-trivially under $SU(4)_c$ and $SU(2)_R$. The following representations detail this:

$$F^i_{\alpha,a} = (\mathbf{4},\mathbf{2},\mathbf{1}) = \begin{pmatrix} u_{L,R} & u_{L,G} & u_{L,B} & \nu \\ d_{L,R} & d_{L,G} & d_{L,B} & e_L \end{pmatrix}^i \tag{2.22}$$

$$\overline{F}^{i\,\alpha,x} = (\overline{\mathbf{4}},\mathbf{1},\mathbf{2}) = \begin{pmatrix} \overline{d}_{R,R} & \overline{d}_{R,G} & \overline{d}_{R,B} & \overline{e}_R \\ \overline{u}_{R,R} & \overline{u}_{R,G} & \overline{u}_{R,B} & N \end{pmatrix}^i \ . \tag{2.23}$$

Note that the index i denotes the generation of matter, the first subscript describes the handedness (L,R), and the second subscript details the colour (Red, Green, Blue, and lepton flavour as the fourth colour). As it is our intention to explore the supersymmetric version of the Pati-Salam model, the right-handed field degrees of freedom have already been CP-conjugated to obtain left-handed fields in order to construct a holomorphic superpotential.

The SM (MSSM) Higgs doublet field(s) must transform as $(\mathbf{1},\mathbf{2},\mathbf{2})$ under $G_{\rm PS}$ for the non-SUSY (SUSY) Pati-Salam model, in order to allow gauge singlet Yukawa terms. Thus

$$h = (\mathbf{1},\mathbf{2},\mathbf{2}) = \begin{pmatrix} h_u^+ & h_d^0 \\ h_u^0 & h_d^- \end{pmatrix} \ . \tag{2.24}$$

To suppress operators that break baryon and lepton number by converting quarks into leptons, this gauge group must be broken at a very high energy scale. In order to

spontaneously break $G_{\rm PS}$, we introduce a new set of 'heavy' Higgs fields $H, \overline{H}$, which gain VEVs that break the Pati-Salam gauge symmetry down to the SM, $G_{\rm PS} \to G_{\rm SM}$.

$$H = (4,1,\mathbf{2}) = \begin{pmatrix} H_{u_R} & H_{u_G} & H_{u_B} & H_\nu \\ H_{d_R} & H_{d_G} & H_{d_B} & H_e \end{pmatrix} \tag{2.25}$$

$$\overline{H} = (\overline{4},1,\mathbf{2}) = \begin{pmatrix} \overline{H}_{d_R} & \overline{H}_{d_G} & \overline{H}_{d_B} & \overline{H}_e \\ \overline{H}_{u_R} & \overline{H}_{u_G} & \overline{H}_{u_B} & \overline{H}_N \end{pmatrix} . \tag{2.26}$$

It is an unfortunate quality of the notation for H that requires H_2 to describe the first row (up-type) and H_1 to describe the second row (down-type). The 'neutrino' components of these heavy Higgs fields develop VEVs around the GUT scale $M_{\rm GUT}$,

$$\langle H_{\alpha,a} \rangle = v_H \delta^4_\alpha \delta^2_a \quad , \quad \langle \overline{H}_{\alpha,x} \rangle = v_{\overline{H}} \delta^4_\alpha \delta^2_x \ . \tag{2.27}$$

In breaking $G_{\rm PS}$ to the Standard Model gauge group, $SU(4)_c$ contains $SU(3)_c$, and the hypercharge $U(1)_Y$ is a linear combination of the residual $U(1)$ subgroups in $SU(4)_c \otimes SU(2)_R$. Even though both $U(1)$ subgroups are broken, and $B-L$, which is a generator of $SU(4)_c$, is broken when $G_{\rm PS}$ breaks, the linear combination of these that makes up the hypercharge remains unbroken:

$$\frac{Y}{2} = I_{3R} + \frac{1}{2}(B-L) \ . \tag{2.28}$$

This symmetry breaking splits the Higgs bi-doublet apart into the two MSSM Higgs doublets. The left-handed matter representation is also split, and it becomes the left-handed quark and lepton doublets. The right-handed representation is similarly broken into the up quark, down quark, electron, and neutrino fields.

Analogously to the discussion of the Higgs mechanism in Section 1.2, the gauge bosons corresponding to the broken generators of the Pati-Salam model become massive, while the gauge bosons of the unbroken (now SM) generators remain massless. Diagonalising the mass matrices yields the following massive gauge bosons:

- 1 $U(1)_{B-L}$ boson with mass squared $(v_H^2 + v_{\overline{H}}^2)(g_{2R}^2/4 + 3g_4^2/8)$,
- 2 $SU(2)_R$ bosons with mass squared $(v_H^2 + v_{\overline{H}}^2)g_{2R}^2/4$,
- 6 $SU(4)$ bosons with mass squared $(v_H^2 + v_{\overline{H}}^2)g_4^2/4$,

where g_4 and g_{2R} are the gauge couplings for $SU(4)_c$ and $SU(2)_R$ respectively. They are related to the hypercharge coupling g' via

$$\frac{1}{g'^2} = \frac{1}{g_{2R}^2} + \frac{2}{3g_4^2} \ . \tag{2.29}$$

Right-handed Majorana mass terms can also be generated at non-renormalisable order,

$$O_N = \overline{F}\overline{F}\frac{\overline{H}\overline{H}}{M_X} \ , \tag{2.30}$$

where M_X is the scale at which the symmetry is broken.

Due to the structure of the VEVs, Majorana mass terms like that above are only generated for the right-handed neutrinos. In the supersymmetric version of the Pati-Salam model, such right-handed masses are generated at almost exactly the correct order of magnitude necessary to make the see-saw mechanism work without the need for fine tuning. So the SUSY Pati-Salam model not only predicts neutrino masses, but it delivers them at the correct order of magnitude too.

One could indeed further the unification process by amalgamating everything into a single multiplet under a larger group, such as $SO(10)$, with a single gauge coupling. This, however, causes certain technical problems, such as predicting experimentally viable proton decay rates and the 'doublet-triplet' splitting problem. The problem of doublet-triplet splitting arises when the Higgs representations become unified. In order for Higgs-mediated proton decay to be sufficiently suppressed, the colour triplet part of the Higgs fields must go super-heavy, whilst the electroweak doublet part must retain a

mass at the electroweak scale. A fundamental Pati-Salam model does not have to deal with these problems.

2.5 A string Pati-Salam model

We now draw on the knowledge attained so far in this chapter to unite the ideas of string theory and the Pati-Salam model. We will discuss a string model for which the supersymmetric Pati-Salam model discussed in Section 2.4 becomes the appropriate effective field theory when the super-heavy exotic states are integrated out. We will summarise the relevant parts of this model, and explore both the model building aspects [49] and the string theoretical details [50].

The model we consider is a type I string model with two intersecting stacks of D5-branes named the 5_1-brane and 5_2-brane. The gauge group on each 5_i-brane in the full string model is $U(4)^{(i)} \otimes U(2)_a \otimes U(2)_b$. We consider the gauge group on the 5_2-brane to have been broken to $U(4)^{(2)}$, where the superscript index in parentheses indicates which brane this gauge group is associated with. So to achieve the correct model, the gauge group on the 5_1-brane must be $U(4)^{(1)} \otimes U(2)_L \otimes U(2)_R$. This set-up is presented in Figure 2.3.

Table 2.1 details the group representations of the field content, where F_i is the i^{th} generation of left-handed matter, $\overline{F}_j$ is the j^{th} generation of right-handed matter, h denotes the MSSM Higgs, and $H, \overline{H}$ are the Higgs fields responsible for breaking $SU(4) \otimes SU(2) \otimes SU(2) \rightarrow SU(3) \otimes SU(2) \otimes U(1)$. Thus the gauge symmetry of the model is $SU(4)^{(2)} \otimes SU(4)^{(1)} \otimes SU(2)_L \otimes SU(2)_R \otimes U(1)^4$. Note that the third matter family arises purely from the 5_1 sector, whereas the first two matter families are localised at the intersection.

The work of Shiu and Tye [50] gives us the gauge symmetry breaking pattern for

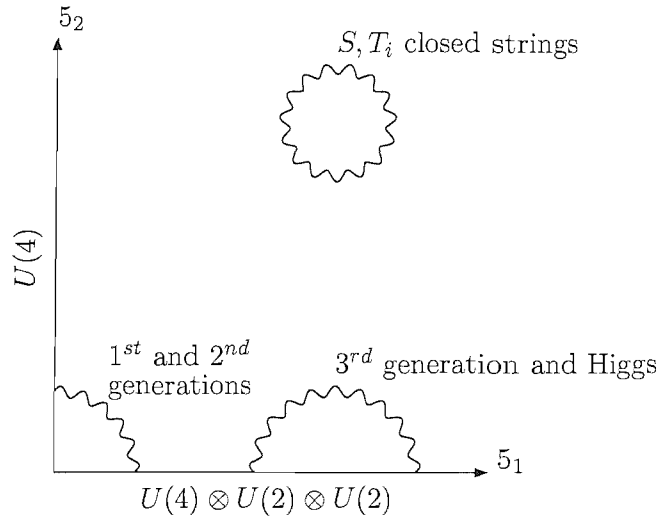

Figure 2.3: Brane set-up of the '4224' model. The first and second generations of matter are localised at the origin as $C^{5_1 5_2}$ intersection states; the third generation, Pati-Salam, and electroweak breaking Higgs fields arise as $C_i^{5_1}$ states; the dilaton and moduli closed strings are free to move throughout the bulk.

Field	$SU(4)^{(1)}$	$SU(2)_L$	$SU(2)_R$	$SU(4)^{(2)}$	$Q_4^{(1)}$	Q_{2L}	Q_{2R}	$Q_4^{(2)}$	Brane assignment
h	1	2	2	1	0	1	-1	0	$C_1^{5_1}$
F_3	4	2	1	1	1	-1	0	0	$C_2^{5_1}$
$\overline{F}_3$	$\overline{4}$	1	2	1	-1	0	1	0	$C_3^{5_1}$
$F_{1,2}$	1	2	1	4	0	-1	0	1	$C^{5_1 5_2}$
$\overline{F}_{1,2}$	1	1	2	$\overline{4}$	0	0	1	-1	$C^{5_1 5_2}$
H	4	1	2	1	1	0	-1	0	$C_1^{5_1}$
$\overline{H}$	$\overline{4}$	1	2	1	-1	0	1	0	$C_2^{5_1}$
φ_1	4	1	1	$\overline{4}$	1	0	0	-1	$C^{5_1 5_2}$
φ_2	$\overline{4}$	1	1	4	-1	0	0	1	$C^{5_1 5_2}$
$D_6^{(+)}$	6	1	1	1	2	0	0	0	$C_1^{5_1}$
$D_6^{(-)}$	6	1	1	1	-2	0	0	0	$C_2^{5_1}$

Table 2.1: The particle content of the '4224' string Pati-Salam model. We have used the isomorphism $U(N_a) = U(1)_a \otimes SU(N_a)$ to write each $U(N_a)$ representation as a $U(1)_a$ charge and an $SU(N_a)$ representation.

three families. This approach considers two stages to the symmetry breaking, which are assumed to occur close to the unification scale M_U. The first stage is controlled by the VEVs of the Higgs bifundamentals φ_1, φ_2, which act, as the name suggests, in the fundamental representation of the gauge groups of both D5-branes. This stage breaks $U(4)^{(1)} \otimes U(4)^{(2)}$ to the diagonal $U(4)$ subgroup identified as $U(4)_c$, which is the part of the Pati-Salam model that takes lepton flavour as a fourth quark colour. The resulting theory is a Pati-Salam group enhanced by three anomalous $U(1)$ symmetries that are expected to decouple before the second stage of breaking.

The second stage is where the Pati-Salam Higgs fields $H, \overline{H}$, are used to break the Pati-Salam group down to the MSSM group. The breaking should occur along 'flat' directions in order to preserve supersymmetry; D-flatness should only be spoilt by terms of the order of the soft parameters. The symmetry breaking pattern is thus

$$\begin{aligned} U(4)^{(2)} \otimes U(4)^{(1)} \otimes U(2)_L \otimes U(2)_R &\xrightarrow{\langle \varphi_{1,2} \rangle} U(4)_c \otimes U(2)_L \otimes U(2)_R \\ &\xrightarrow{\langle H, \overline{H} \rangle} SU(3)_c \otimes SU(2)_L \otimes U(1)_Y \otimes U(1)^3 \ . \end{aligned} \tag{2.31}$$

Simultaneously requiring (approximate) D-flatness and diagonal symmetry breaking gives us the VEVs of the bifundamental Higgs fields,

$$\langle (\varphi_1)_{a\alpha} \rangle = \delta_{a\alpha} v_1 \qquad , \qquad \langle (\varphi_2)_{a\alpha} \rangle = \delta_{a\alpha} v_2 \ , \tag{2.32}$$

where a denotes the $U(4)^{(2)}$ gauge index, and α denotes that of $U(4)^{(1)}$.

However, there now exist a number of combinations that are overall colour triplets, which could lead to a high rate of proton decay. In order to reduce the proton decay rate to an acceptable level, the colour sextet fields $D_6^{(\pm)}$, give these triplets super-heavy mass terms. [49] presents further details on this topic, which is beyond the scope of this thesis.

2.5.1 MSSM couplings

The string model gives us a predictive insight into the MSSM, which is the appropriate effective field theory below the GUT scale of $M_U \approx 10^{16}\,\mathrm{GeV}$. We can make quantitative statements about how the couplings in the MSSM relate to the couplings of the D5-branes. There are two string couplings, one associated with each 5_i-brane, whereas in the MSSM, there are three couplings, one associated with each symmetry group. These are related as follows [49]:

$$\begin{aligned} g_3 &= \frac{g_{5_1} g_{5_2}}{\sqrt{g_{5_1}^2 + g_{5_2}^2}} \\ g_2 &= g_{5_1} \\ g_1 &= \frac{\sqrt{3} g_{5_1} g_{5_2}}{\sqrt{2 g_{5_1}^2 + 5 g_{5_2}^2}} \,. \end{aligned} \tag{2.33}$$

Eq. (2.33) applies at the string scale $M_* \sim 10^{16} GeV$, and $g_1 = \sqrt{\frac{3}{5}}$.

We now consider the Yukawa couplings. We have chosen the string assignments to allow only a third family-Higgs Yukawa coupling. In Eq. (2.19), we see that the term $C_1^{5_1} C_2^{5_1} C_3^{5_1}$ is allowed, yielding an $\mathcal{O}(1)$ Yukawa coupling to $F_3 \overline{F}_3 h$. The terms that would give $Y_{ij}\,, Y_{i3}$ and Y_{3i} for $(i, j = \{1, 2\})$, however, do not appear, so the form of the superpotential and the string assignments in Table 2.1 limit the Yukawa textures to allow only the $(3, 3)$ element at renormalisable order. The model predicts third family Yukawa unification, and therefore required large $\tan\beta \approx 50$ to ensure the correct m_t/m_b ratio.

Non-renormalisable operators are responsible for the small (non-zero) values of the first and second generation Yukawa couplings, as well as the right-handed Majorana mass matrix. These elements could be generated by operators of the form $F_i \overline{F}_j h(H\overline{H}^n)$ [51], by Froggatt-Nielsen operators for models extended by a family symmetry, or by a combination of the two approaches [52].

The soft couplings can be written down in the phenomenological manner of [53] using just a few Goldstino parameters. We make the usual assumption that the auxiliary fields of the moduli make the dominant contribution to the soft terms over the subdominant auxiliary members of the Higgs superfields $\varphi_i, H, \overline{H}$. This is not necessarily true for the soft trilinears A_{ijk} [21]. We begin with a parameterisation of the auxiliary fields, then use expressions in Section 2.2 to obtain the gaugino soft masses, the scalar soft masses, and the trilinear soft couplings for the MSSM in terms of the Goldstino parameters X_α, and the gravitino mass $m_{3/2}$. Thus the auxiliary fields of the dilaton S and moduli T_i are

$$F^S = \sqrt{3}(S+S^*)m_{3/2}X_S\, e^{i\alpha_S} \tag{2.34}$$

$$F^{T_i} = \sqrt{3}(T_i+T_i^*)m_{3/2}X_{T_i}\, e^{i\alpha_{T_i}} \ . \tag{2.35}$$

The Goldstino parameters sum square to unity within a set[15],

$$\sum_i X_{T_i}^2 = 1 \ , \tag{2.36}$$

and in general the auxiliary fields can have arbitrary phases α_S, α_{T_i}. The masses of the 4224 gauginos are then

$$m_4^{(1)} = m_{2L} = m_{2R} = \sqrt{3}m_{3/2}X_{T_1}\, e^{-i\alpha_{T_1}} \tag{2.37}$$

$$m_4^{(2)} = \sqrt{3}m_{3/2}X_{T_2}\, e^{-i\alpha_{T_2}} \ . \tag{2.38}$$

[15]The Goldstino parameter for the dilaton is in a set of its own, but the three moduli controlling Goldstino parameters are in a set together.

This provides us with the following MSSM gaugino masses:

$$m_3 = \frac{\sqrt{3}m_{3/2}}{(T_1+T_1^*)+(T_2+T_2^*)}\Big[(T_1+T_1^*)X_{T_1}\,e^{-i\alpha_{T_1}} + (T_2+T_2^*)X_{T_2}\,e^{-i\alpha_{T_2}}\Big] \tag{2.39}$$

$$m_2 = \sqrt{3}m_{3/2}X_{T_1}\,e^{-i\alpha_{T_1}} \tag{2.40}$$

$$m_1 = \frac{\sqrt{3}m_{3/2}}{\frac{5}{3}(T_1+T_1^*)+\frac{2}{3}(T_2+T_2^*)}\left[\frac{5}{3}(T_1+T_1^*)X_{T_1}\,e^{-i\alpha_{T_1}} + \frac{2}{3}(T_2+T_2^*)X_{T_2}\,e^{-i\alpha_{T_2}}\right]. \tag{2.41}$$

The scalar masses are solely dependent on their string assignments, so using Table 2.1 and Eqs. (2.9), (2.12), and (4.14) - (4.18), they can be written down as [49]

$$m_h^2 = m_{H_u}^2 = m_{H_d}^2 = m_{3/2}^2(1-3X_S^2) \tag{2.42}$$

$$m_{Q_3}^2 = m_{L_3}^2 = m_{3/2}^2(1-3X_{T_3}^2) \tag{2.43}$$

$$m_{U_3}^2 = m_{D_3}^2 = m_{E_3}^2 = m_{N_3}^2 = m_{3/2}^2(1-3X_{T_2}^2) \tag{2.44}$$

$$m_{Q_{1,2}}^2 = m_{L_{1,2}}^2 = m_{3/2}^2\Big(1-\frac{3}{2}(X_S^2+X_{T_3}^2)\Big) \tag{2.45}$$

$$m_{U_{1,2}}^2 = m_{D_{1,2}}^2 = m_{E_{1,2}}^2 = m_{N_{1,2}}^2 = m_{3/2}^2\Big(1-\frac{3}{2}(X_S^2+X_{T_3}^2)\Big). \tag{2.46}$$

The trilinear parameters $\tilde{A}_{ij}$ can then be written down in terms of A_{ij} and the Yukawa couplings Y_{ij} as a matrix

$$\tilde{A}_{ij} = \begin{bmatrix} d_1Y_{11} & d_1Y_{12} & d_2Y_{13} \\ d_1Y_{21} & d_1Y_{22} & d_2Y_{23} \\ d_3Y_{31} & d_3Y_{32} & d_4Y_{33} \end{bmatrix}, \tag{2.47}$$

where the d_i are defined as

$$d_1 = \sqrt{3}m_{3/2}\left(X_S\,e^{-i\alpha_S} - X_{T_1}\,e^{-i\alpha_{T_1}} - X_{T_2}\,e^{-i\alpha_{T_2}}\right) \tag{2.48}$$

$$d_2 = \sqrt{3}m_{3/2}\left(\frac{1}{2}X_S\,e^{-i\alpha_S} - X_{T_1}\,e^{-i\alpha_{T_1}} - \frac{1}{2}X_{T_3}\,e^{-i\alpha_{T_3}}\right) \tag{2.49}$$

$$d_3 = \sqrt{3}m_{3/2}\left(\frac{1}{2}X_S\,e^{-i\alpha_S} - X_{T_1}\,e^{-i\alpha_{T_1}} - X_{T_2}\,e^{-i\alpha_{T_2}} + \frac{1}{2}X_{T_3}\,e^{-i\alpha_{T_3}}\right) \tag{2.50}$$

$$d_4 = -\sqrt{3}m_{3/2}X_{T_1}\,e^{-i\alpha_{T_1}}. \tag{2.51}$$

The μ term in the MSSM is disallowed by the string-derived superpotential. The μ and $B\mu$ terms must be generated in the effective theory, such as by the Giudice-Masiero mechanism [19], but this is dependent on the model considered, and we shall not consider it further. Their magnitudes will, however, be set by the requirements of radiative electroweak symmetry breaking.

Chapter 3

Abelian Family Symmetry and Yukawa Operators

3.1 Preamble

This chapter aims to build on the knowledge attained in Chapters 1 and 2, detailing the Abelian family symmetry that augments the string Pati-Salam model, how to obtain the $U(1)_F$ charge structure, and how to derive the D-terms that arise upon the spontaneous breaking of this $U(1)_F$ symmetry. We also discuss the specific Yukawa and Majorana operator structures that we use to explore the parameter space, and find that the rates of LFV processes are sensitive to specific Yukawa elements being turned on from zero. We shall begin by outlining the specific model that we are using here.

3.2 A string Pati-Salam model with an Abelian family symmetry

In order to study the effects of lepton flavour violation it is necessary to specialise to a particular effective non-minimal SUGRA model which addresses the question of flavour (i.e. provides a theory of the Yukawa couplings). The specific model we shall discuss is defined in Table 3.1. This model is an extension of the Supersymmetric Pati-Salam model discussed in [49], based on two D5-branes which intersect at 90 degrees and preserve SUSY down to the TeV energy scale.

3.2.1 Symmetries and symmetry breaking

The generic D-brane set-up that we use is illustrated in Figure 2.3, where the string assignment notation is defined. The gauge group of the 5_1 sector is $U(4)^{(1)} \times U(2)_L^{(1)} \times U(2)_R^{(1)}$, and the gauge group of the 5_2 sector is $U(4)^{(2)}$ (e.g., we assume the $U(2)_{L,R}$ of the 5_2 sector are broken). The symmetry breaking pattern of this model takes place in two stages, which we assume occur at very similar scales $\sim M_X$. In the first stage, the $U(4)$ groups are broken to the diagonal subgroup via diagonal VEVs of bifundamentals; the resulting theory is an effective Pati-Salam model (with additional $U(1)$'s) which then breaks to the MSSM (and a number of additional $U(1)'s$) via the usual Higgs pair of bifundamentals. The string scale is taken to be equal to the GUT scale, about 3×10^{16} GeV.

The symmetry breaking pattern leads to the following relations among the gauge couplings of the SM gauge groups in terms of the gauge couplings g_{5_1} and g_{5_2} associated

with the gauge groups of the 5_1 and 5_2 sectors [49], as in Eqs. (2.33):

$$g_3 = \frac{g_{5_1} g_{5_2}}{\sqrt{g_{5_1}^2 + g_{5_2}^2}} = g_4 \ , \tag{3.1}$$

$$g_2 = g_{5_1} = g_{2R} \ , \tag{3.2}$$

$$g_Y = \frac{\sqrt{3} g_3 g_2}{\sqrt{3 g_3^2 + 2 g_2^2}} \ . \tag{3.3}$$

The extension is to include an additional $U(1)_F$ family symmetry and the Froggatt-Nielsen (FN) operators as in [52] (see also [51]). The charges under the Abelian symmetry $U(1)_F$ are left arbitrary for now. The present '42241' model is the same as the model considered in [54], with the following modifications considered; firstly, we allow the Froggatt-Nielsen field $\overline{\theta}$ to be either an intersection state or attached to the 5_1 brane. The location of $\overline{\theta}$ dramatically changes the value of the D-term contribution to the scalar masses coming from the FN sector as we shall see in Section 4.3.4.

The quark and lepton fields are contained in the representations $F, \overline{F}$ which are assigned charges under the $U(1)_F$ symmetry. In Table 3.1 we list the $U(1)_F$ charges, string assignments and representations under the string gauge group $U(4)^{(1)} \otimes U(2)_L \otimes U(2)_R \otimes U(4)^{(2)}$.

The field h represents both Electroweak Higgs doublets that we are familiar with from the MSSM. The fields H and $\overline{H}$ are the Pati-Salam Higgs scalars,[1] the bar on the second is used to note that it is in the conjugate representation compared to the unbarred field.

The extra Abelian $U(1)_F$ gauge group is a family symmetry, and is broken at the high energy scale by the VEVs of the FN fields [17] $\theta, \overline{\theta}$, which have charges -1 and $+1$ respectively under $U(1)_F$. We assume that the singlet field θ arises as an intersection state between the two D5-branes, transforming under the remnant $U(1)$s in the 4224

[1] We will also refer to these as "heavy Higgs" fields – this has nothing to do with the MSSM heavy neutral Higgs state H^0.

Field	$SU(4)^{(1)}$	$SU(2)_L$	$SU(2)_R$	$SU(4)^{(2)}$	Ends	$U(1)_F$ charge
h	1	2	2	1	$C_1^{5_1}$	0
F_3	4	2	1	1	$C_2^{5_1}$	q_{L3}
$\overline{F}_3$	$\overline{4}$	1	2	1	$C_3^{5_1}$	q_{R3}
F_2	1	2	1	4	$C^{5_1 5_2}$	q_{L2}
$\overline{F}_2$	1	1	2	$\overline{4}$	$C^{5_1 5_2}$	q_{R2}
F_1	1	2	1	4	$C^{5_1 5_2}$	q_{L1}
$\overline{F}_1$	1	1	2	$\overline{4}$	$C^{5_1 5_2}$	q_{R1}
H	4	1	2	1	$C_1^{5_1}$	q_H
$\overline{H}$	$\overline{4}$	1	2	1	$C_2^{5_1}$	$-q_H$
φ_1	4	1	1	$\overline{4}$	$C^{5_1 5_2}$	–
φ_2	$\overline{4}$	1	1	4	$C^{5_1 5_2}$	–
$D_6^{(+)}$	6	1	1	1	$C_1^{5_1}$	–
$D_6^{(-)}$	6	1	1	1	$C_2^{5_2}$	–
θ	1	1	1	1	$C^{5_1 5_2}$	-1
$\overline{\theta}$	1	1	1	1	All	1

Table 3.1: The particle content of the 42241 model and the brane assignments of the corresponding string. Note that the string assignment of $\overline{\theta}$ is allowed to be any of $\{C^{5_1 5_2}, C_1^{5_1}, C_2^{5_1}, C_3^{5_1}\}$, giving a slightly different model in each case. Different values for the $U(1)_F$ family charges are explored in this chapter and the next, which also generate different models for each case. We will return to this in more detail in Sections 3.5.1 and 3.5.2.

gauge structure. In general the FN fields are expected to have non-zero F-term VEVs.

The two $SU(4)$ gauge groups are broken to their diagonal subgroup at a high scale due to the assumed VEVs of the bifundamental Higgs fields φ_1, φ_2 [49]. The symmetry breaking at the scale M_X,

$$\mathrm{SU}(4) \otimes \mathrm{SU}(2)_L \otimes \mathrm{SU}(2)_R \rightarrow \mathrm{SU}(3) \otimes \mathrm{SU}(2)_L \otimes \mathrm{U}(1)_Y \ , \tag{3.4}$$

is achieved by the heavy Higgs fields H, $\overline{H}$ which are assumed to gain VEVs [51]

$$\langle H^{\alpha b} \rangle = \langle \nu_H \rangle = V \delta_4^\alpha \delta_2^b \sim M_X \quad ; \quad \langle \overline{H}_{\alpha x} \rangle = \langle \overline{\nu}_H \rangle = \overline{V} \delta_\alpha^4 \delta_x^2 \sim M_X \ . \tag{3.5}$$

This symmetry breaking splits the Higgs field h into the two electroweak Higgs doublets h_1, h_2. Their neutral components then gain weak-scale VEVs,

$$\langle h_1^0 \rangle = v_1 \quad ; \quad \langle h_2^0 \rangle = v_2 \quad ; \quad \tan\beta = v_2/v_1 \ . \tag{3.6}$$

The low energy limit of this model contains the MSSM with right-handed neutrinos. We will return to the right-handed neutrinos when we consider operators in Section 3.5 including the heavy Higgs fields H, $\overline{H}$ which lead to effective Yukawa contributions and effective Majorana mass matrices when the heavy Higgs fields gain VEVs.

3.3 Anomalies and charge structures

If a classical symmetry of the Lagrangian of a theory is broken by the quantum corrections, then the theory is said to have an anomaly[2]. Discussions of anomalies and their cancellation can be found in [2] and [55]. We shall now discuss the anomalies that arise within the proposed model, and show the conditions necessary to cancel the anomalies, detailing how to generate the anomaly free charges that are associated with the $U(1)_F$ family symmetry.

[2]Many types of anomaly exist: chiral anomaly, gauge anomaly, gravitational anomaly, for example. Each one mentioned here refers to the symmetry that is not preserved if the anomalies persist.

3.3.1 Anomaly cancellation conditions

In a gauge theory in which gauge bosons couple to fermions in a chiral way, the one-loop corrections to the three-gauge-boson vertex function develop dangerous triangle diagrams. The Ward identity for this amplitude is violated by the anomalous terms. So only gauge theories in which the anomalous contribution somehow vanishes can be gauge invariant. Fortunately, one can arrange to cancel these anomalies when one sums over all possible fermion species that can circulate in these triangle diagrams. Working from the last stage of the symmetry breaking pattern shown in Eq. (2.31), the Feynman diagrams yielding anomalies that we can cancel are shown in Figure 3.1.

We assign an anomalous term A_n to each of these triangle diagrams, then these anomalous terms must combine in such a way as to cancel each other by satisfying Green-Schwarz [25] anomaly cancellation conditions:

$$A_3 = A_2 = \frac{3}{5} A_1 \ , \tag{3.7}$$

$$A_1' = 0 \ , \tag{3.8}$$

where A_1' must cancel on its own.

These anomaly coefficients are proportional to the trace over the generators of the gauge groups in the triangle,

$$A_n \propto \mathrm{tr}[\{t^a, t^b\} t^c] \ . \tag{3.9}$$

Other triangle diagrams that arise all cancel trivially, for instance the anomaly of three $SU(2)$ bosons is zero due to a special property of the Pauli sigma matrices

$$\{\sigma^a, \sigma^b\} = 2\delta^{ab} 1 \ , \tag{3.10}$$

which implies that the trace in Eq. (3.9) will vanish. The anomalies involving only one

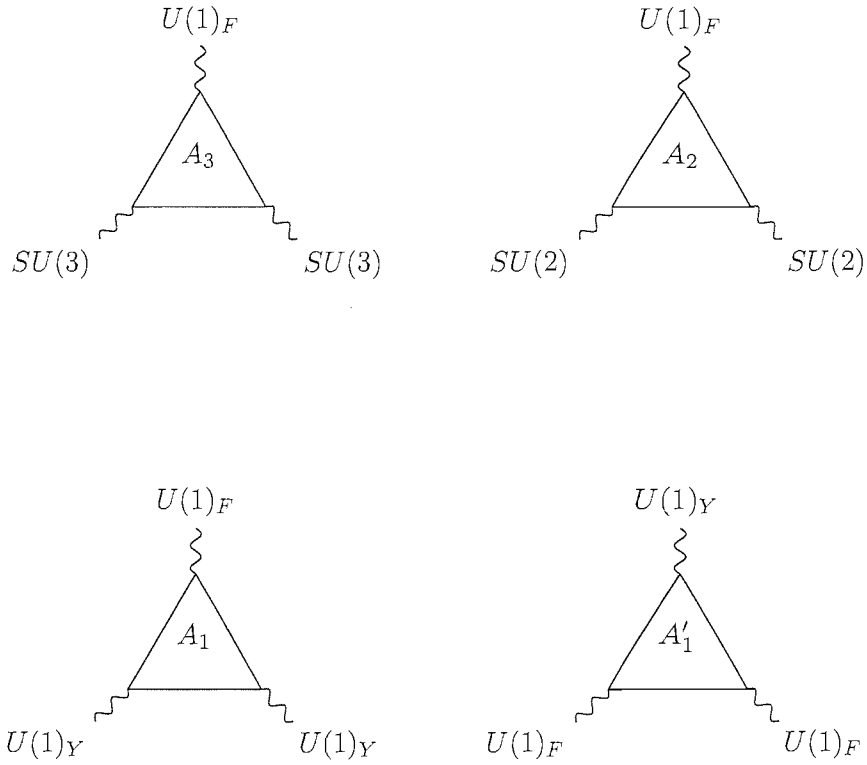

Figure 3.1: The triangle diagrams that we are interested in for this model, which cancel to allow gauge invariance as shown in [56]. The first three cancel each other, and the last one, A_1', must be zero.

Superfield	Q_i	u_i^c	d_i^c	L_i	e_i^c	ν_i^c	H_u	H_d
$U(1)_F$ symm.	q_i	u_i	d_i	l_i	e_i	n_i	h_u	h_d

Table 3.2: Notation used to denote the superfields as $U(1)_F$ symmetries for the purpose of anomaly cancellation. $i \in \{1,2,3\}$ is the family index, 3 indicating the heaviest generation.

$SU(2)$ or $SU(3)$ boson are proportional to

$$\mathrm{tr}[t^c] = 0 \ . \tag{3.11}$$

Now we must address the remaining non-trivial anomalies, shown in Figure 3.1. Group theory states that for vertices with two $SU(2)$ gauge bosons, the anticommutator in Eq. (3.9) is, from Eq. (3.10),

$$\{t^a, t^b\} = 2\delta^{ab}\mathbf{1} \ , \tag{3.12}$$

and for two $U(1)_Y$ bosons, the anticommutator becomes

$$\{t^Y, t^Y\} = 2Y^2\mathbf{1} \ . \tag{3.13}$$

Similarly we work out the anomaly coefficients using the formalism presented in [57], where the notation used for the fields is shown in Table 3.2,

$$A_3 = \frac{1}{2}\left[\sum_{i=1}^{3}(2q_i + u_i + d_i)\right] \ , \tag{3.14}$$

$$A_2 = \frac{1}{2}\left[\sum_{i=1}^{3}(3q_i + l_i) + h_u + h_d\right] \ , \tag{3.15}$$

$$\frac{3}{5}A_1 = \frac{1}{2}\left[\sum_{i=1}^{3}\left(\frac{1}{5}q_i + \frac{8}{5}u_i + \frac{2}{5}d_i + \frac{3}{5}l_i + \frac{6}{5}e_i\right) + \frac{3}{5}(h_u + h_d)\right] \ , \tag{3.16}$$

$$A_1' = \sum_{i=1}^{3}(q_i^2 - 2u_i^2 + d_i^2 - l_i^2 + e_i^2) + h_u^2 - h_d^2 \ . \tag{3.17}$$

These equations are brought together to satisfy the anomaly cancellation conditions in Eqs. (3.7) and (3.8). We rewrite the sums over the charges in terms of arbitrary

parameters, and require that these must satisfy the anomaly cancellation conditions when they are substituted into Eqs. (3.14) -- (3.17). These new definitions are[3]

$$\begin{aligned}
\sum q_i &= x+u\ , \\
\sum u_i &= x+2u\ , \\
\sum d_i &= y+v\ , \\
\sum l_i &= y\ , \\
\sum e_i &= x\ , \\
h_u &= -z\ , \\
h_d &= z+u+v\ .
\end{aligned} \tag{3.18}$$

We consider the case where $u = v = 0$ for simplicity, and using Eqs. (3.18), the anomaly coefficients become

$$A_3 = A_2 = \frac{3}{5}A_1 = \frac{3}{2}x + \frac{1}{2}y\ , \tag{3.19}$$

and

$$A_1' = 0\ . \tag{3.20}$$

So we see that the anomaly cancellation conditions, Eqs. (3.7) and (3.8) are satisfied.

From Eqs. (3.18), with $u = v = 0$, we see that the only case consistent with the Pati-Salam model is to set $x = y$. We shall follow [56] to show that this leads to an anomaly free Pati-Salam group realisation of the mass matrices.

3.3.2 Anomaly free Pati-Salam case

In this case, applying the Pati-Salam constraints on the charges (that $x = y$ in Eqs. (3.18)) so that the left-handed sector fields all have one charge for each gener-

[3]Right-handed neutrinos have no coupling to the bosons $U(1)_Y$, $SU(2)_L$, $SU(3)_c$. They are singlets under all Standard Model groups, so we do not consider them in Eqs. (3.18).

ation

$$q_i = l_i \equiv q_i^L \ , \tag{3.21}$$

and the right-handed sector fields all have another charge for each family

$$u_i = d_i = e_i = n_i \equiv q_i^R \ , \tag{3.22}$$

one can immediately see that the family dependent part of Eq. (3.17) vanishes. We note that these constraints, with Eqs. (3.18), demand that the sum of the left-handed charges is equal to the sum of the right-handed charges. We shall cover this in more detail in Section 3.3.3. We have also included the right-handed neutrino charges that do not enter into the anomaly cancellation conditions Eqs. (3.14) - (3.17), but with a Pati-Salam group they should obey the relation (3.22). Thus in this case all the mass matrices will have the form

$$Y^f \ = \ \begin{pmatrix} \epsilon^{|l_1+e_1+h_f|} & \epsilon^{|l_1+e_2+h_f|} & \epsilon^{|l_1+e_3+h_f|} \\ \epsilon^{|l_2+e_1+h_f|} & \epsilon^{|l_2+e_2+h_f|} & \epsilon^{|l_2+e_3+h_f|} \\ \epsilon^{|l_3+e_1+h_f|} & \epsilon^{|l_3+e_2+h_f|} & \epsilon^{|l_3+e_3+h_f|} \end{pmatrix} \ , \tag{3.23}$$

for $h_f = h_u, h_d$. As we always need to satisfy $x = y$ we can put one of the charges in terms of the other two and the parameters $x = y$

$$e_1 = x - (e_2 + e_3) \quad , \quad l_1 = x - (l_2 + l_3) \quad \Rightarrow \quad e_1 + e_2 + e_3 = l_1 + l_2 + l_3 \ . \tag{3.24}$$

Thus the sum of the right-handed charges equals the sum of the left-handed charges as mentioned above. We already noted that the Pati-Salam constraints on the charges imply that the anomaly A_1' automatically vanishes, and it is also a remarkable fact that the constraints in Eq. (3.24) do not, in practice, lead to any physical constraints on the form of the Yukawa texture in Eq. (3.23).

Family	L_A	R_A
1	1	4
2	0	2
3	0	0

Table 3.3: The anomalous charges for left- and right-handed fields of each generation for Model 1. The left-handed light scalar fields are q_i, l_i with their right-handed counter-parts $u_i^c, d_i^c, e_i^c, \nu_i^c$.

3.3.3 Anomalous and anomaly free charges

The D-terms associated with the family symmetry depend on the charges of the left-handed and right-handed matter representations $F, \overline{F}$ under the family symmetry. It is well known[4] that for Pati-Salam models, one can choose any set of charges, and there will be an equivalent, shifted set of charges that are anomaly free due to the Green-Schwarz anomaly cancellation mechanism. The charges used for the D-term calculation should be the anomaly free charges.

So starting with the anomalous charges for Model 1, Table 3.3, we apply an equal and opposite shift to the left- and right-handed charges such that we obtain the same number when we sum over the families of both the left- and right-handed charges. This shift is $+\frac{5}{6}$ for left-handed charges, and $-\frac{5}{6}$ for right-handed charges, resulting in our anomaly-free charges, Table 3.4. Both left- and right-handed charges sum to $\frac{21}{6}$.

We also define another set of anomalous charges for Model 2, Table 3.5 that should act to suppress the effects of the $(1-2)$ sector $U(1)_F$ derived lepton flavour changing currents, as the left-handed charges are now universal, and hence diminish the effects

[4]For an explanation, see for example [56].

Family	L_{AF}	R_{AF}
1	$\frac{11}{6}$	$\frac{19}{6}$
2	$\frac{5}{6}$	$\frac{7}{6}$
3	$\frac{5}{6}$	$-\frac{5}{6}$

Table 3.4: The anomaly free charges for left- and right-handed fields of each generation for Model 1.

Family	L'_A	R'_A
1	0	4
2	0	2
3	0	0

Table 3.5: The anomalous charges for left- and right-handed fields of each generation for Model 2.

of the left-handed sector D-terms. The anomaly free charges for this second model are found in the same way as before, where the shift to the left-handed charges is $+1$ and the shift to the right-handed charges is -1, which results in Table 3.6. Both left- and right-handed charges now sum to 3.

The $U(1)_F$ charge of H must be equal and opposite in sign to $\overline{F}_3$, and $\overline{H}$ must be the negative of H. This is due to the (3,3) element of the right-handed Majorana mass being allowed at renormalisable order, so the $U(1)_F$ charges of $\overline{F}_3$ and H must conspire to cancel for the operator of the Majorana fermions to be renormalisable.

So for Model 1 the $U(1)_F$ charges of H and $\overline{H}$ are $q_H = \frac{5}{6}$ and $q_{\overline{H}} = -\frac{5}{6}$, and for

Family	L'_{AF}	R'_{AF}
1	1	3
2	1	1
3	1	-1

Table 3.6: The anomaly free charges for left- and right-handed fields of each generation for Model 2.

Model 2 the $U(1)_F$ charges of H and $\overline{H}$ are $q_H = 1$ and $q_{\overline{H}} = -1$ respectively. One can use the relevant equations above to check that the anomaly coefficients do indeed satisfy the anomaly cancellation conditions. To put this in the context of D-terms, D_H^2 depends on q_H, so this gives us a different D_H-term for Models 1 and 2 (compare Eqs. (3.55) and (3.57) in Section 3.4), whereas D_θ^2 is the same for both models, as in Eq. (3.56).

3.4 Derivation of the D-terms

A spontaneously broken family symmetry can give large contributions to LFV processes via D-terms that arise when the gauge group is broken. This section delivers a full derivation of D_H and D_θ from the superpotential of the $U(1)_F$ extended supersymmetric Pati-Salam 42241 model, as detailed in Section 3.2.

The relevant parts of the superpotential for the 42241 model are those concerning the Higgs and Froggatt-Nielsen fields which have different gauge singlets S, S'.[5]

$$\Delta W = S\lambda_S(\overline{H}H - M_H^2) + S'\lambda_{S'}(\overline{\theta}\theta - M_\theta^2) \ , \tag{3.25}$$

[5]Note that these must still have the same quantum numbers as they are both singlets, and therefore in the same representation of the gauge group.

where the M_H and M_θ are GUT scale masses associated with the Higgs and Froggatt-Nielsen VEVs respectively. We have assumed that the heavy Higgs develop VEVs along the neutrino directions only, such that

$$\langle \overline{H} \rangle = \langle \overline{H}_\nu \rangle \quad ; \quad \langle H \rangle = \langle H_\nu \rangle \ . \tag{3.26}$$

This is because charged objects gaining VEVs would break their charge group at the GUT scale, causing problems[6] which the neutral components avoid. Similarly, the Froggatt-Nielsen VEVs are concisely written as

$$\langle \overline{\theta} \rangle \quad ; \quad \langle \theta \rangle \ . \tag{3.27}$$

The F-terms associated with the singlet fields are

$$|F_S|^2 = |\lambda_S(\overline{H}H - M_H^2)|^2 \ , \tag{3.28}$$

and

$$|F_{S'}|^2 = |\lambda_{S'}(\overline{\theta}\theta - M_\theta^2)|^2 \ . \tag{3.29}$$

We use these to form our Higgs potential,

$$V_H = V_D + V_F + V_{\text{soft}} \ . \tag{3.30}$$

The F-term potential is trivially obtained from Eqs. (3.28) and (3.29), and the soft terms are simply written down with mass-squared terms for each of the soft SUSY breaking scalar masses associated with the Higgs and FN VEVs, as we will later see. The D-term potential takes a little more work, so we shall cover that here. The general form for the D-term potential is

$$V_D = \frac{1}{2} g_F^2 D_F^1 D_F^1 + \frac{1}{2} g_{2R}^2 \sum_{a=1}^{3} D_{2R}^a D_{2R}^a + \frac{1}{2} g_4^2 \sum_{m=1}^{15} D_4^m D_4^m \ , \tag{3.31}$$

[6] A colour charged object, for example, would imply that QCD is broken at the GUT scale, which would lead to a very massive gluon.

where g_F is the gauge coupling for $U(1)_F$, g_{2R} is for $SU(2)_R$, and g_4 is for $SU(4)_c$.

We focus on the $a = 3$ and $m = 15$ contributions to Eq. (3.31) which involve the

$$\tau_R^3 = \text{diag}\left(\frac{1}{2}, -\frac{1}{2}\right) , \tag{3.32}$$

and

$$T_4^{15} = \sqrt{\frac{3}{2}}\text{diag}\left(\frac{1}{6}, \frac{1}{6}, \frac{1}{6}, -\frac{1}{2}\right) , \tag{3.33}$$

the diagonal generators of the $SU(2)_R$ and $SU(4)$ groups. There is no sum in the $U(1)$ part of Eq. (3.31) because this group is the unit matrix $\mathbf{1}$, so the only generator is

$$T_F^1 = \mathbf{1} q_F . \tag{3.34}$$

where q_F is the charge of the $U(1)_F$ group for each field. When applying Eqs. (3.32) and (3.33) to conjugate fields we have to complex conjugate the generator and multiply it by -1, but for the $U(1)_F$ group we just use Eq. (3.34) where it is known that the q_F charges are different for right-handed fields.

Using Table 3.1 we find that D_F^1, D_{2R}^3, and D_4^{15} are given by

$$\begin{aligned} D_F^1 &= \overline{H}^\dagger(q_F)_{\overline{H}}\overline{H} + H^\dagger(q_F)_H H + \overline{\theta}^\dagger(q_F)_{\overline{\theta}}\overline{\theta} + \theta^\dagger(q_F)_\theta\theta \\ &\quad + \overline{F}_i^\dagger(q_F)_{\overline{F}_i}\overline{F}^j\delta_i^j + F_i^\dagger(q_F)_{F_i}F^j\delta_i^j + h^\dagger(q_F)_h h , \end{aligned} \tag{3.35}$$

$$D_{2R}^3 = \overline{H}^\dagger(-\tau_R^{3*})\overline{H} + H^\dagger(\tau_R^3)H + \overline{F}^\dagger(-\tau_R^{3*})\overline{F} + h^\dagger(\tau_R^3)h , \tag{3.36}$$

$$D_4^{15} = \overline{H}^\dagger(-T_4^{15*})\overline{H} + H^\dagger(T_4^{15})H + \overline{F}^\dagger(-T_4^{15*})\overline{F} + F^\dagger(T_4^{15})F . \tag{3.37}$$

In Eq. (3.35), $i, j \in \{1, 2, 3\}$ are family indices. We used δ_i^j to pick out the trace of the outer products $F_i^\dagger F^j$ and $\overline{F}_i^\dagger\overline{F}^j$, thereby giving us the dot product.

The scalar components of the left-handed matter superfield F are q and l. The scalar components of the right-handed matter superfield $\overline{F}$ are u^c, d^c, ν^c, and e^c. The tensorial conventions are shown in [58] for D_{2R}^3 and D_4^{15}. For D_F^1, all diagonal elements are equal to unity for the generator, so the tensor notation is trivial.

Now we square D_F^1, D_{2R}^3, and D_4^{15} (as they are squared in the D-term potential), then consider the cross terms, as we are only interested in those terms that look like $(mass)^2 \times (field)^2$. The $(mass)^2$ terms come from the VEVs of the heavy Higgs and Froggatt-Nielsen fields $\langle\overline{H}\rangle^2, \langle H\rangle^2, \langle\overline{\theta}\rangle^2, \langle\theta^2\rangle$. The $(field)^2$ terms come from $|F_i|^2, |\overline{F}_i|^2$, where the i is a family index running from 1 to 3.

To follow the established convention of [52, 54, 58], we shall place a square on the D-terms such as D_H^2, but one must note that this is purely convention - the D-term still has mass dimension 2, so it will appear as $(D_H^2)^2$ in the potential which has mass dimension 4. We have followed [58] in choosing our designation of D_H^2, but D_θ^2 is new as it was not considered in that work. So D_H^2 is defined to be

$$D_H^2 = \frac{1}{8}(\langle\overline{H}\rangle^2 - \langle H\rangle^2) \ , \tag{3.38}$$

and similarly we have defined D_θ^2 to be

$$D_\theta^2 = -q_\theta(\langle\overline{\theta}\rangle^2 - \langle\theta\rangle^2) - q_H(\langle\overline{H}\rangle^2 - \langle H\rangle^2) \ , \tag{3.39}$$

where q_θ is defined to be -1 and q_H is defined to be $-q_{R3}$.[7] So from Eq. (3.31), using the expressions above in Eqs. (3.38) and (3.39), we have

$$V_D = \frac{1}{2}g_F^2(D_\theta^2)^2 + 8(g_{2R}^2 + 3g_4^2)(D_H^2)^2 \ . \tag{3.40}$$

Working explicitly within Model 1, where $q_H = \frac{5}{6}$, we shall proceed to rewrite these D-terms as functions of the calculable soft SUSY breaking masses and gauge couplings. So we arrive at the D-term potential V_D, which, when put together with V_F and V_{soft},

[7] In Section 3.3 we saw that $q_H = 1$ for Model 2 differs from $q_H = \frac{5}{6}$ for Model 1. Models 1 and 2 are the two different $U(1)_F$ charge structure models considered in this thesis.

forms the Higgs potential:

$$\begin{aligned} V_{\text{Higgs}} &= \frac{1}{2}g_F^2\left[\frac{25}{36}(\langle\overline{H}\rangle^2-\langle H\rangle^2)^2+(\langle\bar{\theta}\rangle^2-\langle\theta\rangle^2)^2-\frac{5}{3}(\langle\overline{H}\rangle^2-\langle H\rangle^2)(\langle\bar{\theta}\rangle^2-\langle\theta\rangle^2)\right] \\ &+\frac{1}{8}(g_{2R}^2+\frac{3}{2}g_4^2)(\langle\overline{H}\rangle^2-\langle H\rangle^2)^2+\lambda_S^2(\langle\overline{H}\rangle\langle H\rangle-M_H^2)^2+\lambda_{S'}^2(\langle\bar{\theta}\rangle\langle\theta\rangle-M_\theta^2)^2 \\ &+m_{\overline{H}}^2\langle\overline{H}\rangle^2+m_H^2\langle H\rangle^2+m_{\bar{\theta}}^2\langle\bar{\theta}\rangle^2+m_\theta^2\langle\theta\rangle^2\ , \end{aligned} \tag{3.41}$$

where V_D comprises the terms with gauge couplings, V_F is made up of the terms with dilaton lambda factors, and V_{soft} contains the terms that have TeV scale soft SUSY breaking scalar masses $m_{\overline{H}}^2, m_H^2, m_{\bar{\theta}}^2, m_\theta^2$. M_H and M_θ are GUT scale masses.

To find the form of the D-terms, we must minimise this potential with respect to the fields $\langle\overline{H}\rangle$, $\langle H\rangle$, $\langle\bar{\theta}\rangle$, $\langle\theta\rangle$, and then set these minimisation relations equal to zero.

$$\begin{aligned} \frac{\partial V}{\partial\langle\overline{H}\rangle} &= \frac{1}{2}g_F^2\left[\frac{25}{9}(\langle\overline{H}\rangle^2-\langle H\rangle^2)-\frac{10}{3}(\langle\bar{\theta}\rangle^2-\langle\theta\rangle^2)\right]\langle\overline{H}\rangle+\frac{1}{2}(g_{2R}^2+\frac{3}{2}g_4^2)(\langle\overline{H}\rangle^2-\langle H\rangle^2)\langle\overline{H}\rangle \\ &+2\lambda_S^2(\langle\overline{H}\rangle\langle H\rangle-M_H^2)\langle H\rangle+2m_{\overline{H}}^2\langle\overline{H}\rangle=0 \end{aligned} \tag{3.42}$$

$$\begin{aligned} \frac{\partial V}{\partial\langle H\rangle} &= -\frac{1}{2}g_F^2\left[\frac{25}{9}(\langle\overline{H}\rangle^2-\langle H\rangle^2)-\frac{10}{3}(\langle\bar{\theta}\rangle^2-\langle\theta\rangle^2)\right]\langle H\rangle-\frac{1}{2}(g_{2R}^2+\frac{3}{2}g_4^2)(\langle\overline{H}\rangle^2-\langle H\rangle^2)\langle H\rangle \\ &+2\lambda_S^2(\langle\overline{H}\rangle\langle H\rangle-M_H^2)\langle\overline{H}\rangle+2m_H^2\langle H\rangle=0 \end{aligned} \tag{3.43}$$

$$\begin{aligned} \frac{\partial V}{\partial\langle\bar{\theta}\rangle} &= \frac{1}{2}g_F^2\left[4(\langle\bar{\theta}\rangle^2-\langle\theta\rangle^2)-\frac{10}{3}(\langle\overline{H}\rangle^2-\langle H\rangle^2)\right]\langle\bar{\theta}\rangle \\ &+2\lambda_{S'}^2(\langle\bar{\theta}\rangle\langle\theta\rangle-M_\theta^2)\langle\theta\rangle+2m_{\bar{\theta}}^2\langle\bar{\theta}\rangle=0 \end{aligned} \tag{3.44}$$

$$\begin{aligned} \frac{\partial V}{\partial\langle\theta\rangle} &= -\frac{1}{2}g_F^2\left[4(\langle\bar{\theta}\rangle^2-\langle\theta\rangle^2)-\frac{10}{3}(\langle\overline{H}\rangle^2-\langle H\rangle^2)\right]\langle\theta\rangle \\ &+2\lambda_{S'}^2(\langle\bar{\theta}\rangle\langle\theta\rangle-M_\theta^2)\langle\bar{\theta}\rangle+2m_\theta^2\langle\theta\rangle=0\ . \end{aligned} \tag{3.45}$$

As these are set to zero, any linear combination of them is also zero, so taking the following combinations and rearranging them, we have two minimisation conditions

$$\begin{aligned} \frac{\partial V}{\partial\langle\overline{H}\rangle}-\frac{\partial V}{\partial\langle H\rangle} \Rightarrow &\left\{\frac{1}{4}\left[\frac{25}{9}g_F^2+g_{2R}^2+\frac{3}{2}g_4^2\right](\langle\overline{H}\rangle+\langle H\rangle)^2-\lambda_S^2(\langle\overline{H}\rangle\langle H\rangle-M_H^2)\right\}(\langle\overline{H}\rangle-\langle H\rangle) \\ &-\frac{5}{6}g_F^2(\langle\bar{\theta}\rangle+\langle\theta\rangle)(\langle\bar{\theta}\rangle-\langle\theta\rangle)(\langle\overline{H}\rangle+\langle H\rangle)=-m_{\overline{H}}^2\langle\overline{H}\rangle+m_H^2\langle H\rangle\ , \end{aligned} \tag{3.46}$$

$$\begin{aligned} \frac{\partial V}{\partial\langle\bar{\theta}\rangle}-\frac{\partial V}{\partial\langle\theta\rangle} \Rightarrow &\frac{1}{6}g_F^2\left[6(\langle\bar{\theta}\rangle^2-\langle\theta\rangle^2)-5(\langle\overline{H}\rangle^2-\langle H\rangle^2)\right](\langle\bar{\theta}\rangle+\langle\theta\rangle) \\ &-\lambda_{S'}^2(\langle\bar{\theta}\rangle\langle\theta\rangle-M_\theta^2)(\langle\bar{\theta}\rangle-\langle\theta\rangle)=-m_{\bar{\theta}}^2\langle\bar{\theta}\rangle+m_\theta^2\langle\theta\rangle\ , \end{aligned} \tag{3.47}$$

where we have used equalities such as

$$\begin{aligned}(\langle\overline{H}\rangle^2 - \langle H\rangle^2)\langle\overline{H}\rangle + (\langle\overline{H}\rangle^2 - \langle H\rangle^2)\langle H\rangle &= \langle\overline{H}\rangle^3 - \langle\overline{H}\rangle\langle H\rangle^2 + \langle\overline{H}\rangle^2\langle H\rangle - \langle H\rangle^3 \\ &= (\langle\overline{H}\rangle^3 + 2\langle\overline{H}\rangle^2\langle H\rangle + \langle\overline{H}\rangle\langle H\rangle^2) - (\langle\overline{H}\rangle^2\langle H\rangle + 2\langle\overline{H}\rangle\langle H\rangle^2 + \langle H\rangle^3) \\ &= (\langle\overline{H}\rangle + \langle H\rangle)^2(\langle\overline{H}\rangle - \langle H\rangle) \ . \end{aligned} \tag{3.48}$$

For D-flatness, it is necessary to set $\langle\overline{H}\rangle^2 = \langle H\rangle^2$ and $\langle\overline{\theta}\rangle^2 = \langle\theta\rangle^2$, which results in $V_D = 0$. For F_S-flatness and $F_{S'}$-flatness, it is necessary to set $\langle\overline{H}\rangle\langle H\rangle = M_H^2$ and $\langle\overline{\theta}\rangle\langle\theta\rangle = M_\theta^2$, yielding zero valued F-terms. We wish to perturb away from these flat directions, so we impose

$$\langle\overline{H}\rangle = M_H - \overline{m} \quad ; \quad \langle H\rangle = M_H - m \ , \tag{3.49}$$

$$\langle\overline{\theta}\rangle = M_\theta - \overline{m}' \quad ; \quad \langle\theta\rangle = M_\theta - m' \ , \tag{3.50}$$

where $\overline{m}$, m, $\overline{m}'$, and m' are all TeV scale masses.

Thus the two minimisation conditions, Eqs. (3.46) and (3.47), become[8]

$$g_H^2(m - \overline{m})M_H - \frac{10}{3}g_F^2(m' - \overline{m}')M_\theta = m_H^2 - m_{\overline{H}}^2 \ , \tag{3.51}$$

$$\frac{2}{3}g_F^2\left[6(m' - \overline{m}')M_\theta - 5(m - \overline{m})M_H\right] = m_\theta^2 - m_{\overline{\theta}}^2 \ . \tag{3.52}$$

Now putting the small perturbations, Eqs. (3.49) and (3.50), into Eqs. (3.38) and (3.39) for the D-terms, we have, to leading order,

$$D_H^2 = \frac{1}{4}(m - \overline{m})M_H \ , \tag{3.53}$$

$$D_\theta^2 = \frac{1}{3}\left[6(m' - \overline{m}')M_\theta - 5(m - \overline{m})M_H\right] \ . \tag{3.54}$$

So, using Eqs. (3.51) and (3.52) in the above Eqs. (3.53) and (3.54), we have the following expressions for our D-terms for Model 1, as functions of the soft SUSY breaking

[8] After rearranging and taking the leading order in the GUT scale masses M_H and M_θ.

masses, GUT scale masses and gauge couplings

$$D_H^2 = \frac{1}{4g_{2R}^2 + 6g_4^2}\left[m_H^2 - m_{\overline{H}}^2 + \frac{5}{6}(m_{\bar{\theta}}^2 - m_{\overline{\theta}}^2)\right] , \tag{3.55}$$

$$D_{\bar{\theta}}^2 = \frac{m_{\bar{\theta}}^2 - m_{\overline{\theta}}^2}{2g_F^2} . \tag{3.56}$$

Note that Eq. (3.56) was used in obtaining Eq. (3.55). This is the form of the D-terms as used in our updated version of SOFTSUSY [59] to compute the slepton mass data for the lepton flavour violating branching ratios for Model 1, using Eqs. (4.36) - (4.43).

For Model 2, the derivation is very similar, with the factor of $q_H = 1$ being the only difference, and so we obtain the form of D_H^2 below, with $D_{\bar{\theta}}^2$ being the same in both models,

$$D_H^2 = \frac{(m_H^2 - m_{\overline{H}}^2) + (m_{\bar{\theta}}^2 - m_{\overline{\theta}}^2)}{4g_{2R}^2 + 6g_4^2} . \tag{3.57}$$

In both cases, we can see that the Pati-Salam limit is obtained when the Froggatt-Nielsen scalar masses are degenerate, $m_{\bar{\theta}}^2 = m_{\overline{\theta}}^2$. This gives zero D_θ contributions, and also means that $m_{\bar{\theta}}^2 - m_{\overline{\theta}}^2 = 0$ and consequently does not contribute to D_H^2. The result here differs from [58] due to a different derivation procedure.

3.5 Yukawa and Majorana operators

The 'effective' Yukawa couplings are generated by operators with the following structure[9] [51]

$$\mathcal{O} = F_i \overline{F}_j h \left(\frac{H\overline{H}}{M_X^2}\right)^n \left(\frac{\theta}{M_X}\right)^{p(i,j)} , \tag{3.58}$$

[9]The field $\bar{\theta}$ will not enter the Yukawa operators because $F_i \overline{F}_j h$ will be positive for any i, j.

where the integer $p(i,j)$ is the total $U(1)_F$ charge of $F_i + \overline{F}_j + h$, and $H\overline{H}$ has a $U(1)_F$ charge of zero. The tensor structure of the operators in Eq. (3.58) is

$$(\mathcal{O})^{\alpha\rho yw}_{\beta\gamma xz} = F^{\alpha a}\overline{F}_{\beta x} h^y_a \overline{H}_{\gamma z} H^{\rho w} \theta^{p(i,j)} \ . \tag{3.59}$$

One constructs $SU(4)_{PS}$ invariant tensors $C^{\beta\gamma}_{\alpha\rho}$ that combine 4 and $\overline{4}$ representations of $SU(4)_{PS}$ into **1**, **6**, **10**, $\overline{\mathbf{10}}$ and **15** representations [51]. Similarly we construct $SU(2)_R$ tensors R^{xz}_{yw} that combine the **2** representations of SU(2) into singlet and triplet representations. These tensors are contracted together and into $\mathcal{O}^{\alpha\rho yw}_{\beta\gamma xz}$ to create singlets of $SU(4)_{PS}$, $SU(2)_L$ and $SU(2)_R$. Depending on which operators are used, different Clebsch-Gordan coefficients (CGCs) will emerge. We will return to these in Section 3.5.1, when we define the first of two models that we will be using for the numerical analysis. Section 3.5.2 details the operator structure and $U(1)_F$ charges for the second model.

We are interested in Majorana fermions because they can contribute neutrino masses of the correct order of magnitude via the see-saw effect. The operators for Majorana fermions are of the form

$$\mathcal{O}_{ij} = \overline{F}_i \overline{F}_j \left(\frac{HH}{M_X}\right) \left(\frac{H\overline{H}}{M_X^2}\right)^{n-1} \left(\frac{\theta}{M_X}\right)^{q(i,j)} \ . \tag{3.60}$$

$q(i,j)$ is analogous to $p(i,j)$ but for Majorana fermions, so it is the integer sum of the $U(1)_F$ charges of the $\overline{F_i} + \overline{F}_j + H + H$ fields. There do not exist renormalisable elements of this infinite series of operators, so $n < 1$ Majorana operators are not defined, except in the $(3,3)$ Majorana matrix element. We assume that a $(3,3)$ neutrino mass term is allowed at leading (but non-renormalisable) order. A similar analysis to that of the Dirac fermions is followed, however the structures only ever give masses to the neutrinos, not to the electrons or the quarks.

3.5.1 Operator structure and $U(1)_F$ charges in Model 1

In this section and the next, we shall be detailing two different models distinguished primarily by their $U(1)_F$ family charges. The intention is to consider two models which have the same Yukawa textures, but different $U(1)_F$ charge structure. This can be achieved by changing the magnitude of the operators in the Yukawa textures and the arbitrary couplings $a, a', ...$ to compensate for the change in the charge structure. The point of this first model is to highlight the dangerously large contributions to flavour violation that can arise from hitherto unconsidered D-terms.

For convenience, we define ϵ and δ as

$$\epsilon = \left(\frac{\langle\theta\rangle}{M_X}\right) \quad ; \quad \delta = \left(\frac{\langle H\rangle\langle\overline{H}\rangle}{M_X^2}\right) \ , \tag{3.61}$$

such that $\epsilon = \delta = 0.22$.

This model is almost the model studied in [52, 54], but with an extra operator in the $(1,2)$ and $(1,3)$ Yukawa matrix elements to allow non-zero Y_{12}^e and Y_{13}^e values. The operator texture is

$$\mathcal{O} = \begin{bmatrix} (a_{11}\mathcal{O}^{Fc} + a''_{11}\mathcal{O}^{''Ae})\epsilon^5 & (a_{12}\mathcal{O}^{Ee} + a'_{12}\mathcal{O}^{'Cb} + a''_{12}\mathcal{O}^{''Ec})\epsilon^3 & (a_{13}\mathcal{O}^{Ec} + a'_{13}\mathcal{O}^{'Cf} + a''_{13}\mathcal{O}^{''Ee})\epsilon \\ (a_{21}\mathcal{O}^{Dc})\epsilon^4 & (a_{22}\mathcal{O}^{Bc} + a'_{22}\mathcal{O}^{'Ff})\epsilon^2 & (a_{23}\mathcal{O}^{Ee} + a'_{23}\mathcal{O}^{'Bc}) \\ (a_{31}\mathcal{O}^{Fc})\epsilon^4 & (a_{32}\mathcal{O}^{Ac} + a'_{23}\mathcal{O}^{'Fe})\epsilon^2 & a_{33} \end{bmatrix} . \tag{3.62}$$

The operator nomenclature is defined in Appendix B and Appendix C. This leads

to the following Yukawa textures:

$$Y^u(M_X) = \begin{bmatrix} a''_{11}\sqrt{2}\delta^3\epsilon^5 & a'_{12}\sqrt{2}\delta^2\epsilon^3 & a'_{13}\frac{2}{\sqrt{5}}\delta^2\epsilon \\ 0 & a'_{22}\frac{8}{5\sqrt{5}}\delta^2\epsilon^2 & 0 \\ 0 & a'_{32}\frac{8}{5}\delta^2\epsilon^2 & a_{33} \end{bmatrix}, \tag{3.63}$$

$$Y^d(M_X) = \begin{bmatrix} a_{11}\frac{8}{5}\delta\epsilon^5 & -a'_{12}\sqrt{2}\delta^2\epsilon^3 & a'_{13}\frac{4}{\sqrt{5}}\delta^2\epsilon \\ a_{21}\frac{2}{\sqrt{5}}\delta\epsilon^4 & (a_{22}\sqrt{\frac{2}{5}} + a'_{22}\frac{16}{5\sqrt{5}}\delta)\delta\epsilon^2 & a'_{23}\sqrt{\frac{2}{5}}\delta^2 \\ a_{31}\frac{8}{5}\delta\epsilon^4 & a_{32}\sqrt{2}\delta\epsilon^2 & a_{33} \end{bmatrix}, \tag{3.64}$$

$$Y^e(M_X) = \begin{bmatrix} a_{11}\frac{6}{5}\delta\epsilon^5 & a''_{12}2\delta^2\epsilon^3 & a_{13}2\delta^2\epsilon \\ a_{21}\frac{4}{\sqrt{5}}\delta\epsilon^4 & (-a_{22}3\sqrt{\frac{2}{5}} + a'_{22}\frac{12}{5\sqrt{5}}\delta)\delta\epsilon^2 & -a'_{23}\sqrt{\frac{2}{5}}\delta^2 \\ -a_{31}\frac{6}{5}\delta\epsilon^4 & a_{32}\sqrt{2}\delta\epsilon^2 & a_{33} \end{bmatrix}, \tag{3.65}$$

$$Y^\nu(M_X) = \begin{bmatrix} a''_{11}\sqrt{2}\delta^3\epsilon^5 & a_{12}2\delta\epsilon^3 & a''_{13}2\delta^3\epsilon \\ 0 & a'_{22}\frac{6}{5\sqrt{5}}\delta^2\epsilon^2 & a_{23}2\delta \\ 0 & a'_{32}\frac{6}{5}\delta^2\epsilon^2 & a_{33} \end{bmatrix}. \tag{3.66}$$

The values of the arbitrary coefficients are laid out in Table 3.7. This gives numerical values for the Yukawa elements which can be used in either model, with the relevant

δ	0.22
ϵ	0.22
a_{11}	-0.92
a_{12}	0.33
a_{13}	0.00
a_{21}	1.67
a_{22}	1.12
a_{23}	0.89
a_{31}	-0.21
a_{32}	2.08
a_{33}	0.55
a'_{12}	0.77
a'_{13}	0.53
a'_{22}	0.66
a'_{23}	0.40
a'_{32}	1.80
a''_{11}	0.28
a''_{12}	0.00
a''_{13}	0.00
A_{11}	0.94
A_{12}	0.48
A_{13}	2.10
A_{22}	0.52
A_{23}	1.29
A_{33}	1.88

Table 3.7: The $\mathcal{O}(1)$ coefficients from [54] for the Yukawa and Majorana textures in Model 1. The values of a''_{12} and a_{13} will be varied in Section 3.5.3.

values of Y^e_{12} and Y^e_{13} inserted instead of the texture zeros.

$$Y^u(M_X) = \begin{bmatrix} 2.159 \times 10^{-06} & 5.606 \times 10^{-04} & 5.090 \times 10^{-03} \\ 0.000 & 1.105 \times 10^{-03} & 0.000 \\ 0.000 & 6.733 \times 10^{-03} & 5.841 \times 10^{-01} \end{bmatrix}, \quad (3.67)$$

$$Y^d(M_X) = \begin{bmatrix} -1.661 \times 10^{-04} & -5.606 \times 10^{-04} & 1.018 \times 10^{-02} \\ 7.683 \times 10^{-04} & -5.343 \times 10^{-03} & 1.216 \times 10^{-02} \\ -1.769 \times 10^{-04} & 3.133 \times 10^{-02} & 3.933 \times 10^{-01} \end{bmatrix}, \quad (3.68)$$

$$Y^e(M_X) = \begin{bmatrix} -1.246 \times 10^{-04} & 0.000 & 0.000 \\ 1.537 \times 10^{-03} & 2.432 \times 10^{-02} & -3.649 \times 10^{-02} \\ -1.327 \times 10^{-04} & 3.133 \times 10^{-02} & 5.469 \times 10^{-01} \end{bmatrix}, \quad (3.69)$$

$$Y^\nu(M_X) = \begin{bmatrix} 2.159 \times 10^{-06} & 1.525 \times 10^{-03} & 0.000 \\ 0.000 & 8.290 \times 10^{-04} & 3.923 \times 10^{-01} \\ 0.000 & 5.050 \times 10^{-03} & 5.469 \times 10^{-01} \end{bmatrix}. \quad (3.70)$$

These numerical values for the Yukawa elements can also be used for Model 2. In the numerical analysis we vary the values of the Y^e_{12} and Y^e_{13} electron Yukawa elements, so we will have to substitute in the appropriate values instead of the texture zeros that appear in Eq. (3.69).

The values of the family charges were explained in Section 3.3, but for ease, we shall present here them in Table 3.8.

The RH Majorana neutrino mass matrix is

$$\frac{M_{RR}(M_X)}{M_{33}} = \begin{bmatrix} A_{11}\delta\epsilon^8 & A_{12}\delta\epsilon^6 & A_{13}\delta\epsilon^4 \\ A_{12}\delta\epsilon^6 & A_{22}\delta\epsilon^4 & A_{23}\delta\epsilon^2 \\ A_{13}\delta\epsilon^4 & A_{23}\delta\epsilon^2 & A_{33} \end{bmatrix}. \quad (3.71)$$

Field	Model 1 Charge
F_1	$\frac{11}{6}$
F_2	$\frac{5}{6}$
F_3	$\frac{5}{6}$
$\overline{F}_1$	$\frac{19}{6}$
$\overline{F}_2$	$\frac{7}{6}$
$\overline{F}_3$	$-\frac{5}{6}$

Table 3.8: The $U(1)_F$ family charges for Model 1.

The numerical values for the Majorana mass matrix are

$$\frac{M_{RR}(M_X)}{M_{33}} = \begin{bmatrix} 3.508 \times 10^8 & 3.686 \times 10^9 & 3.345 \times 10^{11} \\ 3.686 \times 10^9 & 8.313 \times 10^{10} & 5.886 \times 10^{12} \\ 3.345 \times 10^{11} & 5.886 \times 10^{12} & 5.795 \times 10^{14} \end{bmatrix} . \tag{3.72}$$

3.5.2 Operator structure and $U(1)_F$ charges in Model 2

In Section 3.5.1 we outlined the operator structure and family charges of Model 1. We now move on to consider Model 2. The point of this second model is that all of the $U(1)_F$ charges of left-handed matter are the same, causing the $U(1)_F$ D-term for left-handed scalar mass matrices to give less flavour violation than in the first model. This choice is a small change to the model, since two of the 'left-handed' charges were the same anyway, but is made because the left-handed contribution *usually* dominates over the right-handed contribution.

Model 2 differs from Model 1 in the charges under the Abelian family symmetry, and the compensating changes to ensure the same Yukawa textures. Again, ϵ and δ are

defined as in Eq. (3.61), so $\epsilon = \delta = 0.22$. The powers of ϵ in the first row of the Yukawa textures are one lower, and we compensate that by increasing the power of δ in these first rows. We do not have to shift the values of the a, a', a'', a''' parameters since $\delta = \epsilon$. Were this not the case, we would have to shift the values by a factor of $\frac{\epsilon}{\delta}$. Model 2 is not meant to be a natural or realistic model, we use it as a tool to investigate the contribution to flavour violation from the $U(1)_F$ D-term correction to the left-handed scalar masses. The family charges for Model 2 are taken from Table 3.6.

The $U(1)_F$ charge of H must be equal and opposite to $\overline{F}_3$, and $\overline{H}$ must be the negative of this. This is due to the (3,3) element of the right-handed Majorana mass being allowed at leading order, so the $U(1)_F$ charges of $\overline{F}_3$ and H must conspire to cancel for the operator of the Majorana fermions to be renormalisable.

So for Model 2, the $U(1)_F$ charges of H and $\overline{H}$ are 1 and -1 respectively. One can use the relevant equations above to check that the anomaly coefficients do indeed satisfy the anomaly cancellation conditions. This gives us a different D_H-term for Model 2 Eq. (3.57), but the D_θ-term is the same in both models, Eq. (3.56).

The operator texture for Model 2 is

$$\mathcal{O} = \begin{bmatrix} (a'_{11}\mathcal{O}'^{Fc} + a'''_{11}\mathcal{O}'''^{Ae})\epsilon^4 & (a'_{12}\mathcal{O}'^{Ee} + a''_{12}\mathcal{O}''^{Cb} + a'''_{12}\mathcal{O}'''^{Ec})\epsilon^2 & (a_{13}\mathcal{O}^{Ec} + a''_{13}\mathcal{O}''^{Cf} + a'''_{13}\mathcal{O}'''^{Ee}) \\ (a_{21}\mathcal{O}^{Dc})\epsilon^4 & (a_{22}\mathcal{O}^{Bc} + a'_{22}\mathcal{O}'^{Ff})\epsilon^2 & (a_{23}\mathcal{O}^{Ee} + a'_{23}\mathcal{O}'^{Bc}) \\ (a_{31}\mathcal{O}^{Fc})\epsilon^4 & (a_{32}\mathcal{O}^{Ac} + a'_{23}\mathcal{O}'^{Fe})\epsilon^2 & a_{33} \end{bmatrix} . \tag{3.73}$$

The operator nomenclature is defined in Appendix B and Appendix C. The new

operator setup leads to the following Yukawa textures:

$$Y^u(M_X) = \begin{bmatrix} a'''_{11}\sqrt{2}\delta^4\epsilon^4 & a''_{12}\sqrt{2}\delta^3\epsilon^2 & a''_{13}\frac{2}{\sqrt{5}}\delta^3 \\ 0 & a'_{22}\frac{8}{5\sqrt{5}}\delta^2\epsilon^2 & 0 \\ 0 & a'_{32}\frac{8}{5}\delta^2\epsilon^2 & a_{33} \end{bmatrix}, \tag{3.74}$$

$$Y^d(M_X) = \begin{bmatrix} a'_{11}\frac{8}{5}\delta^2\epsilon^4 & -a''_{12}\sqrt{2}\delta^3\epsilon^2 & a''_{13}\frac{4}{\sqrt{5}}\delta^3 \\ a_{21}\frac{2}{\sqrt{5}}\delta\epsilon^4 & (a_{22}\sqrt{\frac{2}{5}} + a'_{22}\frac{16}{5\sqrt{5}}\delta)\delta\epsilon^2 & a'_{23}\sqrt{\frac{2}{5}}\delta^2 \\ a_{31}\frac{8}{5}\delta\epsilon^4 & a_{32}\sqrt{2}\delta\epsilon^2 & a_{33} \end{bmatrix}, \tag{3.75}$$

$$Y^e(M_X) = \begin{bmatrix} a'_{11}\frac{6}{5}\delta^2\epsilon^4 & a'''_{12}2\delta^3\epsilon^2 & a_{13}2\delta^3 \\ a_{21}\frac{4}{\sqrt{5}}\delta\epsilon^4 & (-a_{22}3\sqrt{\frac{2}{5}} + a'_{22}\frac{12}{5\sqrt{5}}\delta)\delta\epsilon^2 & -a'_{23}\sqrt{\frac{2}{5}}\delta^2 \\ -a_{31}\frac{6}{5}\delta\epsilon^4 & a_{32}\sqrt{2}\delta\epsilon^2 & a_{33} \end{bmatrix}, \tag{3.76}$$

$$Y^\nu(M_X) = \begin{bmatrix} a'''_{11}\sqrt{2}\delta^4\epsilon^4 & a'_{12}2\delta^2\epsilon^2 & a'''_{13}2\delta^4 \\ 0 & a'_{22}\frac{6}{5\sqrt{5}}\delta^2\epsilon^2 & a_{23}2\delta \\ 0 & a'_{32}\frac{6}{5}\delta^2\epsilon^2 & a_{33} \end{bmatrix}. \tag{3.77}$$

The numerical values for the Yukawa textures are the same as in Model 1 before, Eqs. (3.67) – (3.70), and in Section 3.5.3 we vary the values of the $(1,2)$ and $(1,3)$ electron Yukawa elements. Y^e_{12} is varied from 0 to 1.5×10^{-3} and Y^e_{13} is turned on from 0 to 1.5×10^{-2}. A larger value of the $(1,3)$ element is needed to have the same impact as the $(1,2)$ element. These Yukawas are turned on for both models, and the results of the effects they have on the branching ratio of $\mu \to e\gamma$ are given in Section 4.5.3.

The values of the arbitrary couplings are laid out in Table 3.9. The family charges for Model 2 are laid out in Table 3.10 for convenience.

The RH Majorana neutrino mass matrix is the same as in Model 1,

$$\frac{M_{RR}(M_X)}{M_{33}} = \begin{bmatrix} A_{11}\delta\epsilon^8 & A_{12}\delta\epsilon^6 & A_{13}\delta\epsilon^4 \\ A_{12}\delta\epsilon^6 & A_{22}\delta\epsilon^4 & A_{23}\delta\epsilon^2 \\ A_{13}\delta\epsilon^4 & A_{23}\delta\epsilon^2 & A_{33} \end{bmatrix}, \tag{3.78}$$

δ	0.22
ϵ	0.22
a'_{11}	-0.92
a'_{12}	0.33
a_{13}	0.00
a_{21}	1.67
a_{22}	1.12
a_{23}	0.89
a_{31}	-0.21
a_{32}	2.08
a_{33}	0.55
a''_{12}	0.77
a''_{13}	0.53
a'_{22}	0.66
a'_{23}	0.40
a'_{32}	1.80
a'''_{11}	0.28
a'''_{12}	0.00
a'''_{13}	0.00
A_{11}	0.94
A_{12}	0.48
A_{13}	2.10
A_{22}	0.52
A_{23}	1.29
A_{33}	1.88

Table 3.9: The $\mathcal{O}(1)$ coefficients for the Yukawa and Majorana textures in Model 2. The values of a'''_{12} and a_{13} will be varied in Section 3.5.3.

Field	Model 2 Charge
F_1	1
F_2	1
F_3	1
$\overline{F}_1$	3
$\overline{F}_2$	1
$\overline{F}_3$	-1

Table 3.10: The $U(1)_F$ family charges for Model 2.

and the numerical values are also the same, see Eq. (3.72).

3.5.3 Varying Y^e_{12} and Y^e_{13}

Normally, the chargino contribution to LFV dominates. Since the Feynman diagram for this includes the left-handed sfermions, we would expect the D-term corrections to the left-handed slepton mass matrix to dominate the flavour violation. However, Model 2, as defined in Section 3.5.2, is set up to have universal left-handed charges, so the D-term correction from the breaking of $U(1)_F$ will not contribute to flavour violation in the left-handed sector (except that it will either add or remove some mass suppression). The D-term is limited in magnitude by the difference of $m^2_{\theta} - m^2_{\bar{\theta}}$, and although this is not a strong correction to the soft masses, in general it can contribute significantly to the lepton flavour violating branching ratios.

The difference in $\mu \to e\gamma$ between Model 1 and Model 2 is negligible for either $Y^e_{12} = 0$ or $Y^e_{13} = 0$. This should not be surprising, since the texture zero coming from either element will yield small mixing angles, resulting in small lepton flavour violation,

and especially so in the case of $Y^e_{12} = Y^e_{13} = 0$. We will see this in Figures 4.6 and 4.7 in Section 4.5.3.

In order to get a picture of how great an effect the D-term contributions could have on the soft masses, it was necessary to examine a range of different values of Y^e_{12} and Y^e_{13}. Extra operator contributions were added to the textures in Model 1 and Model 2, when compared to the model previously studied [54], to allow for variations of the order $Y^e_{12} \approx 10^{-3}$ and $Y^e_{13} \approx 10^{-2}$. The gives $\mathcal{O}(1)$ parameters a''_{12} and a'''_{12} for Models 1 and 2 respectively, and an $\mathcal{O}(1)$ parameter a_{13} for both models.[10]

[10] $Y^e_{12} = 1.5 \times 10^{-3}$ corresponds to $a''_{12} = a'''_{12} = 0.32$. $Y^e_{13} = 1.5 \times 10^{-2}$ corresponds to $a_{13} = 3.20$.

Chapter 4

Lepton Flavour Violation in Non-Minimal Supergravity Models with D-terms

Realistic effective supergravity models have a variety of sources of lepton flavour violation (LFV) which can drastically affect the predictions relative to the scenarios usually considered in the literature based on minimal supergravity and the supersymmetric see-saw mechanism. The aim of this chapter is to bring new light to recent research [54] and consequently correct the results therein. We catalogue the additional sources of LFV which occur in realistic supergravity models including the effect of D-terms arising from an Abelian $U(1)$ family symmetry, non-aligned trilinear contributions from scalar F-terms, as well as non-minimal supergravity contributions and the impact of changing specific Yukawa elements. In order to quantify these effects, we investigate a string inspired effective supergravity model arising from intersecting D-branes supplemented by an additional $U(1)$ family symmetry, and calculate the branching ratios for $\mu \to e\gamma$ and

$\tau \rightarrow \mu\gamma$ for different benchmark points designed to isolate the different non-minimal contributions.

4.1 Preamble

Lepton flavour violation is a sensitive probe of new physics in supersymmetric (SUSY) models [60, 61]. In SUSY models, LFV arises due to off-diagonal elements in the slepton mass matrices in the 'super-CKM' (SCKM) basis, in which the quark and lepton mass matrices are diagonal [62]. In supergravity (SUGRA) mediated SUSY breaking the soft SUSY breaking masses are generated at the Planck scale, and the low energy soft masses relevant for physical processes such as LFV are therefore subject to radiative corrections in running from the Planck scale to the weak scale. Off-diagonal Yukawa couplings in the SCKM basis can arise both directly at the high energy scale (due to the effective SUGRA theory which is responsible for them), or can be radiatively generated by renormalisation group running from the Planck scale to the weak scale, for example due to right-handed neutrinos in see-saw models which have masses intermediate between these two scales.

Neutrino experiments confirming the Large Mixing Angle (LMA) MSW solution to the solar neutrino problem [14] taken together with the atmospheric neutrino data [6] show that neutrino masses are inevitable [63]. The presence of right-handed neutrinos, as required by the see-saw mechanism for generating neutrino masses, will lead inevitably to LFV, due to running effects, even in minimal SUGRA (mSUGRA) which has no LFV at the high energy GUT or Planck scale [64, 65]. Therefore, merely assuming SUSY and the see-saw mechanism, one expects LFV to be present. This has been studied, for example, in mSUGRA models with a natural neutrino mass hierarchy [66]. There is a large literature on the case of minimal LFV arising from mSUGRA and the

see-saw mechanism [67].

Despite the fact that most realistic string models lead to a low energy effective *non-minimal* SUGRA theory, such theories have not been extensively studied in the literature, although a general analysis of flavour changing effects in the mass insertion approximation has recently been performed [68]. Such effective non-minimal SUGRA models predict non-universality of the soft masses at the high energy scale, dependent on the structure of the Yukawa matrices. Moreover there can be additional sources of LFV which also enter the analysis. For example, realistic effective SUGRA theories arising from string inspired models will also typically involve some gauged family symmetry which can give an additional direct (as opposed to renormalisation group induced) source of LFV. This is because the D-term contributions to the scalar masses generated when the family symmetry spontaneously breaks add differently to each generation in the 'theory' basis. This is the basis in which these contributions are diagonal, thus the non-universal terms generate non-zero off-diagonal elements in the SCKM basis, leading to LFV. This effect depends on the strength of the D-term contribution, which is expected to be close in size to the magnitude of the uncorrected scalar masses. There can also be a significant contribution to non-universal trilinear soft masses leading to flavour violation [54, 69, 70] arising from the F-terms of scalars associated with the Yukawa couplings (for example the flavons of Froggatt-Nielsen theories).

The purpose of the present chapter is to catalogue and quantitatively study the importance of all the different sources of LFV present in a general non-minimal SUGRA framework, including the effects of gauged family symmetry. Although the different effects have all been identified in the literature, there has not so far been a coherent and quantitative dedicated study of LFV processes, beyond the mass insertion approximation, which includes all these effects within a single framework. In order to quantify the

importance of the different effects it is necessary to investigate these disparate sources of LFV numerically, both in isolation and in association with one another, within some particular SUGRA model. To be concrete we shall study the effective SUGRA models of the kind considered in [54] which have a sufficiently rich structure to enable all of the effects to be studied within a single framework. Within this class of models we shall consider specific benchmark points in order to illustrate the different effects. Some of these benchmark points were previously considered in [54]. However in the previous study the important effect of D-terms arising from the Abelian family symmetry was not considered. Here we shall show that such D-terms are in fact calculable within the framework of the model considered here, and can lead to significant enhancement (or suppression) of LFV rates, depending on the particular model considered.

4.2 Sources of lepton flavour violation

There are two parts to the flavour problem. The first is understanding the origin of the Yukawa couplings (and heavy Majorana masses for the see-saw mechanism), which lead to low energy quark and lepton mixing angles. In low energy SUSY, we also need to understand why flavour changing and/or CP violating processes induced by SUSY loops have such small branching ratios. A theory of flavour must address both problems simultaneously. For a full discussion of this see the review [62].

There are two contributions that can lead to large amounts of flavour violation. The first is the non-alignment of the trilinear soft coupling matrices with the corresponding Yukawa matrices, due to the contribution $F_m \partial_m \ln Y$, $m = \{H, \overline{H}, \theta, \overline{\theta}\}$. The reasons why this can lead to large flavour violation have been given before [54], where a numerical investigation of a model very similar to those considered herein finds that there is some amount of flavour violation. The second contribution can come from scalar mass

matrices which are not proportional to the identity in the theory basis, and lead to off-diagonal entries in the SCKM basis, resulting in flavour violation.

In this section we begin by defining the SCKM basis, and in the following subsections we systematically discuss a number of distinct sources of lepton flavour violation (LFV) in SUGRA models. As well as considering generic SUGRA models, we also allow for a family symmetry, which easily leads to non-universal scalar mass matrices and non-aligned trilinear matrices[1].

4.2.1 The SCKM basis

The most convenient basis to work in for considering flavour violating decays, such as $\mu \to e\gamma$ is the super-CKM (SCKM) basis, which is the basis where the Yukawa matrices are diagonal. As we deal with LFV in this thesis we shall only consider the slepton case here, but [62] explains the SCKM in more detail.

Using the $SU(2)$ representation of sleptons,

$$\widetilde{L}_i = \begin{pmatrix} \widetilde{N}_{L_i} \\ \widetilde{E}_{L_i} \end{pmatrix} , \tag{4.1}$$

[1]By non-aligned trilinears, we mean that $\tilde{A}_{ij}/Y_{ij} \neq$ constant (no sum)

we define the SCKM basis with the following equations:

$$\widetilde{E}_L^{SCKM} = \begin{pmatrix} \widetilde{e}_L \\ \widetilde{\mu}_L \\ \widetilde{\tau}_L \end{pmatrix} = V_{E_L} \begin{pmatrix} \widetilde{E}_{L_1} \\ \widetilde{E}_{L_2} \\ \widetilde{E}_{L_3} \end{pmatrix} , \tag{4.2}$$

$$\widetilde{E}_R^{SCKM} = \begin{pmatrix} \widetilde{e}_R \\ \widetilde{\mu}_R \\ \widetilde{\tau}_R \end{pmatrix} = V_{E_R} \begin{pmatrix} \widetilde{E}_{R_1} \\ \widetilde{E}_{R_2} \\ \widetilde{E}_{R_3} \end{pmatrix} , \tag{4.3}$$

$$\widetilde{N}_L^{SCKM} = \begin{pmatrix} \widetilde{\nu}_{eL} \\ \widetilde{\nu_{\mu L}} \\ \widetilde{\nu}_{\tau L} \end{pmatrix} = V_{N_L} \begin{pmatrix} \widetilde{N}_{L_1} \\ \widetilde{N}_{L_2} \\ \widetilde{N}_{L_3} \end{pmatrix} , \tag{4.4}$$

where the heavy right-handed sneutrinos have been integrated out.

Flavour violation is proportional to the off-diagonal elements in the SCKM basis, and is suppressed by the diagonal values. As the Yukawas are 3 by 3 matrices, the selectron mass matrix is 6 by 6, and the sneutrino mass matrix is 3 by 3.[2] The selectron mass matrix is

$$m^2_{\tilde{E}} = \begin{pmatrix} Y^e Y^{e\dagger} v_1^2 + \frac{1}{4} v^2 (g_2^2 - g_1^2)\mathbf{1} + m^2_{L_L} & -Y^e v_2 \mu + \tilde{A}^e v_1 \\ -Y^{e\dagger} v_2 \mu^* + \tilde{A}^{e\dagger} v_1 & Y^{e\dagger} Y^e v_1^2 + \frac{1}{2} v^2 g_1^2 \mathbf{1} + m^2_{E_R} \end{pmatrix} , \tag{4.5}$$

where $v^2 = v_2^2 - v_1^2$. The sneutrino mass matrix is then

$$m^2_{\tilde{N}} = \left(Y^\nu Y^{\nu\dagger} v_2^2 + \frac{1}{4} v^2 g_1^2 \mathbf{1} + m^2_{L_L} \right) . \tag{4.6}$$

Off diagonal elements in any of the 3 by 3 submatrices in the SCKM basis will lead to flavour violation. We will now consider the LL block of $m^2_{\tilde{E}}$. The arguments follow similar lines for any other block of $m^2_{\tilde{E}}$ or $m^2_{\tilde{N}}$. The transformation to the SCKM basis

[2]The heavy right handed neutrinos cause the right-handed part of the sneutrino mass matrix to decouple by the electroweak scale.

is carried out by

$$(m^{2\,SCKM}_{\tilde{E}})_{LL} = V_{E_L}\left(Y^e Y^{e\dagger} v_1^2 + \frac{1}{4}v^2(g_2^2 - g_1^2)\mathbf{1} + m^2_{L_L}\right)V^\dagger_{E_L} \ . \tag{4.7}$$

Using properties of the unitary Hermitian matrices $V_{E_L}, V^\dagger_{E_L}$, we see that the first term is diagonal and the second term is trivially proportional to the identity, so any non-zero off-diagonal elements must therefore be generated by the third term $V_{E_L} m^2_{L_L} V^\dagger_{E_L}$. If this is proportional to the identity at the GUT scale, it will be approximately equal to the identity at the electroweak scale, which is the scale we should be working at. The fact that this is only approximate is due to the presence of the right handed neutrino fields in the running of the soft scalar mass squared matrices. If, however, the soft mass squared matrices are not proportional to the identity at the GUT scale, then large off-diagonal values will be generated when rotating to the SCKM basis, unless the rotation happens to be small, which it generally is not. Since the family D-term contribution is not proportional to the identity[3] this will usually be the case here[4] and so we expect large flavour violation in models with Abelian family symmetries when the D-terms correct the scalar mass matrices.

4.2.2 The relevance of the Yukawa textures

There is one subtlety concerning the size of the off-diagonal elements of the scalar mass matrices in the SCKM basis. This comes back to the definition of the SCKM basis as the basis in which the Yukawa matrices are diagonal. The larger the SCKM

[3]This statement assumes that the generational charges are not the same for both left- and right-handed fields. This would remove the point of the family symmetry generating the sfermion mass hierarchy.

[4]One can, however, imagine some model with particular points in its parameter space where a non-universal non-zero D-term corrects a non-universal base mass matrix to result in a net *universal* mass matrix. This has not been seen before and is actually shown in panel (ii) of Figure 4.4.

transformation between any 'theory' basis and the mass eigenstate basis for the Yukawa matrices, the larger the SCKM transformation that must be performed on the scalar mass matrices in going to the SCKM basis, hence the larger the off-diagonal elements of the scalar mass matrices in the SCKM basis generated from non-equal diagonal elements in the 'theory' basis. [5] The larger the off-diagonal entries in the SCKM basis compared to the diagonal ones, the greater will be the flavour violation. Also, the greater the mass difference between the diagonal elements in the 'theory' basis, the greater the size of the off-diagonal entries produced when rotating from the 'theory' basis, hence the larger the flavour violating effect. Clearly these effects are sensitive to the size of the transformation required to go to the SCKM basis, which in turn is sensitive to the particular choice of Yukawa textures in the 'theory' basis. In this way, the choice of Yukawa texture can play an important part in controlling the magnitude of flavour violation, and we shall see examples of this later.

4.2.3 Running effects

Consider the case where, at the high energy scale, the scalar mass matrices are proportional to the identity matrix and each soft trilinear coupling matrix is aligned to the corresponding Yukawa matrix:

$$\left(m_f^2\right)_{ij} = m_{0,f}^2 \delta_{ij} \quad , \quad \left(\tilde{A}^f\right)_{ij} = A_0^f Y_{ij}^f \ . \tag{4.8}$$

This is often referred to as mSUGRA. In the quark sector, due to the quark flavour violation responsible for CKM mixing, when the scalar squark mass matrices are run down to the electroweak scale, they will run to non-universal scalar mass matrices and

[5] Note that the D-terms make us sensitive to right-handed mixings in the Yukawa matrices, so the non-universal family charge structure for the right-handed scalar masses may lead to a non-universal generational hierarchy in the right-handed scalar mass matrices.

non-aligned trilinear coupling matrices. If this is the case, then in the SCKM basis, which is the basis where the Yukawa matrices are diagonal, off-diagonal elements in the scalar squark mass matrices or the trilinear squark mass matrices lead to flavour violation.

In the lepton sector, in the absence of neutrino masses the separate lepton flavour numbers are conserved and mSUGRA will not lead to any LFV induced by running the matrices down to low energy. However, in the presence of neutrino masses, with right-handed neutrino fields included to allow a see-saw explanation of neutrino masses and mixing angles, the separate lepton flavour numbers will be violated and, even in the mSUGRA type scenario, running effects will generate off-diagonal elements in the scalar mass matrices in the SCKM basis, resulting in low energy LFV.

4.2.4 Non-universal diagonal scalar mass matrices

In non-minimal SUGRA the scalar mass matrices may be diagonal at the high-energy scale, but not proportional to the unit matrix. In this case, there will be non-zero off-diagonal elements in the SCKM basis even with no contribution from running effects or from the trilinear coupling matrices.

One way of getting diagonal mass matrices not proportional to the unit matrix is from a SUGRA model corresponding to the low energy limit of a string model with D-branes. If each generation from the field theory viewpoint corresponds to a string attaching to different branes, then the masses predicted in the SUGRA can be different. This leads to diagonal but non-universal scalar mass matrices.

Another way of getting diagonal non-universal mass matrices is by having a model with a gauge family symmetry which is broken spontaneously, leading to D-term contributions to the soft masses. When the Higgs that breaks the family group gets a

VEV it gives a squark (slepton) mass contribution through the four point scalar gauge interaction, which has two flavons and two squarks (sleptons).

To make the point more explicitly, consider a $U(1)$ family group. The mass contribution is then proportional to the charge under the family symmetry. As the point of a family symmetry is to explain the hierarchy of fermion masses, small quark mixing angles and large neutrino mixing angles, the charges of each generation are usually different.

Then, even if the mass matrix starts off as a universal matrix, it will be driven non-universal by the D-term contribution

$$m^2_{L_L} = \begin{bmatrix} m_0^2 & & \\ & m_0^2 & \\ & & m_0^2 \end{bmatrix} + \begin{bmatrix} q_{L1} & & \\ & q_{L2} & \\ & & q_{L3} \end{bmatrix} D^2 \, . \tag{4.9}$$

4.2.5 Non-aligned trilinears

One way of getting non-aligned trilinear matrices is by having the same sort of non-minimal SUGRA setup that leads to diagonal but non-universal mass matrices, as described in Section 4.2.4. From the supergravity equations of Section 2.2, the trilinears that appear in the soft Lagrangian, $\tilde{A}_{ij}$ will be non-aligned if the trilinears predicted by the SUGRA model, A_{ij} are not democratic, i.e. if $A_{ij} \neq$ constant. From a string-inspired/SUGRA standpoint, if each generation is assigned to a different brane and extra-dimensional vibrational direction, then in general we expect A_{abc} to be different, due to the differing values of the Kähler metrics $\tilde{K}_a$ for the different brane assignments C^i_j. When $\tilde{A}_{ij}$ is transformed to the SCKM basis at the electroweak scale, there will then be large off-diagonal elements which contribute to flavour violating processes.

In general, when one considers a family symmetry in order to understand the origin

of the Yukawa couplings, the new fields arising from this can develop F-term VEVs, and contribute to the supersymmetry breaking F-terms in a non-universal way. This also leads to a dangerous source of flavour violating non-aligned trilinears [54, 69, 70, 71],

$$\Delta A = F_\theta \partial_\theta \ln Y \ , \tag{4.10}$$

where the Yukawa coupling Y in Eq. (4.10) arises from the effective FN operator and is a polynomial of the FN field θ, $Y \sim \theta^n$, leading to

$$\Delta A \sim F_\theta \partial_\theta \ln \theta^n \sim F_\theta \frac{n}{\theta}. \tag{4.11}$$

However, the auxiliary field is proportional to the scalar component,

$$F_\theta \propto m_{3/2}\theta \ \Rightarrow \ \Delta A \propto n m_{3/2} \ . \tag{4.12}$$

An example of this with an arbitrary $U(1)$ family symmetry is

$$Y_{ij} = a_{ij}\left(\frac{\theta}{M}\right)^{p(i,j)} \ \Rightarrow \ \Delta A_{ij} \sim m_{3/2} p(i,j) \ , \tag{4.13}$$

where the a_{ij} are arbitrary couplings, all of which should be $\mathcal{O}(1)$ for the symmetry to be considered natural. The $p(i,j)$ are integers appearing as a power for the ij^{th} element of the above Yukawa, and they comprise the sum of the family charges for the i^{th}-generation left-handed field and j^{th}-generation right-handed field. In principle, if the Yukawa texture is set up so that each power is different, then each element in A_{ij} will be different from the others, and the physical trilinear matrix $\tilde{A}_{ij}$ will be non-aligned to the corresponding Yukawa. Due to the dependence on the charges of the different fields, this contribution to the trilinears is not diagonalised when we transform to the SCKM basis. With either source of non-aligned trilinear, when $\tilde{A}_{ij}$ is transformed to the SCKM basis at the electroweak scale, there will be large off-diagonal elements which contribute to flavour violating processes.

4.3 Soft supersymmetry breaking masses

Section 2.2 summarised the standard way of obtaining soft SUSY breaking terms from supergravity. So using the knowledge therein, we construct the SUSY breaking F-terms, scalar masses, D-term contributions, soft gaugino masses, and soft trilinear couplings.

4.3.1 Supersymmetry breaking F-terms

In [49] it was assumed that the Yukawas were field-independent, and hence the only F-VEVs of importance were that of the dilaton S, and the untwisted moduli T_i. Here we set out the parameterisation for the F-term VEVs, including the contributions from the FN field θ and the heavy Higgs fields $H, \overline{H}$. Note that the field dependent part follows from the assumption that the family symmetry field, θ is an intersection state.

$$F_S = \sqrt{3} m_{3/2} \left(S + \overline{S}\right) X_S \ , \tag{4.14}$$

$$F_{T_i} = \sqrt{3} m_{3/2} \left(T_i + \overline{T}_i\right) X_{T_i} \ , \tag{4.15}$$

$$F_{H^{\alpha b}} = \sqrt{3} m_{3/2} H^{\alpha b} \left(S + \overline{S}\right)^{\frac{1}{2}} X_H \ , \tag{4.16}$$

$$F_{\overline{H}_{\alpha x}} = \sqrt{3} m_{3/2} \overline{H}_{\alpha x} \left(T_3 + \overline{T}_3\right)^{\frac{1}{2}} X_{\overline{H}} \ , \tag{4.17}$$

$$F_\theta = \sqrt{3} m_{3/2} \theta \left(S + \overline{S}\right)^{\frac{1}{4}} \left(T_3 + \overline{T}_3\right)^{\frac{1}{4}} X_\theta \ . \tag{4.18}$$

We introduce a shorthand notation,

$$F_H H = \sum_{\alpha b} F_{H^{\alpha b}} H^{\alpha b} \quad ; \quad F_{\overline{H}} \overline{H} = \sum_{\alpha x} F_{\overline{H}_{\alpha x}} \overline{H}_{\alpha x} \ . \tag{4.19}$$

In [54], it was assumed that $\langle S \rangle + \langle \overline{S} \rangle$ and $\langle T_i \rangle + \langle \overline{T_i} \rangle$ were large due to an assumption made about the gauge coupling factors controlling the size of these VEVs. However, the values of $\langle S \rangle$ and $\langle T_i \rangle$ are tied to the values of the brane gauge couplings, which themselves are constrained. The F-terms above use values of S and T_i which are given

in terms of the gauge couplings as Eqs. (2.20):

$$\Re S = \frac{4\pi}{g_9^2} \quad ; \quad \Re T_i = \frac{4\pi}{g_{5_i}^2} \ . \tag{4.20}$$

The gauge couplings g_{5_1}, g_{5_2} are given from Eqs. (3.1) – (3.3) [49] as

$$g_{5_1} = g_2 \quad ; \quad g_{5_2} = \frac{g_2 g_3}{\sqrt{g_2^2 - g_3^2}} \ , \tag{4.21}$$

where we shall assume that at the scale M_X we have,

$$g_2 = 0.7345 \quad ; \quad g_3 = 0.6730 \ . \tag{4.22}$$

The values of g_9, g_{5_3} are assumed to be equal and are obtained from the string relation

$$32\pi^2 \left(\frac{M_*}{M_{Pl}}\right)^2 = g_9 g_{5_1} g_{5_2} g_{5_3} \ , \tag{4.23}$$

as

$$g_9 = g_{5_3} = 0.0266 \ , \tag{4.24}$$

where we have taken

$$\left(\frac{M_*}{M_{Pl}}\right)^2 = 2.77 \times 10^{-6} \ . \tag{4.25}$$

These rather small gauge couplings imply

$$\Re S = \Re T_3 = 0.877. \tag{4.26}$$

In [54] the string relation was not used and it was assumed incorrectly that $g_9 = g_{5_3} = g_2$ which resulted in $\Re S = 27.7$. With these now consistent values of $\langle S \rangle$ and $\langle T_i \rangle$, we get the corrected results as seen in Section 4.5.

4.3.2 Soft scalar masses

There are two contributions to scalar mass squared matrices, coming from SUGRA and from D-terms. In this subsection we calculate the SUGRA predictions for the matrices at the GUT scale, and in the Section 4.3.3 we add on the D-term contributions.

The method for obtaining the SUGRA contributions to soft masses is detailed in Section 2.2.1. From Eq. (2.9) we can get the family dependent form for the squared scalar masses,

$$m_L^2 = m_{3/2}^2 \begin{pmatrix} a & & \\ & a & \\ & & b_L \end{pmatrix} , \tag{4.27}$$

$$m_R^2 = m_{3/2}^2 \begin{pmatrix} a & & \\ & a & \\ & & b_R \end{pmatrix} , \tag{4.28}$$

$$m_h^2 = m_{3/2}^2(1 - 3X_S^2) , \tag{4.29}$$

$$m_H^2 = m_{3/2}^2(1 - 3X_S^2) , \tag{4.30}$$

$$m_{\overline{H}}^2 = m_{3/2}^2(1 - 3X_{T_3}^2) , \tag{4.31}$$

$$m_\theta^2 = m_{3/2}^2 \left[1 - \frac{3}{2}(X_S^2 + X_{T_3}^2)\right] , \tag{4.32}$$

where

$$a = 1 - \frac{3}{2}(X_S^2 + X_{T_3}^2) , \tag{4.33}$$

$$b_L = 1 - 3X_{T_3}^2 , \tag{4.34}$$

$$b_R = 1 - 3X_{T_2}^2 . \tag{4.35}$$

Here m_L^2 represents the left-handed scalar mass squared matrices $m_{Q_L}^2$ and $m_{L_L}^2$. m_R^2 represents the right-handed scalar mass squared matrices $m_{U_R}^2$, $m_{D_R}^2$, $m_{E_R}^2$ and $m_{N_R}^2$. A discussion of the equations for $m_{\overline{\theta}}^2$ can be found in Section 4.3.4.

4.3.3 D-term contributions

Section 3.4 contains a full derivation of the D-terms that arise in the 42241 model considered here. Now we shall give an idea as to how these D-terms contribute to the

sfermion mass spectrum.

D-terms arise when a gauge symmetry is spontaneously broken, and can give large contributions to lepton flavour violating processes. There are two D-term contributions to the scalar masses for the $U(1)_F$ extended Pati-Salam model. The first is the well known [58, 54] contribution from the breaking of the Pati-Salam group to the MSSM group. It has a subscript H to denote that it arises when the $H, \overline{H}$ Higgs fields break the Pati-Salam symmetry. Note that these D-terms are different to those quoted in the references above as we now also consider the D-term contributions generated by breaking the family symmetry. This second D-term comes solely from the breaking of the $U(1)_F$ symmetry by the Froggatt-Nielsen fields $\theta, \overline{\theta}$, and is denoted by the subscript

θ. The corrections lead to the following mass matrices:

$$m^2_{Q_L} = m^2_L + 1(g_4^2)D_H^2 + \begin{pmatrix} q_{L1} & & \\ & q_{L2} & \\ & & q_{L3} \end{pmatrix} g_F^2 D_\theta^2 \ , \tag{4.36}$$

$$m^2_{L_L} = m^2_L - 1(3g_4^2)D_H^2 + \begin{pmatrix} q_{L1} & & \\ & q_{L2} & \\ & & q_{L3} \end{pmatrix} g_F^2 D_\theta^2 \ , \tag{4.37}$$

$$m^2_{U_R} = m^2_R - 1(g_4^2 - 2g_{2R}^2)D_H^2 + \begin{pmatrix} q_{R1} & & \\ & q_{R2} & \\ & & q_{R3} \end{pmatrix} g_F^2 D_\theta^2 \ , \tag{4.38}$$

$$m^2_{D_R} = m^2_R - 1(g_4^2 + 2g_{2R}^2)D_H^2 + \begin{pmatrix} q_{R1} & & \\ & q_{R2} & \\ & & q_{R3} \end{pmatrix} g_F^2 D_\theta^2 \ , \tag{4.39}$$

$$m^2_{E_R} = m^2_R + 1(3g_4^2 - 2g_{2R}^2)D_H^2 + \begin{pmatrix} q_{R1} & & \\ & q_{R2} & \\ & & q_{R3} \end{pmatrix} g_F^2 D_\theta^2 \ , \tag{4.40}$$

$$m^2_{N_R} = m^2_R + 1(3g_4^2 + 2g_{2R}^2)D_H^2 + \begin{pmatrix} q_{R1} & & \\ & q_{R2} & \\ & & q_{R3} \end{pmatrix} g_F^2 D_\theta^2 \ , \tag{4.41}$$

$$m^2_{h_u} = m^2_{h_2} - 2g_{2R}^2 D_H^2 \ , \tag{4.42}$$

$$m^2_{h_d} = m^2_{h_1} + 2g_{2R}^2 D_H^2 \ . \tag{4.43}$$

The charges q_{Li}, q_{Rj} are the charges under $U(1)_F$ of F_i and $\overline{F}_j$ respectively, as shown in Table 3.8 for Model 1. We now choose an explicit example for both the left- and right-handed sectors using the $U(1)_F$ family charges for the left- and right-handed

fields for Model 1:

$$m^2_{L_L} = m^2_L - 1(3g_4^2)D_H^2 + \begin{pmatrix} 11/6 & 0 & 0 \\ 0 & 5/6 & 0 \\ 0 & 0 & 5/6 \end{pmatrix} g_F^2 D_\theta^2 \,, \tag{4.44}$$

$$m^2_{E_R} = m^2_R + 1(3g_4^2 - 2g_{2R}^2)D_H^2 + \begin{pmatrix} 19/6 & 0 & 0 \\ 0 & 7/6 & 0 \\ 0 & 0 & -5/6 \end{pmatrix} g_F^2 D_\theta^2 \,. \tag{4.45}$$

For Model 2, the sparticle mass matrices are the same as those before, Eqs. (4.36) – (4.41), but with the Model 2 charges in Table 3.10 instead of the Model 1 charges. So to show an explicit example for both the left- and right-handed sectors, we replace the $U(1)_F$ charges in Eqs. (4.44) and (4.45), so we can again clearly see the role played by the $U(1)_F$ family charges – this time for Model 2:

$$m^2_{L_L} = m^2_L - 1(3g_4^2)D_H^2 + \begin{pmatrix} 1 & 0 & 0 \\ 0 & 1 & 0 \\ 0 & 0 & 1 \end{pmatrix} g_F^2 D_\theta^2 \,, \tag{4.46}$$

$$m^2_{E_R} = m^2_R + 1(3g_4^2 - 2g_{2R}^2)D_H^2 + \begin{pmatrix} 3 & 0 & 0 \\ 0 & 1 & 0 \\ 0 & 0 & -1 \end{pmatrix} g_F^2 D_\theta^2 \,. \tag{4.47}$$

The correction factors D_θ^2, D_H^2 are calculated explicitly in Section 3.4 in terms of the gauge couplings and soft masses as[6]

$$D_H^2 = \frac{1}{4g_{2R}^2 + 6g_4^2}\left[m_H^2 - m_{\overline{H}}^2 + q_H(m_\theta^2 - m_{\overline{\theta}}^2)\right] \,, \tag{4.48}$$

$$D_\theta^2 = \frac{m_\theta^2 - m_{\overline{\theta}}^2}{2g_F^2} \,. \tag{4.49}$$

[6] q_H is defined to be $-q_{R3}$, thus $q_H = \frac{5}{6}$ for Model 1 and $q_H = 1$ for Model 2. See Section 3.4 for more details.

Thus we obtain the soft scalar masses for both Models 1 and 2 by using Eqs. (4.36) – (4.41), with the appropriate $U(1)_F$ charges in Tables 3.8 and 3.10, and using the correct D-terms of course.

The gauge couplings[7] and mass parameters in Eqs. (4.48) and (4.49) are predicted from the model, in terms of the X parameters and gravitino mass $m_{3/2}$ as shown in Eqs. (4.30) – (4.32) and Eqs. (4.51) – (4.53). Note that the D-terms will be zero if $X_S = X_{T_i}$, or if the $\overline{\theta}$ brane assignment is the same as θ. Choosing the second of these conditions is useful since it gives a comparison case where there are no $U(1)_F$ D-terms, ($D_\theta = 0$). This comparison will make the D-term contribution to flavour violation immediately apparent.

4.3.4 Magnitude of D_θ-terms for different $\overline{\theta}$ assignments

The main point worth emphasising here is that in this string model the magnitudes of the D-terms are *calculable*. We have assumed throughout that the FN field θ is an intersection string state $C^{5_1 5_2}$, but have not specified the string assignment of $\overline{\theta}$. Thus $m^2_{\overline{\theta}}$ takes various values depending on the string assignment for $\overline{\theta}$.

From Eq. (4.49), we see that we have calculable D_θ-terms,

$$2g_F^2 D_\theta^2 = m_\theta^2 - m_{\overline{\theta}}^2 \,, \tag{4.50}$$

so the value of D_θ^2 depends on the choice of where the $\overline{\theta}$ field lives. We use Table 3.1 and Eqs. (4.27) – (4.35) to quantify the D_θ-term for each possible $\overline{\theta}$ string assignment. As θ always lives at the intersection $C^{5_1 5_2}$, our first choice of $\overline{\theta}$ on $C^{5_1 5_2}$ is trivial: it gives $D_\theta^2 = 0$, as $m^2_{\overline{\theta}} = m^2_\theta$ in this case.

[7] We note that the factors of g_F^2 appearing in the mass matrices are cancelled by the $\frac{1}{g_F^2}$ in the definition of D_θ^2, so the size of the coupling for the $U(1)_F$ gauge group does not affect the size of the scalar masses.

For $\overline{\theta}$ on $C_1^{5_1}$, $m_{\overline{\theta}}^2$ is equivalent to m_h^2, as this is also on $C_1^{5_1}$. So using Eq. (4.29) for $m_{\overline{\theta}}^2$ and Eq. (4.32) for m_{θ}^2 in Eq. (4.50), we have

$$C_1^{5_1} \quad : \quad 2g_F^2 D_\theta^2 = \frac{3}{2} m_{3/2}^2 (X_S^2 - X_{T_3}^2) \ . \tag{4.51}$$

Similarly, the other two choices yield

$$C_2^{5_1} \quad : \quad 2g_F^2 D_\theta^2 = -\frac{3}{2} m_{3/2}^2 (X_S^2 - X_{T_3}^2) \ , \tag{4.52}$$

$$C_3^{5_1} \quad : \quad 2g_F^2 D_\theta^2 = -\frac{3}{2} m_{3/2}^2 (X_S^2 - X_{T_2}^2) \ . \tag{4.53}$$

In this thesis, all models use $X_{T_3}^2 = X_{T_2}^2 = X_{T_1}^2 = X_T^2$, so Eqs. (4.52) and (4.53) are equal to each other, and opposite in sign to Eq. (4.51).

4.3.5 Soft gaugino masses

The soft gaugino masses are the same as in [49], which we quote here for completeness. The results follow from Eq. (2.10) applied to the $\mathrm{SU}(4) \otimes \mathrm{SU}(2)_L \otimes \mathrm{SU}(2)_R$ gauginos, which then mix into the $\mathrm{SU}(3) \otimes \mathrm{SU}(2)_L \otimes \mathrm{U}(1)_Y$ gauginos whose masses are given by

$$M_3 = \frac{\sqrt{3} m_{3/2}}{(T_1 + \overline{T}_1) + (T_2 + \overline{T}_2)} \left[(T_1 + \overline{T}_1) X_{T_1} + (T_2 + \overline{T}_2) X_{T_2} \right] \ , \tag{4.54}$$

$$M_2 = \sqrt{3} m_{3/2} X_{T_1} \ , \tag{4.55}$$

$$M_1 = \frac{\sqrt{3} m_{3/2}}{\frac{5}{3}(T_1 + \overline{T}_1) + \frac{2}{3}(T_2 + \overline{T}_2)} \left[\frac{5}{3} (T_1 + \overline{T}_1) X_{T_1} + \frac{2}{3} (T_2 + \overline{T}_2) X_{T_2} \right] \ . \tag{4.56}$$

The values of $T_1 + \overline{T}_1$ and $T_2 + \overline{T}_2$ are proportional to the brane gauge couplings g_{5_1} and g_{5_2}, which are related in a simple way to the MSSM couplings at the unification scale, as shown by Eqs. (4.21). This is discussed in [49].

When we run the MSSM gauge couplings up and solve for g_{5_1} and g_{5_2} we find that approximate gauge coupling unification is achieved by $T_1 + \overline{T_1} \gg T_2 + \overline{T}_2$. Then we find the simple approximate result

$$M_1 \approx M_3 \approx M_2 = \sqrt{3} m_{3/2} X_{T_1} \ . \tag{4.57}$$

4.3.6 Soft trilinear couplings

So far we have considered the scalar masses and the gaugino masses. The gaugino masses are the same as in [49]. The soft masses have had both D_H and D_θ contributions added onto the base values from [49]. The contributions to the soft masses and gaugino masses from the FN and heavy Higgs auxiliary fields are completely negligible due to the small size of their F-terms. However, for the soft trilinear masses these contributions are of order $\mathcal{O}(m_{3/2})$ despite having small F-terms, so FN and Higgs contributions will give very important additional contributions beyond those considered in [49].

From Section 2.2.1 we see that the canonically normalised equation for the trilinear is

$$A_{abc} = F_I \left[\overline{K}_I + \partial_I \ln Y_{abc} - \partial_I \ln \left(\tilde{K}_a \tilde{K}_b \tilde{K}_c \right) \right] , \tag{4.58}$$

where $I, J = h, C_a$, so we also sum over all the hidden sector fields $S, T_i, H, \overline{H}, \theta$.

This general form for the trilinear accounts for contributions from non-moduli F-terms. These contributions are, in general, expected to be of the same magnitude as the moduli contributions despite the fact that the non-moduli F-terms are much smaller [21]. Specifically, if the Yukawa hierarchy is taken to be generated by a FN field, θ such that $Y_{ij} \sim \theta^{p(i,j)}$, then we expect $F_\theta \sim m_{3/2}\theta$, and then $\Delta A_{ij} = F_\theta \partial_\theta \ln Y_{ij} \sim p(i,j)\, m_{3/2}$ and so even though these fields are expected to have heavily sub-dominant F-terms[8] they contribute to the trilinears at the same order $\mathcal{O}(m_{3/2})$ as the moduli, but in a flavour off-diagonal way.

In the specific D-brane model of interest here, the general results for soft trilinear masses, including the contributions for general effective Yukawa couplings are given in Appendix A. From Eqs. (3.58) and (3.59) we can read off the effective Yukawa

[8] In our model the FN and heavy Higgs VEVs are of order the unification scale, compared to the moduli VEVs which are of order of the Planck scale.

couplings,

$$Y_{hF\overline{F}}hF\overline{F} \equiv \underbrace{(c)^{\beta\gamma}_{\alpha\rho}(r)^{xz}_{yw}\overline{H}_{\gamma z}H^{\rho w}\theta^{p}}_{Y^{\beta x}_{hF\overline{F}\alpha y}} h^{y}_{a}F^{\alpha a}\overline{F}_{\beta x} \ . \tag{4.59}$$

Note the extra group indices that the effective Yukawa coupling $Y^{\beta x}_{hF\overline{F}\alpha y}$ has, and proper care must be taken of the tensor structure when deriving trilinears from a given operator. We can write down the trilinear soft masses, A, by substituting the operators in Eq. (3.62) into the results in Appendix A. Having done this we find the result:[9]

$$A = \sqrt{3}m_{3/2}\begin{bmatrix} d_1+d_H+p(i,j)d_\theta & d_1+d_H+p(i,j)d_\theta & d_2+d_H+p(i,j)d_\theta \\ d_1+d_H+p(i,j)d_\theta & d_1+d_H+p(i,j)d_\theta & d_2+d_H+p(i,j)d_\theta \\ d_3+d_H+p(i,j)d_\theta & d_3+d_H+p(i,j)d_\theta & d_4 \end{bmatrix} , \tag{4.60}$$

where

$$d_1 = X_S - X_{T_1} - X_{T_2} \ , \tag{4.61}$$

$$d_2 = \frac{1}{2}X_S - X_{T_1} - \frac{1}{2}X_{T_2} \ , \tag{4.62}$$

$$d_3 = \frac{1}{2}X_S - X_{T_1} - X_{T_2} + \frac{1}{2}X_{T_3} \ , \tag{4.63}$$

$$d_4 = -X_{T_1} \ , \tag{4.64}$$

$$d_H = (S+\overline{S})^{\frac{1}{2}}X_H + (T_3+\overline{T}_3)^{\frac{1}{2}}X_{\overline{H}} \ , \tag{4.65}$$

$$d_\theta = (S+\overline{S})^{\frac{1}{4}}(T_3+\overline{T}_3)^{\frac{1}{4}}X_\theta \ . \tag{4.66}$$

These results are independent of which brane assignment we give $\overline{\theta}$.

4.4 Numerical procedure

The code used to generate all the data here was based on SOFTSUSY [59], which is a program that accurately calculates the spectrum of superparticles in the MSSM. [59]

[9] We assume that a $(3,3)$ Yukawa coupling appears at renormalisable order. This is why the A_{33} doesn't include contributions from d_H and d_θ.

is a manual on how the basic SOFTSUSY program works, written by the author of SOFTSUSY. Note though that this version does not include any changes discussed here, and there have been several updates to SOFTSUSY since the version used here was published. It solves the renormalisation group equations with theoretical constraints on soft supersymmetry breaking terms provided by the user. Successful radiative electroweak symmetry breaking is used as a boundary condition, as are weak-scale gauge coupling and fermion mass data (including one-loop finite MSSM corrections). The program can also calculate a measure of fine-tuning. The program structure has, in this case, been adapted to the extension of the MSSM considered in this paper. It is modified to include right-handed neutrino fields, and thus non-zero neutrino masses and mixing angles, generated via the SUSY see-saw mechanism. It is also set up to include the new D-term contributions considered herein, and to run over a series of string assignments for the $\overline{\theta}$ field. We use $\tan\beta \approx 50$ for all models and cases.

Once the code was ready to produce data for the new models, a lot of tests were run and we eventually found out that the spike feature of the figures in [54] was unphysical. We found that the equation governing the fundamental VEV on which all masses in the calculation were based became imaginary, due to a tachyonic Z mass. The scale dependent Z mass VEV is proportional the square root of the sum of the squared Z mass (at the electroweak scale) and its scale dependent self-energy. The first is a positive contribution and the second is a negative contribution. When the code is run up in energy scale, the self-energy of the Z boson increases in magnitude, but the square mass stays constant, as it is at a fixed energy scale. This means that the self-energy comes closer in magnitude to the squared Z mass, and as it had the opposite sign, it grows closer to cancelling out the value of the square Z mass. Thus the number in the square root decreases in value to zero, more rapidly the smaller it gets. This

causes the branching ratios to suddenly spike up in a smooth but exponentially rapid fashion. When the self-energy of the Z boson grows larger than its squared mass at the electroweak scale we are left with a tachyonic Z boson, as we would have a negative mass-squared for the scale dependent VEV, and the square root would become imaginary. The computer program would then automatically set the self energy to zero, causing the branching ratios to immediately drop down several orders of magnitude, and the VEV would then become a preordained constant value leading to the unexplained plateau after the spike observed in earlier work [54]. As there is a tachyonic Z boson and an imaginary VEV with which to compute the masses of the sparticles, the physics must break down at this scale.

Electroweak symmetry breaking provides a significant constraint on the results. The breakdown of electroweak symmetry breaking was responsible for the 'spike' feature that was shown in the plots for benchmark points A and B in [54]. For the data above the spike, radiative electroweak symmetry breaking does not work properly, as the Z boson mass becomes tachyonic. In the work carried out here, such 'bad' regions where electroweak symmetry breaking fails are cut-off, however there is still a remnant of the spike left, which is why one can see a slight rise at the ends of the plots for our benchmark points A and B, as can be seen in Section 4.5. For completeness we include the relevant plots from [54] to show the contrast with the new results computed for this thesis. These plots demonstrate the erroneous spike and plateau features, and can be found in Figures 4.1 and 4.2.

4.4.1 Varying brane assignments for $\overline{\theta}$

The θ field is fixed to reside on the $C^{5_1 5_2}$ brane, but we allow the brane assignment of $\overline{\theta}$ to vary. This means we can derive D-terms that are calculable, not free parameters.

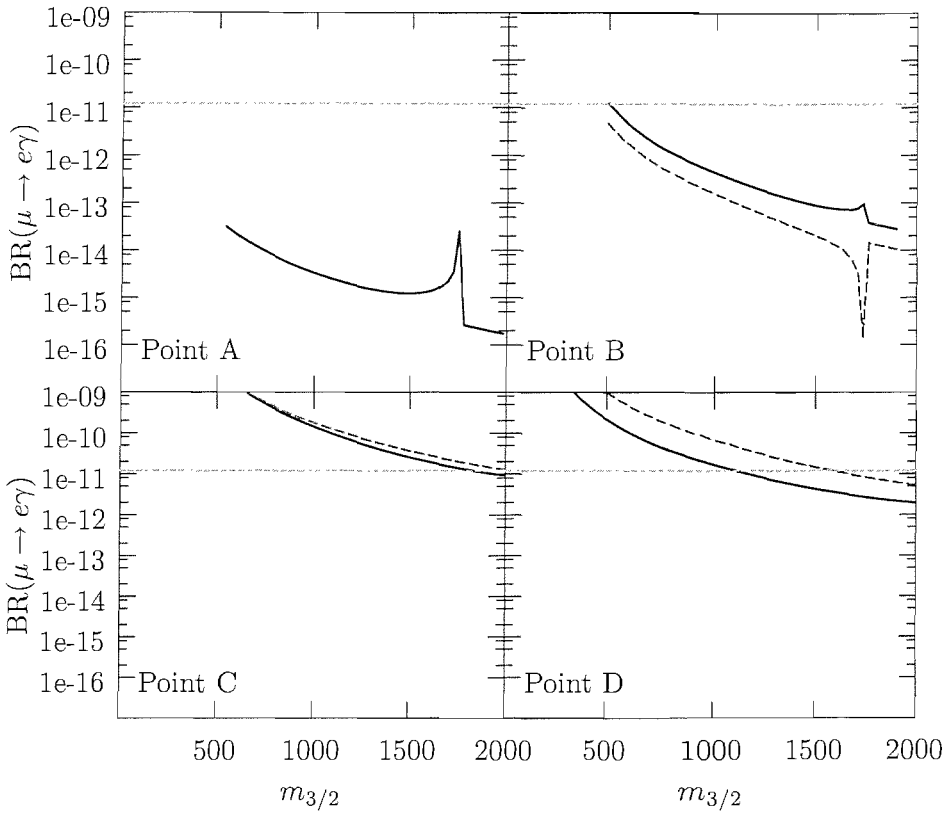

Figure 4.1: BR($\mu \to e\gamma$) for points A-D in Model 1 of [54] as shown by the solid line. The dashed line represents an unphysical model with no right-handed neutrino field whose purpose is only comparison in [54]. The horizontal line is the 2002 experimental limit from [4]. $m_{3/2}$ is in GeV.

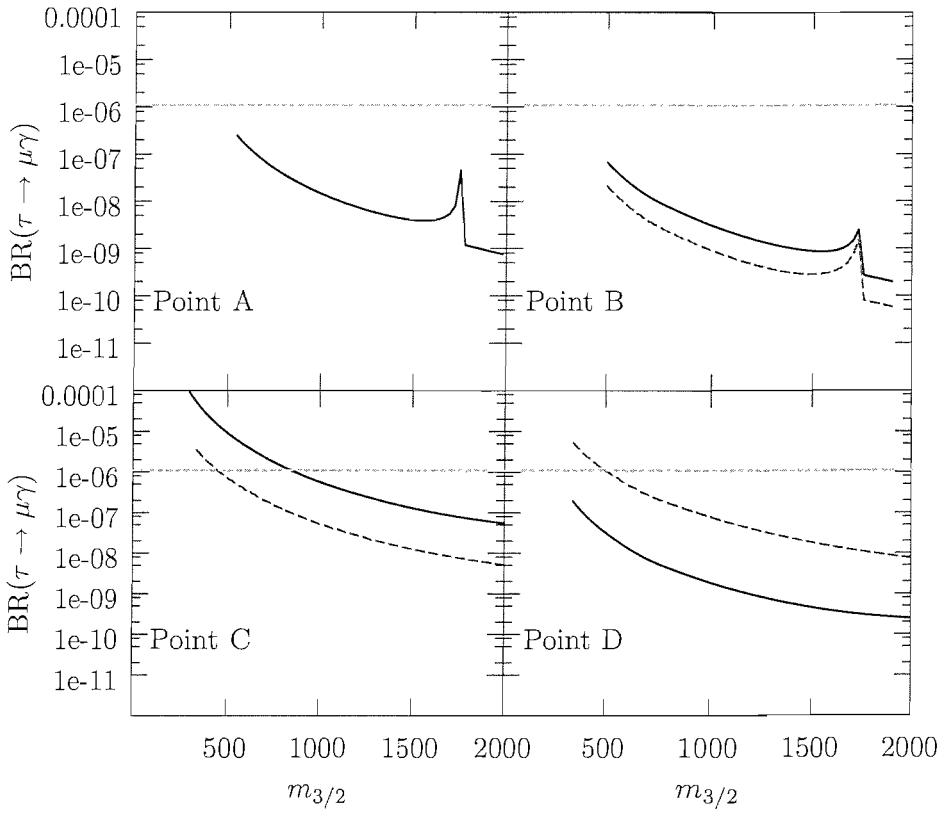

Figure 4.2: BR($\tau \to \mu\gamma$) for points A-D in Model 1 of [54] as shown by the solid line. The dashed line represents an unphysical model with no right-handed neutrino field whose purpose is only comparison in [54]. The horizontal line is the 2002 experimental limit from [4]. $m_{3/2}$ is in GeV.

Possibilities include $C^{5_1 5_2}$, $C_1^{5_1}$, $C_2^{5_1}$ and $C_3^{5_1}$. Since the assignment of $\overline{\theta}$ to $C^{5_1 5_2}$ means that it is at the intersection, along with the θ field, the $U(1)_F$ D-term calculated for this case would be zero. The other possibilities, as given in Eqs. (4.51) - (4.53), will highlight the contribution of the D-terms to lepton flavour violation.

4.5 Results

4.5.1 Benchmark points

Since the parameter space for the models is reasonably expansive, and the intention is to compare different sources of LFV, it is convenient to first consider four benchmark points, as follows. It should be noted that for all these points we have taken all X_{T_i} to be the same, $X_{T_i} = X_T$, and also $X_H = X_{\overline{H}}$. $X_{\overline{\theta}}$ is taken to be zero throughout.

Point	X_S	X_T	X_H	$X_{\overline{H}}$	X_θ	$X_{\overline{\theta}}$
A	0.500	0.500	0.000	0.000	0.000	0.000
B	0.535	0.488	0.000	0.000	0.000	0.000
C	0.270	0.270	0.000	0.000	0.841	0.000
D	0.270	0.270	0.595	0.595	0.000	0.000

Table 4.1: Values of the X parameters for the four benchmark points, A-D.

- Point A is referred to as 'minimum flavour violation'. At the point $X_S = X_T$ the scalar mass matrices m^2 are proportional to the identity, and the trilinears $\tilde{A}$ are aligned with the Yukawas. If we look back to Eqs. (4.48) and (4.49) for the D-terms, with Eqs. (4.30), (4.31) and (4.32) for m_H^2, $m_{\overline{H}}^2$ and m_θ^2, using Eqs. (4.51) - (4.53) for $m_{\overline{\theta}}^2$, we see that the D-terms depend on the difference between X_S and X_T. So with $X_S = X_T$, which is the case for point A (and points C and D) we see

that the value of both D-term contributions is zero $D_\theta^2 = 0 = D_H^2$, since the four relevant soft masses are degenerate at this point, $m^2_{C^{5_1 5_2}} = m^2_{C_1^{5_1}} = m^2_{C_2^{5_1}} = m^2_{C_3^{5_1}}$. As such, both m^2 and $\tilde{A}$ will be diagonal in the SCKM basis in the absence of the RH neutrino field.

- Point B is referred to as 'SUGRA'. With $X_S \neq X_T$ it represents typical flavour violation from the moduli fields; this is the amount of flavour violation that would traditionally have been expected with no contribution from the F_H or F_θ fields. This and benchmark point E are the only points investigated where $D_\theta^2 \neq 0$, and are consequently of most interest here.

- Point C is referred to as 'FN flavour violation'. It represents flavour violation from the Froggatt-Nielsen sector on its own, without any contribution to flavour violation from traditional SUGRA effects, since $X_S = X_T$ as in point A.

- Point D is referred to as 'heavy Higgs flavour violation'. It represents flavour violation from the heavy Higgs sector, without any contribution from either traditional SUGRA effects, since $X_S = X_T$, or from FN fields, since $F_\theta = 0$.

Since the intention is to explore the effect of the $U(1)_F$ D-terms on lepton flavour violating processes, it is convenient to define a new benchmark point E, that is a deviation from point B and consequently has $D_\theta^2 \neq 0$.

- Point E combines features of points B and C, resulting in Froggatt-Nielsen flavour violation from $X_\theta \neq 0$ as in point C, with SUGRA flavour violation from $X_S \neq X_T$ as in point B. This is the only point where we see the joint effect of lepton flavour violation from the Froggatt-Nielsen fields and the $U(1)_F$ D-terms appearing at the same time. The numerical values for this point were obtained by taking the

Point	X_S	X_T	X_H	$X_{\overline{H}}$	X_θ	$X_{\overline{\theta}}$
B	0.535	0.488	0.000	0.000	0.000	0.000
C	0.270	0.270	0.000	0.000	0.841	0.000
E	0.290	0.264	0.000	0.000	0.841	0.000

Table 4.2: Values of the X parameters for the two benchmark points of interest, B and E. Benchmark point C is included to show how point E is created – by taking the ratio of X_S to X_T from point B and applying it to point C.

ratio of X_S and X_T for benchmark point B and applying it to benchmark point C. We note that the $\overline{\theta}$ field has the same string assignments to each of the 5_i-branes as before, $C^{5_1 5_2}$, $C_1^{5_1}$, $C_2^{5_1}$ and $C_3^{5_1}$. The D-terms are then calculated accordingly using Eqs. (3.55), (3.56), and (3.57), with the $U(1)_F$ charges for Model 1 and Model 2 as in Tables 3.8 and 3.10.

We could have presented similar plots for a new benchmark point F, which is an amalgamation of points B and D, but this produces the same kind of results as for point E, telling us that there is a similar interplay between the flavour violating effects arising from the heavy Higgs F-terms and the D-terms as there is between the Froggatt-Nielsen F-terms and the D-terms of benchmark point E. As this does not give any further insight we do not present the results here. For completeness we quote the values for the X parameters for benchmark point F in Table 4.3.

4.5.2 Numerical results with Yukawa texture zeros

We have now defined our first model, Model 1, and a set of four benchmark points in Table 4.1 to examine within the model. We have also listed all the possible brane

Point	X_S	X_T	X_H	$X_{\overline{H}}$	X_θ	$X_{\overline{\theta}}$
D	0.270	0.270	0.595	0.595	0.000	0.000
F	0.290	0.264	0.595	0.595	0.000	0.000

Table 4.3: Values of the X parameters for a possible benchmark point F. Benchmark point D is included to show how point F is created – by taking the ratio of X_S to X_T from point B and applying it to point D.

assignments for the $\overline{\theta}$ field, which yield different D-term contributions to the soft scalar mass matrices.The branching ratio for $\tau \rightarrow e\gamma$ is not shown here as it does not constrain us beyond those limits placed by $\mu \rightarrow e\gamma$ and $\tau \rightarrow \mu\gamma$. The current experimental limit for $\tau \rightarrow e\gamma$, at 2.7×10^{-6}, is in fact far above the predicted rate for this process at all examined parts of the parameter space. The experimental limits used in the plots for BR($\tau \rightarrow \mu\gamma$) and BR($\mu \rightarrow e\gamma$) are 6.8×10^{-8} and 1.2×10^{-11} respectively.

In the following plots, we do not consider the $\overline{\theta}$ assignment to $C_3^{5_1}$ as this is exactly the same as $C_2^{5_1}$, due to the degeneracy of the X_{T_i}. Were we to allow the X_{T_i} to be non-degenerate, the phenomenological results of assigning $\overline{\theta}$ to $C_2^{5_1}$ and $C_3^{5_1}$ would not be the same. The detailed spectrum will look different at each parameter point, but the general trend is for the physical masses to increase in magnitude as the gravitino mass increases, thus the branching ratios for these events decrease. Thus too-high gravitino masses will start to reintroduce the fine-tuning problem resulting from the gluino mass being too high [72], although we shall not discuss the detailed spectrum here. In the next section we will vary the values of the $(1,2)$ and $(1,3)$ electron Yukawa elements to give relative enhancement/suppression of the D-terms. We will also use Model 2 and benchmark point E which we do not consider in this section.

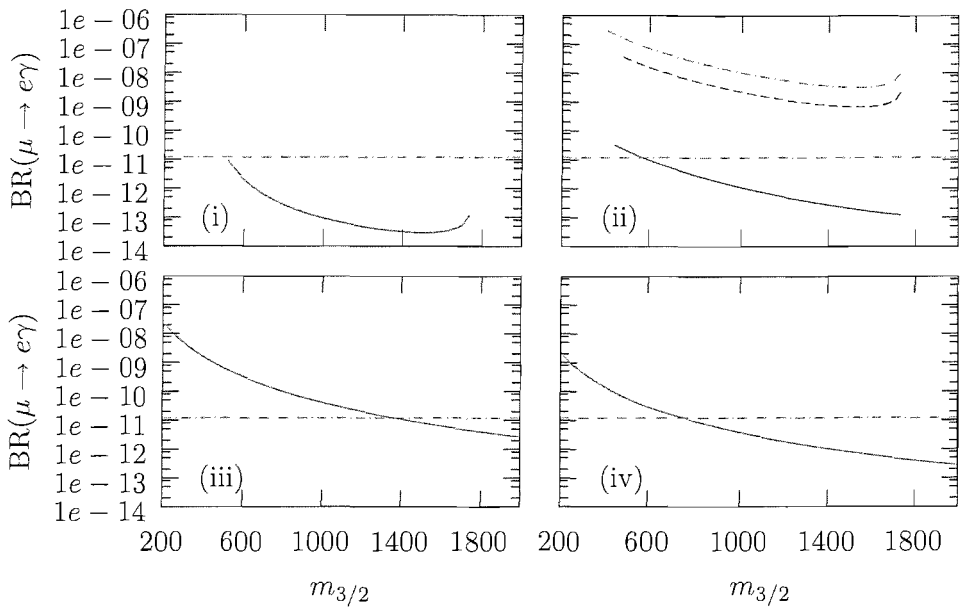

Figure 4.3: Plots showing the Branching Ratio for $\mu \to e\gamma$ for Model 1. Panel (i) corresponds to benchmark point A, panel (ii) is for B, panel (iii) is for C and panel (iv) is for D. The $\overline{\theta}$ assignments are shown with the separate lines: $C^{5_1 5_2}$ (*solid*), $C_1^{5_1}$ (*dashed*), and $C_2^{5_1}$ (*dot-dash*). The 2002 experimental limit [4] is also given by the horizontal line. $m_{3/2}$ is in GeV.

Figure 4.3 shows numerical results for BR($\mu \rightarrow e\gamma$) for Model 1, plotted against the gravitino mass $m_{3/2}$, where each of the four panels (i) – (iv) correspond to each of the four benchmark points A – D. As the gravitino mass $m_{3/2}$ increases, the sparticle spectrum becomes heavier. This will look different at each parameter point, but the physical masses are expected to be of the same order of magnitude as the gravitino mass. As such, high gravitino masses will start to reintroduce the fine-tuning problem of the gluino mass being too high. The solid line on each plot in Figure 4.3 corresponds to the solid lines in Figure 1 of [54], shown above in Figure 4.1. However there were errors in the code used to generate the previous data, and the corrected rates shown here differ to the previous results by up to two orders of magnitude. Furthermore, unlike the results in [54], the results here do not exhibit a sharp spike for benchmark points A and B. For the data above the spike, radiative electroweak symmetry breaking does not work properly, as the Z boson mass becomes tachyonic. This was not realized in the previous analysis.

Panel (i) of Figure 4.3 refers to benchmark point A, corresponding to minimum flavour violation, where the only source of LFV is from the see-saw mechanism, which for Model 1 is well below the experimental limit, shown as the horizontal dot-dash line. Panel (ii) of Figure 4.3 refers to benchmark point B, which has LFV arising from SUGRA, with the FN and heavy Higgs sources of LFV switched off. In this case one can clearly distinguish the additional contributions to LFV arising from the D-terms. This makes benchmark point B the most phenomenologically interesting for the purposes of this study. The differing contributions stem from the $\overline{\theta}$ string assignments, which are shown by the separate lines: $C^{5_1 5_2}$ (*solid*), $C_1^{5_1}$ (*dashed*), and $C_2^{5_1}$ (*dot-dash*). The $C^{5_1 5_2}$ case shows the zero-D-term limit, where θ and $\overline{\theta}$ are both intersection states, and hence conspire to cancel out D_θ via their soft masses being degenerate, $m_\theta^2 - m_{\overline{\theta}}^2 = 0$.

The other two locations for $\overline{\theta}$ then turn on the D_θ-term contributions. With the D-terms switched on, Model 1 is experimentally ruled out over all parameter space shown here. Panel (iii) of Figure 4.3, referring to benchmark point C, is the Froggatt-Nielsen benchmark point, and for this case we see that the experimental limit is satisfied for $m_{3/2}$ over 1400 GeV. This is a correction to the previous results in [54], that brings the predicted rate half an order of magnitude lower. Panel (iv) of Figure 4.3, benchmark point D, shows the heavy Higgs point, for which the experimental limit is satisfied everywhere above 800 GeV. Note that the predictions in this figure are lower than the corresponding figure in [54] due to the corrected values of S, T_3, as discussed in Section 4.3.1.

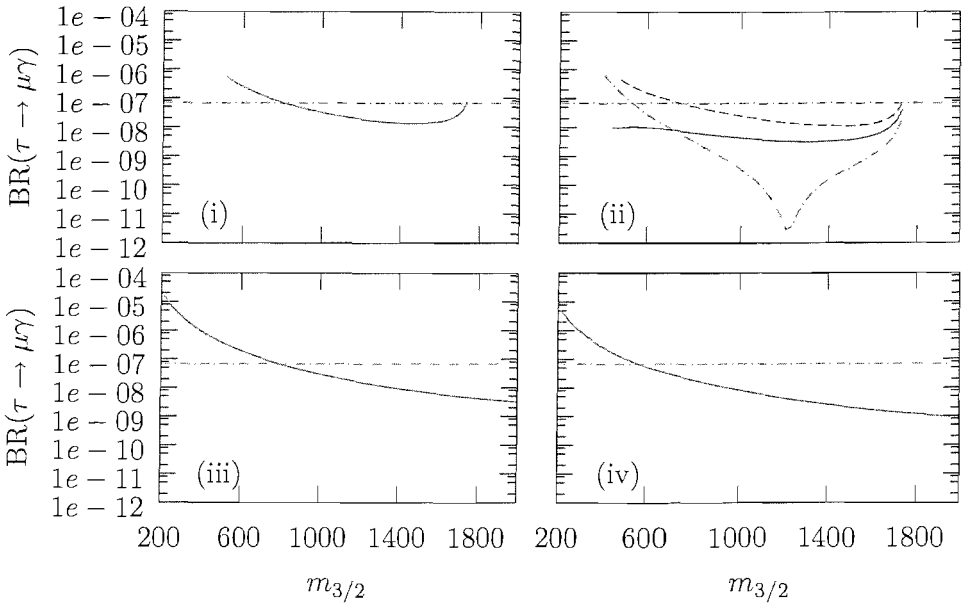

Figure 4.4: Plots showing the Branching Ratio for $\tau \to \mu\gamma$ for Model 1. Panel (i) corresponds to benchmark point A, panel (ii) is for B, panel (iii) is for C and panel (iv) is for D. The $\overline{\theta}$ assignments are shown with the separate lines: $C^{5_1 5_2}$ (*solid*), $C_1^{5_1}$ (*dashed*), and $C_2^{5_1}$ (*dot-dash*). The 2005 experimental limit [73] is also given by the horizontal line. $m_{3/2}$ is in GeV.

Figure 4.4 shows analogous results for BR($\tau \to \mu\gamma$) for Model 1, plotted against the

gravitino mass $m_{3/2}$. All benchmark points come below the experimental limit for a substantial amount of the parameter space. The experimental limit here is more recent, and subsequently much more stringent than the previous limit. For these models in which there is a large (2,3) element in the neutrino Yukawa matrix the branching ratio for $\tau \to \mu\gamma$ is essentially as constraining as that for $\mu \to e\gamma$, as first pointed out in [66]. The D-term coupling to right-handed scalars has a Yukawa mixing angle of order λ^3, compared to λ^2 for $\mu \to e\gamma$. $\lambda \approx 0.22$ is the Wolfenstein parameter, which contributes on an equal footing to ϵ and δ. So the right-handed sector is of equal importance to the left-handed sector. We note that the see-saw effect enters prominently in the left-handed sector, and by considering Eqs. (4.36) and (4.37) for the soft scalar masses in the $(2-3)$ sector for $\tau \to \mu\gamma$, one can show that there is little effect coming from the D-terms coupling to left-handed scalars, since we have universal family charges for the left-handed $(2-3)$ sector, $q_{L_2} = q_{L_3}$. For the right-handed scalars, however, the D-terms do play an important part and can have rather interesting and surprising effects, as we now discuss in some detail.

The solid line in panel (ii) of Figure 4.4 for the $C^{5_1 5_2}$ string assignment of $\overline{\theta}$ has zero contribution from the $U(1)_F$ D-terms, and shows just the effect of non-minimal SUGRA. This actually suppresses the flavour violation arising from the see-saw effect alone, showing an interesting cancellation between the LFV from the see-saw mechanism and the LFV from the non-universal SUGRA contributions. On the other hand the dashed line in panel (ii) for the $C_1^{5_1}$ case is very similar to the see-saw scenario of benchmark point A shown in panel (i). This is due to the D-terms actually conspiring to restore universality in the scalar masses, turning non-minimal SUGRA back into the minimal form. One can easily see this by applying Eq. (4.51) to Eqs. (4.38) – (4.41) for the right-handed scalar mass matrices, as the D-terms bring in an equal but opposite effect

to the non-universal effects from SUGRA, and subsequently force the mass matrices to become universal. It is an amazing consequence of this string assignment for $\overline{\theta}$ that in this model the effects of the non-universal $U(1)_F$ D-terms can exactly cancel the effects of the non-universal SUGRA for the branching ratio of $\tau \rightarrow \mu\gamma$, leading to *universal* scalar mass matrices, even with SUGRA turned on. This is a string effect that directly affects the amount of flavour violation predicted in this scenario. For the $C_2^{5_1}$ case shown by the dot-dash line, applying Eq. (4.52) to the right-handed scalar mass matrices Eqs. (4.38) – (4.41) shows that the D-terms in this case actually enhance the effect of non-minimal SUGRA, causing the scalar mass matrices to become even more non-universal.

Section 4.5.3 takes the points of interest raised in this section and expands upon them, exploring the second model with changes to the Yukawa textures in both models, and the extra benchmark point E that combines the flavour violation of benchmark points B and C – the joint effect of SUGRA and Froggatt-Nielsen flavour violation.

4.5.3 Numerical results with varying Yukawa textures

We have defined our second model, Model 2, and a further benchmark point in Table 4.2 with which to examine the model. We have also set up what we will be varying apart from the gravitino mass in this model – the values of Y_{12}^e and Y_{13}^e, and the brane assignment of $\overline{\theta}$ which gives different D-terms. In the following plots, we do not consider the $\overline{\theta}$ assignment to $C_3^{5_1}$ as this is exactly the same as $C_2^{5_1}$, due to the degeneracy of the X_{T_i}. Were we to allow the X_{T_i} to be non-degenerate, the phenomenological results of assigning $\overline{\theta}$ to $C_2^{5_1}$ and $C_3^{5_1}$ would not be the same.

Figure 4.5 shows benchmark point B for Model 1. The four panels show the Y_{12}^e and Y_{13}^e electron Yukawa elements being turned on and off. The results for Figure 4.5(i)

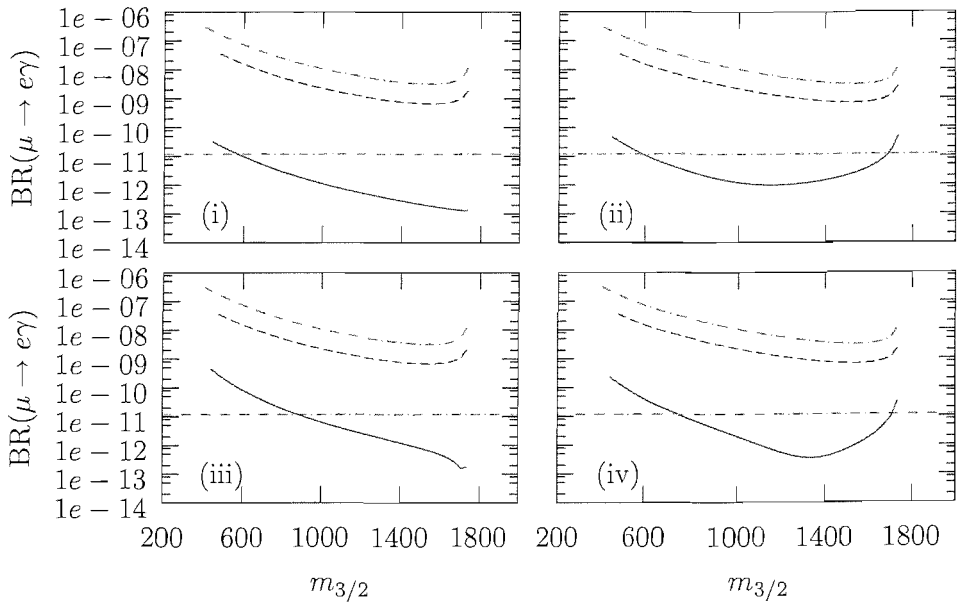

Figure 4.5: Plots showing the Branching Ratio for $\mu \to e\gamma$ for benchmark point B for Model 1 only. Panel (i) has $Y^e_{12} = 0$ and $Y^e_{13} = 0$. Panel (ii) has $Y^e_{12} = 1.5 \times 10^{-3}$ and $Y^e_{13} = 0$. Panel (iii) has $Y^e_{12} = 0$ and $Y^e_{13} = 1.5 \times 10^{-2}$. Panel (iv) has $Y^e_{12} = 1.5 \times 10^{-3}$ and $Y^e_{13} = 1.5 \times 10^{-2}$. The $\overline{\theta}$ assignments are shown with the separate lines: $C^{5_1 5_2}$ (*solid*), $C^{5_1}_1$ (*dashed*), and $C^{5_1}_2$ (*dot-dash*). The 2002 experimental limit [4] is also given by the horizontal line. $m_{3/2}$ is in GeV.

are for $Y^e_{12} = 0$ and $Y^e_{13} = 0$. This is the same as in Figure 4.3(ii), and is the base from which we start. Panel (ii) of Figure 4.5 has $Y^e_{12} = 1.5 \times 10^{-3}$ and $Y^e_{13} = 0$, so we can clearly see the effect of turning Y^e_{12} on. It only affects the $C^{5_1 5_2}$ line, as the D-terms dominate over this effect for the other two string assignments. Panel (iii) of Figure 4.5 uses $Y^e_{12} = 0$ and $Y^e_{13} = 1.5 \times 10^{-2}$, highlighting the effect of just Y^e_{13} alone. Again the zero D-term line of $C^{5_1 5_2}$ is the only one that is sizably affected by this change in Yukawa texture. Panel (iv) of Figure 4.5 shows the effect of turning on both Yukawa elements: $Y^e_{12} = 1.5 \times 10^{-3}$ and $Y^e_{13} = 1.5 \times 10^{-2}$. We see that the shape of the solid line is determined by both Yukawa textures – they seem to have an equal impact on it.

If we make the same changes and explore the effect of the Yukawa elements on Model 2, we see that it yields similar results to Model 1, and we need to investigate our fifth benchmark point in order to show the differences between these two models.

Figure 4.6 shows benchmark point E, which combines the features of benchmark points B and C, thus both $U(1)$ D-term and Froggatt-Nielsen flavour violation appear in the predicted branching ratios shown in this figure. There is some interesting interplay between the FN F-terms in the benchmark point C region of parameter space, and the D-terms in benchmark point B; benchmark point E is designed to show this difference. In Figure 4.6 the results are shown for Model 1 with both Y^e_{12} and Y^e_{13} Yukawa elements turned on and off. The shape of the curves are as in benchmark point C due to X_θ being turned on, and the results are numerically similar to those of benchmark point C, showing that the dominant contribution comes from Froggatt-Nielsen flavour violation. However, as in benchmark point B, the different D-terms corresponding to different $\overline{\theta}$ assignments leads to noticeable shifts in the results. In panel (i) with $Y^e_{12} = 0$ and $Y^e_{13} = 0$ it is seen that the presence of non-zero D-terms actually reduces the LFV rate somewhat compared to the solid curve with zero D-terms, corresponding to a region of

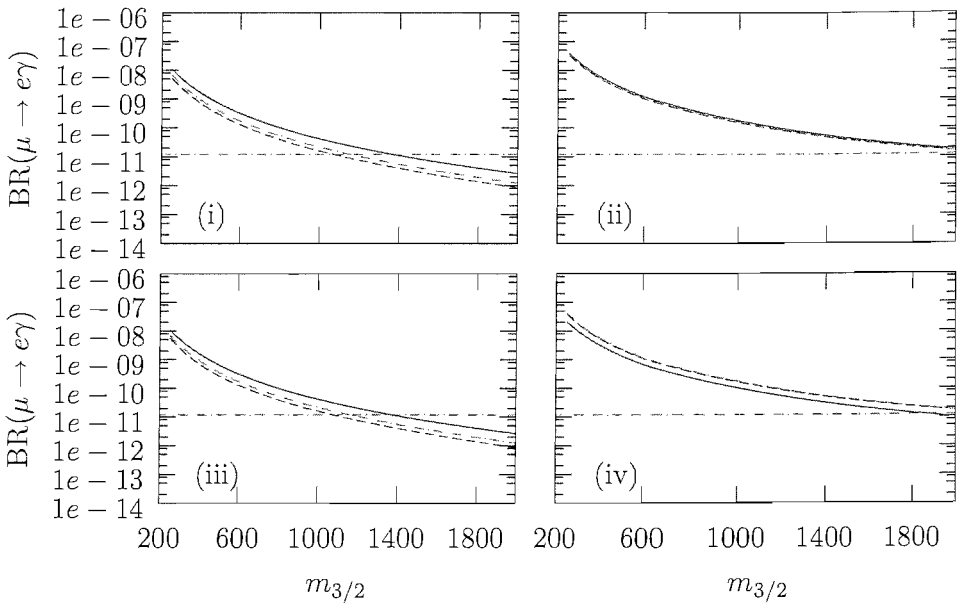

Figure 4.6: Plots showing the Branching Ratio for $\mu \to e\gamma$ for benchmark point E for Model 1 only. Panel (i) has $Y^e_{12} = 0$ and $Y^e_{13} = 0$. Panel (ii) has $Y^e_{12} = 1.5 \times 10^{-3}$ and $Y^e_{13} = 0$. Panel (iii) has $Y^e_{12} = 0$ and $Y^e_{13} = 1.5 \times 10^{-2}$. Panel (iv) has $Y^e_{12} = 1.5 \times 10^{-3}$ and $Y^e_{13} = 1.5 \times 10^{-2}$. The $\overline{\theta}$ assignments are shown with the separate lines: $C^{5_1 5_2}$ (*solid*), $C^{5_1}_1$ (*dashed*), and $C^{5_1}_2$ (*dot-dash*). The 2002 experimental limit [4] is also given by the horizontal line. $m_{3/2}$ is in GeV.

parameter space where there is some cancellation between the flavour violation from the Froggatt-Nielsen fields and that caused by the $U(1)_F$ D-terms. The other panels show variation of the Yukawa elements as in Figure 4.5, for example panel (iv) corresponds to both Y^e_{12} and Y^e_{13} Yukawa elements being non-zero. Note that the solid curve in panel (iv) is slightly lower than the solid curve in panel (ii), showing that sometimes a non-zero Yukawa coupling can reduce LFV.

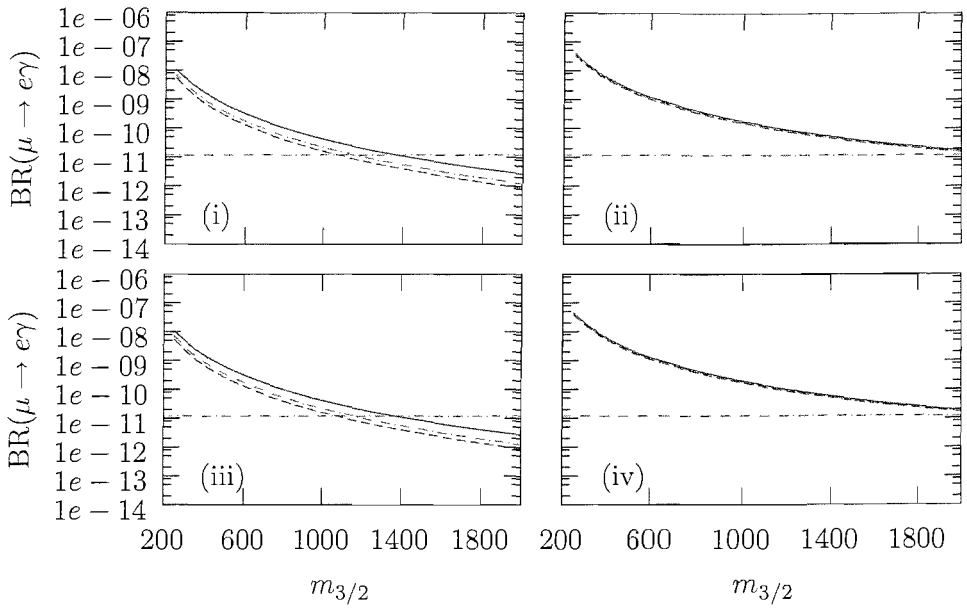

Figure 4.7: Plots showing the Branching Ratio for $\mu \to e\gamma$ for benchmark point E for Model 2 only. Panel (i) has $Y^e_{12} = 0$ and $Y^e_{13} = 0$. Panel (ii) has $Y^e_{12} = 1.5 \times 10^{-3}$ and $Y^e_{13} = 0$. Panel (iii) has $Y^e_{12} = 0$ and $Y^e_{13} = 1.5 \times 10^{-2}$. Panel (iv) has $Y^e_{12} = 1.5 \times 10^{-3}$ and $Y^e_{13} = 1.5 \times 10^{-2}$. The $\overline{\theta}$ assignments are shown with the separate lines: $C^{5_1 5_2}$ (*solid*), $C_1^{5_1}$ (*dashed*), and $C_2^{5_1}$ (*dot-dash*). The 2002 experimental limit [4] is also given by the horizontal line. $m_{3/2}$ is in GeV.

Figure 4.7 shows the effects of the Yukawa elements for benchmark point E using Model 2, where Model 2 has the same Yukawa structure as Model 1, but has the feature that the left-handed family charges are the same for all three families, resulting in universal D-terms in the left-handed sector. Comparing Figure 4.7 to Figure 4.6, we

see that in panel (i) of both figures with $Y^e_{12} = 0$ and $Y^e_{13} = 0$ there is no observable difference between the predictions of the two models. This is also the case for panels (ii) and (iii). This negligible difference between the branching ratios of $\mu \to e\gamma$ for Model 1 and Model 2 should not be surprising, since the texture zero coming from either (or both) element(s) will yield small mixing angles, resulting in small lepton flavour violation. However comparing panels (iv) of Figure 4.7 and Figure 4.6 we see that with non-zero Y^e_{12} and Y^e_{13}, the universal left-handed $U(1)_F$ family charges of Model 2 have the effect of reducing the LFV resulting from the D-terms.

4.6 Conclusions

We have investigated the impact of lepton flavour violation coming from a number of sources, including the D-terms associated with the breaking of an Abelian family symmetry in a D-brane inspired model based on supergravity mediated supersymmetry breaking. There are five sources of LFV in such models: see-saw induced, arising from the running effects of right-handed neutrino fields; supergravity, due to the non-universal structure of the supergravity model; FN (Higgs) flavour violation, due to the F-terms associated with FN (Higgs) fields developing VEVs, and contributing in a non-universal way to the soft trilinear terms; and finally, D-term flavour violation, where the D-term mass correction from the breaking of an Abelian family symmetry drives the scalar mass matrices to be non-universal.

In order to quantify the relative importance of these ways of generating lepton flavour violation, we studied a model based on a type I string-inspired Pati-Salam model with an Abelian family symmetry. We have derived the soft supersymmetry breaking terms, including the effect of the calculable D-terms associated with breaking the family symmetry. We then performed a numerical analysis of the five sources.

Supergravity and D-term flavour violation always appear together in these models.

Much work was done on the computer code that generates this data. Whole new cases for the string assignments needed to be created, new models for the $U(1)_F$ charge structure and varying Yukawa elements needed to be fitted into the existing program. The spike feature that appeared in previous work [54] had to be figured out – whether it was a physical threshold effect or an artifact of the code.

The most striking conclusion here is how dangerously large the calculable D-term contribution to flavour violation can be, at least for the class of models studied. However it should be emphasised that while the D-terms are calculable in these models they are also model dependent, and it is always possible to simply switch off the D-terms by selecting the $\overline{\theta}$ field to have the same string assignment as the θ intersection state. However other choices (when the $\overline{\theta}$ field is chosen to be fixed to the 5_1-brane) will lead to non-zero but calculable D-terms, which can be dangerously large, or can massively suppress flavour violation. For example the curves with non-zero D-terms in Figure 4.5 all exceed the experimental limit for the branching ratio for $\mu \to e\gamma$, showing that D-term effects have the potential to greatly exceed the other contributions to LFV from SUGRA, the see-saw mechanism, FN and Higgs, depending on the choice of Yukawa textures. However in some cases the D-terms generated by breaking the $U(1)_F$ family symmetry can actively suppress the branching ratio for $\mu \to e\gamma$, as shown in panels (i) and (iii) of Figures 4.6 and 4.7. Thus including non-zero $U(1)_F$ D-terms in this model helps to predict realistic supergravity models with reduced lepton flavour violation.

A notable feature is the effect of Yukawa texture on the results. The Yukawa texture has $Y^e_{12} = Y^e_{13} = 0$, and we have shown that turning on non-zero values of these Yukawa couplings can greatly enhance the branching ratio for $\mu \to e\gamma$ almost arbitrarily. The reason is that the rotations to the SCKM basis are controlled by these

Yukawa elements and the larger these rotations the larger will be the off-diagonal soft masses in the SCKM basis. The non-zero magnitudes of Y^e_{12} and Y^e_{13} were therefore chosen to be large enough to show the variations in the branching ratios of the different models, but small enough to keep within the currently experimentally allowed range.

In this thesis we have worked with a particular Yukawa texture in which there is a large (2,3) element in the neutrino Yukawa matrix leading to large see-saw induced LFV and a branching ratio for $\tau \to \mu\gamma$ which is as constraining as that for $\mu \to e\gamma$ [66]. However we have seen that in some cases the D-terms can lead to a large suppression of the rate for particular values of $m_{3/2}$, as seen in panel (ii) of Figure 4.4. For other cases the effects of the non-universal $U(1)_F$ D-terms can exactly cancel the effects of the non-universal SUGRA model leading to universal scalar mass matrices, thereby restoring universality even for a non-minimal SUGRA model. Such effects are only possible in certain string set-ups and thus LFV provides an observable signal which may discriminate between different underlying string models.

Chapter 5

Conclusions

Throughout this thesis we have considered a string inspired Pati-Salam model of intersecting D-branes supplemented by an additional $U(1)$ family symmetry. We studied the connections between the physics arising from this model and low energy observable physics in the context of unified supersymmetric theories. In particular, we explored the effect of new D-terms associated with the breaking of the family symmetry that had not previously been considered in the literature. We saw how they could cause dangerously large contributions to lepton flavour violating processes, exceeding experimental limits for the branching ratios of flavour changing processes, and in contrast how they could actively suppress the amount of flavour violation arising in certain scenarios.

In Chapter 1,we gave a general introduction to the physics of the Standard Model and its supersymmetric extensions. Then in Chapter 2 we introduced the formulae necessary to define the string inspired Pati-Salam model on which the models presented in Chapter 3 are based. In Chapter 3, we discussed the specific class of models that we investigated in this work, showing how to obtain the anomaly free $U(1)_F$ charges and how to derive the D-terms. We detailed the operator structure that was used in the numerical analysis, giving specific values that were used to generate the data. We

also outlined a second model that had universal $U(1)_F$ family charges in the left-hand sector, suppressing the $(1-2)$ sector flavour violation effects brought about by the $U(1)_F$ D-terms.

In Chapter 4 we catalogued and quantitatively studied the importance of all the different sources of LFV present in a general non-minimal SUGRA framework, including the effects of gauged family symmetry. We discussed five different sources of LFV in such models: see-saw induced LFV arising from the running effects of right-handed neutrino fields; supergravity induced LFV due to the non-universal structure of the supergravity model; FN (Higgs) flavour violation, due to the F-terms associated with FN (Higgs) fields developing VEVs, and contributing in a non-universal way to the soft trilinear terms; D-term flavour violation, where the D-term mass correction from the breaking of the Abelian family symmetry drives the scalar mass matrices to be non-universal; and finally the effects of different choices of Yukawa textures on LFV.

In order to quantify the importance of the different effects we investigated these disparate sources of LFV numerically, both in isolation and in association with one another, within a particular SUGRA model based on a type I string-inspired Pati-Salam model with an Abelian family symmetry, which has a sufficiently rich structure to enable all of the effects to be studied within a single framework. Within this framework we derived the soft supersymmetry breaking terms, including the effect of the D-terms associated with breaking the family symmetry. For these models the D-terms are calculable, but are model dependent, depending on a particular choice of string assignment for the FN fields, and in particular the D-terms are only non-zero for the non-universal SUGRA models. We performed a detailed numerical analysis of the five sources of LFV using five benchmark points designed to highlight the particular effects, and we explored the effect of the variation of Yukawa texture elements on the results.

In conclusion, we have seen that within realistic non-minimal supergravity models there can be several important effects leading to much larger LFV than in the case usually considered in the literature of minimum flavour violation corresponding to just mSUGRA and the see-saw mechanism, and considered here as benchmark point A. We find that the D-term contributions are generally dangerously large, but in certain cases such contributions can lead to a dramatic suppression of LFV rates, for example by cancelling the effect of the see-saw induced LFV in $\tau \longrightarrow \mu\gamma$ models with lop-sided textures. In the class of string models considered here we find the surprising result that the D-terms can sometimes serve to restore universality in the effective non-minimal supergravity theory, so our choice of string set-up at high energy scales can directly impact on the observable physics at low energy scales. Thus D-terms can give very large and very surprising effects in LFV processes, and the physics we observe at low energies can tell us about the underlying high energy theory.

In general there will be a panoply of different sources of LFV in realistic non-minimal SUGRA models, and we have explored the relative importance of some of them within a particular framework. The results here only serve to heighten the expectation that LFV processes such as $\mu \longrightarrow e\gamma$ and $\tau \longrightarrow \mu\gamma$ may be observed soon, although it is clear from our results that the precise theoretical interpretation of such signals will be more non-trivial than is apparent from many previous studies in the literature.

Appendix A

Parameterised Trilinears for the 42241 Model

We here write the general form of the trilinear parameters A_{ijk} assuming nothing about the form of the Yukawa matrices.

$$\begin{aligned} A_{C_1^{5_1} C^{5_1 5_2} C^{5_1 5_2}} &= \sqrt{3} m_{3/2} \left\{ X_S \left[1 + \left(S + \overline{S} \right) \partial_S \ln Y_{abc} \right] \right. \\ &+ X_{T_1} \left[-1 + \left(T_1 + \overline{T}_1 \right) \partial_{T_1} \ln Y_{abc} \right] \\ &+ X_{T_2} \left[-1 + \left(T_2 + \overline{T}_2 \right) \partial_{T_2} \ln Y_{abc} \right] \\ &+ X_{T_3} \left(T_3 + \overline{T}_3 \right) \partial_{T_3} \ln Y_{abc} \\ &+ X_H \left(S + \overline{S} \right)^{\frac{1}{2}} H \partial_H \ln Y_{abc} \\ &+ X_{\overline{H}} \left(T_3 + \overline{T}_3 \right)^{\frac{1}{2}} \overline{H} \partial_{\overline{H}} \ln Y_{abc} \\ &\left. + X_\theta \left(S + \overline{S} \right)^{\frac{1}{4}} \left(T_3 + \overline{T}_3 \right)^{\frac{1}{4}} \theta \partial_\theta \ln Y_{abc} \right\} . \end{aligned} \tag{A.1}$$

$$
\begin{aligned}
A_{C_1^{5_1} C_3^{5_1} C^{5_1 5_2}} &= \sqrt{3} m_{3/2} \Big\{ X_S \left[\frac{1}{2} + \left(S + \overline{S} \right) \partial_S \ln Y_{abc} \right] \\
&+ X_{T_1} \left[-1 + \left(T_1 + \overline{T}_1 \right) \partial_{T_1} \ln Y_{abc} \right] \\
&+ X_{T_2} \left(T_2 + \overline{T}_2 \right) \partial_{T_2} \ln Y_{abc} \\
&+ X_{T_3} \left[-\frac{1}{2} \left(T_3 + \overline{T}_3 \right) \partial_{T_3} \ln Y_{abc} \right] \\
&+ X_H \left(S + \overline{S} \right)^{\frac{1}{2}} H \partial_H \ln Y_{abc} \\
&+ X_{\overline{H}} \left(T_3 + \overline{T}_3 \right)^{\frac{1}{2}} \overline{H} \partial_{\overline{H}} \ln Y_{abc} \\
&+ X_\theta \left(S + \overline{S} \right)^{\frac{1}{4}} \left(T_3 + \overline{T}_3 \right)^{\frac{1}{4}} \theta \partial_\theta \ln Y_{abc} \Big\} \ . \qquad \text{(A.2)}
\end{aligned}
$$

$$
\begin{aligned}
A_{C_1^{5_1} C_2^{5_1} C^{5_1 5_2}} &= \sqrt{3} m_{3/2} \Big\{ X_S \left[\frac{1}{2} + \left(S + \overline{S} \right) \partial_S \ln Y_{abc} \right] \\
&+ X_{T_1} \left[-1 + \left(T_1 + \overline{T}_1 \right) \partial_{T_1} \ln Y_{abc} \right] \\
&+ X_{T_2} \left[-1 + \left(T_2 + \overline{T}_2 \right) \partial_{T_2} \ln Y_{abc} \right] \\
&+ X_{T_3} \left[\frac{1}{2} \left(T_3 + \overline{T}_3 \right) \partial_{T_3} \ln Y_{abc} \right] \\
&+ X_H \left(S + \overline{S} \right)^{\frac{1}{2}} H \partial_H \ln Y_{abc} \\
&+ X_{\overline{H}} \left(T_3 + \overline{T}_3 \right)^{\frac{1}{2}} \overline{H} \partial_{\overline{H}} \ln Y_{abc} \\
&+ X_\theta \left(S + \overline{S} \right)^{\frac{1}{4}} \left(T_3 + \overline{T}_3 \right)^{\frac{1}{4}} \theta \partial_\theta \ln Y_{abc} \Big\} \ . \qquad \text{(A.3)}
\end{aligned}
$$

$$
\begin{aligned}
A_{C_1^{5_1} C_2^{5_1} C_3^{5_1}} \;=\; & \sqrt{3} m_{3/2} \left\{ X_S \left(S + \overline{S} \right) \partial_S \ln Y_{abc} \right. \\
& + X_{T_1} \left[-1 + \left(T_1 + \overline{T}_1 \right) \partial_{T_1} \ln Y_{abc} \right] \\
& + X_{T_2} \left(T_2 + \overline{T}_2 \right) \partial_{T_2} \ln Y_{abc} \\
& + X_{T_3} \left(T_3 + \overline{T}_3 \right) \partial_{T_3} \ln Y_{abc} \\
& + X_H \left(S + \overline{S} \right)^{\frac{1}{2}} H \partial_H \ln Y_{abc} \\
& + X_{\overline{H}} \left(T_3 + \overline{T}_3 \right)^{\frac{1}{2}} \overline{H} \partial_{\overline{H}} \ln Y_{abc} \\
& \left. + X_\theta \left(S + \overline{S} \right)^{\frac{1}{4}} \left(T_3 + \overline{T}_3 \right)^{\frac{1}{4}} \theta \partial_\theta \ln Y_{abc} \right\} \; . \qquad \text{(A.4)}
\end{aligned}
$$

Appendix B

$n = 1$ Operators

The $n = 1$ Dirac operators are the complete set of all operators that can be constructed from the quintilinear $F\overline{F}h\overline{H}H$, by all possible group theoretical contractions of the indices in

$$\mathcal{O}^{\alpha\rho y w}_{\beta\gamma x z} = F^{\alpha a}\overline{F}_{\beta x}h^{y}_{a}\overline{H}_{\gamma z}H^{\rho w} \ . \tag{B.1}$$

The n in question is the superscript n that gives the power to which the $\left(\frac{H\overline{H}}{M_X^2}\right)$ term is raised. This term is found in the operator structure equation, Eq. (3.58), in the Yukawa operator section, Section 3.5, for example. We define some SU(4) invariant

Operator Name	Operator Name in [51]	$Q\bar{U}h_2$	$Q\bar{D}h_1$	$L\bar{E}h_1$	$L\bar{N}h_2$
O^{Aa}	O^{A}	1	1	1	1
O^{Ab}	O^{B}	1	-1	-1	1
O^{Ac}	O^{M}	0	$\sqrt{2}$	$\sqrt{2}$	0
O^{Ad}	O^{T}	$\frac{2\sqrt{2}}{5}$	$\frac{\sqrt{2}}{5}$	$\frac{\sqrt{2}}{5}$	$\frac{2\sqrt{2}}{5}$
O^{Ae}	O^{V}	$\sqrt{2}$	0	0	$\sqrt{2}$
O^{Af}	O^{U}	$\frac{\sqrt{2}}{5}$	$\frac{2\sqrt{2}}{5}$	$\frac{2\sqrt{2}}{5}$	$\frac{\sqrt{2}}{5}$
O^{Ba}	O^{C}	$\frac{1}{\sqrt{5}}$	$\frac{1}{\sqrt{5}}$	$\frac{-3}{\sqrt{5}}$	$\frac{-3}{\sqrt{5}}$
O^{Bb}	O^{D}	$\frac{1}{\sqrt{5}}$	$\frac{-1}{\sqrt{5}}$	$\frac{-3}{\sqrt{5}}$	$\frac{3}{\sqrt{5}}$
O^{Bc}	O^{W}	0	$\sqrt{\frac{2}{5}}$	$-3\sqrt{\frac{2}{5}}$	0
O^{Bd}	O^{X}	$\frac{2\sqrt{2}}{5}$	$\frac{\sqrt{2}}{5}$	$\frac{-3\sqrt{2}}{5}$	$\frac{-6\sqrt{2}}{5}$
O^{Be}	O^{Z}	$\sqrt{\frac{2}{5}}$	0	0	$-3\sqrt{\frac{2}{5}}$
O^{Bf}	O^{Y}	$\frac{\sqrt{2}}{5}$	$\frac{2\sqrt{2}}{5}$	$\frac{-6\sqrt{2}}{5}$	$\frac{-3\sqrt{2}}{5}$
O^{Ca}	O^{a}	$\sqrt{2}$	$\sqrt{2}$	0	0
O^{Cb}	O^{F}	$\sqrt{2}$	$-\sqrt{2}$	0	0
O^{Cc}	O^{E}	0	2	0	0
O^{Cd}	O^{b}	$\frac{4}{\sqrt{5}}$	$\frac{2}{\sqrt{5}}$	0	0
O^{Ce}	O^{N}	2	0	0	0
O^{Cf}	O^{c}	$\frac{2}{\sqrt{5}}$	$\frac{4}{\sqrt{5}}$	0	0
O^{Da}	O^{d}	$\sqrt{\frac{2}{5}}$	$\sqrt{\frac{2}{5}}$	$2\sqrt{\frac{2}{5}}$	$2\sqrt{\frac{2}{5}}$
O^{Db}	O^{e}	$\sqrt{\frac{2}{5}}$	$-\sqrt{\frac{2}{5}}$	$-2\sqrt{\frac{2}{5}}$	$2\sqrt{\frac{2}{5}}$
O^{Dc}	O^{G}	0	$\frac{2}{\sqrt{5}}$	$\frac{4}{\sqrt{5}}$	0
O^{Dd}	O^{H}	$\frac{4}{5}$	$\frac{2}{5}$	$\frac{4}{5}$	$\frac{8}{5}$
O^{De}	O^{O}	$\frac{2}{\sqrt{5}}$	0	0	$\frac{4}{\sqrt{5}}$
O^{Df}	O^{f}	$\frac{2}{5}$	$\frac{4}{5}$	$\frac{8}{5}$	$\frac{4}{5}$
O^{Ea}	O^{g}	0	0	$\sqrt{2}$	$\sqrt{2}$
O^{Eb}	O^{h}	0	0	$-\sqrt{2}$	$\sqrt{2}$
O^{Ec}	O^{i}	0	0	2	0
O^{Ed}	O^{j}	0	0	$\frac{2}{\sqrt{5}}$	$\frac{4}{\sqrt{5}}$
O^{Ee}	O^{I}	0	0	0	2
O^{Ef}	O^{J}	0	0	$\frac{4}{\sqrt{5}}$	$\frac{2}{\sqrt{5}}$
O^{Fa}	O^{P}	$\frac{4\sqrt{2}}{5}$	$\frac{4\sqrt{2}}{5}$	$\frac{3\sqrt{2}}{5}$	$\frac{3\sqrt{2}}{5}$
O^{Fb}	O^{Q}	$\frac{4\sqrt{2}}{5}$	$\frac{-4\sqrt{2}}{5}$	$\frac{-3\sqrt{2}}{5}$	$\frac{3\sqrt{2}}{5}$
O^{Fc}	O^{R}	0	$\frac{8}{5}$	$\frac{6}{5}$	0
O^{Fd}	O^{L}	$\frac{16}{5\sqrt{5}}$	$\frac{8}{5\sqrt{5}}$	$\frac{6}{5\sqrt{5}}$	$\frac{12}{5\sqrt{5}}$
O^{Fe}	O^{K}	$\frac{8}{5}$	0	0	$\frac{6}{5}$
O^{Ff}	O^{S}	$\frac{8}{5\sqrt{5}}$	$\frac{16}{5\sqrt{5}}$	$\frac{12}{5\sqrt{5}}$	$\frac{6}{5\sqrt{5}}$

Table B.1: Operator names, Clebsch-Gordan coefficients and names in [51].

tensors C and some SU(2) invariant tensors R as follows[1]:

$$
\begin{aligned}
(C_1)^{\alpha}_{\beta} &= \delta^{\alpha}_{\beta} \ , \\
(C_6)^{\rho\gamma}_{\alpha\beta} &= \epsilon^{\rho\gamma\omega\chi}_{\alpha\beta\omega\chi} \ , \\
(C_{10})^{\alpha\beta}_{\rho\gamma} &= \delta^{\alpha}_{\rho}\delta^{\beta}_{\gamma} + \delta^{\alpha}_{\gamma}\delta^{\beta}_{\rho} \ , \\
(C_{15})^{\beta\gamma}_{\alpha\rho} &= \delta^{\beta}_{\rho}\delta^{\gamma}_{\alpha} - \frac{1}{4}\delta^{\beta}_{\alpha}\delta^{\gamma}_{\rho} \ , \\
(R_1)^{x}_{y} &= \delta^{x}_{y} \ , \\
(R_3)^{wx}_{yz} &= \delta^{x}_{y}\delta^{w}_{z} - \frac{1}{2}\delta^{x}_{z}\delta^{w}_{y} \ .
\end{aligned}
\tag{B.2}
$$

The six independent SU(4) structures are then

$$
\begin{aligned}
\text{A.} \quad (C_1)^{\beta}_{\alpha}\,(C_1)^{\gamma}_{\rho} &= \delta^{\beta}_{\alpha}\delta^{\gamma}_{\rho} \ , \\
\text{B.} \quad (C_{15})^{\beta\chi}_{\alpha\sigma}\,(C_{15})^{\gamma\sigma}_{\rho\chi} &= \delta^{\beta}_{\rho}\delta^{\gamma}_{\alpha} - \frac{1}{4}\delta^{\beta}_{\alpha}\delta^{\gamma}_{\rho} \ , \\
\text{C.} \quad (C_6)^{\omega\chi}_{\alpha\rho}\,(C_6)^{\beta\gamma}_{\omega\chi} &= 8(\delta^{\beta}_{\alpha}\delta^{\gamma}_{\alpha} - \delta^{\gamma}_{\alpha}\delta^{\beta}_{\rho}) \ , \\
\text{D.} \quad (C_{10})^{\omega\chi}_{\alpha\rho}\,(C_{10})^{\beta\gamma}_{\omega\chi} &= 2(\delta^{\beta}_{\alpha}\delta^{\gamma}_{\rho} + \delta^{\gamma}_{\alpha}\delta^{\beta}_{\rho}) \ , \\
\text{E.} \quad (C_1)^{\beta}_{\rho}\,(C_1)^{\gamma}_{\alpha} &= \delta^{\beta}_{\alpha}\delta^{\gamma}_{\alpha} \ , \\
\text{F.} \quad (C_{15})^{\gamma\chi}_{\alpha\sigma}\,(C_{15})^{\beta\sigma}_{\rho\chi} &= \delta^{\gamma}_{\rho}\delta^{\alpha}_{\beta} - \frac{1}{4}\delta^{\gamma}_{\alpha}\delta^{\beta}_{\rho} \ ,
\end{aligned}
\tag{B.3}
$$

and the six SU(2) structures are

$$
\begin{aligned}
\text{a.} \quad (R_1)^{z}_{w}\,(R_1)^{x}_{y} &= \delta^{z}_{w}\delta^{x}_{y} \ , \\
\text{b.} \quad (R_3)^{zq}_{wr}\,(R_3)^{xr}_{yq} &= \delta^{x}_{w}\delta^{z}_{y} - \frac{1}{2}\delta^{x}_{y}\delta^{z}_{w} \ , \\
\text{c.} \quad \epsilon^{xz}\epsilon_{yw} &= \epsilon^{xz}\epsilon_{yw} \ , \\
\text{d.} \quad \epsilon_{ws}\epsilon^{xt}\,(R_3)^{sq}_{yr}\,(R_3)^{zr}_{tq} &= \delta^{x}_{w}\delta^{z}_{y} - \frac{1}{2}\epsilon_{wy}\epsilon^{xz} \ , \\
\text{e.} \quad (R_1)^{z}_{y}\,(R_1)^{x}_{w} &= \delta^{z}_{y}\delta^{x}_{w} \ , \\
\text{f.} \quad (R_3)^{zq}_{yr}\,(R_3)^{xr}_{wq} &= \delta^{x}_{y}\delta^{z}_{w} - \frac{1}{2}\delta^{x}_{w}\delta^{z}_{y} \ .
\end{aligned}
\tag{B.4}
$$

[1]The subscript denotes the dimension of the representation they can create from multiplying $\mathbf{4}$ or $\overline{\mathbf{4}}$ with $\mathbf{4}$ or $\overline{\mathbf{4}}$. For example $(C_{15})^{\beta\gamma}_{\alpha\rho}\overline{\mathbf{4}}_{\gamma}\mathbf{4}^{\rho} = \mathbf{15}^{\beta}_{\alpha}$.

All possible $n = 1$ operators were then named $O^A ... O^Z O^a ... O^j$ in [51]. We rename them here in a manner consistent with the $n > 1$ operators $O^{(n')}$, so that the names are $O^{\Pi\pi}$ where Π is the SU(4) structure and π is the SU2 structure. See Table B.1 for the translation into the names of [51] and the Clebsch-Gordan coefficients (CGCs).

All of these operators are operators for the case without a U(1) family symmetry. In the case when there is, we follow the prescription

$$\mathcal{O}_{ij} \to \mathcal{O}_{ij} \left(\frac{\theta}{M_X} \right)^{p(i,j)} . \tag{B.5}$$

Where $p(i,j) = |X_{\mathcal{O}_{ij}}|$ is the modulus of the charge of the operator. If the charge of the operator is negative, then the field θ should be replaced by the field $\overline{\theta}$. The prescription makes the operator chargeless under the $U(1)_F$ while simultaneously not changing the dimension.

Appendix C

$n > 1$ Operators

In the case that $n > 1$, there will be more indices to contract, which allows more representations, and hence more Clebsch coefficients. To generalise the notation, it is necessary only to construct the new tensors which create the new structures. However, it will always be possible to contract the new indices between the H and $\overline{H}$ fields to create a singlet $H\overline{H}$ which has a Clebsch of 1 in each sector u, d, e, ν. In this case, the first structures are the same as the old structures, but with extra δ symbols which construct the $H\overline{H}$ singlet.

Thus taking an $n = 2$ operator, say $\mathcal{O}'^{Fb}$, which forms a representation that could have been attained by a $n = 1$ operator, the Clebsch coefficients are the same. This is what we mean by $\mathcal{O}^{n'\,\Pi\pi}$, as we have only used $n > 1$ coefficients which are in the subset that have $n = 1$ analogues.

Appendix D

Branching ratios for $l_j^- \longrightarrow l_i^- \gamma$

The expressions used in the computer code to generate the data to one-loop for the branching ratios of the lepton flavour violating processes considered in this thesis were taken from [64]. In this appendix we shall briefly discuss these formulae.

The decay rate for $l_j^- \to l_i^- \ \gamma$ is easily calculated using the amplitude in Eq. (D.2) with the coefficients as defined in Eq. (D.3),

$$\Gamma(l_j^- \to l_i^- \ \gamma) = \frac{e^2}{16\pi} m_{l_j}^5 (|A_2^L|^2 + |A_2^R|^2) \ . \tag{D.1}$$

The amplitude for $l_j^- \to l_i^- \gamma$ is generally written as

$$T = e\epsilon^\alpha \bar{u}_i(p-q) \left[q^2 \gamma_\alpha (A_1^L P_L + A_1^R P_R) + m_{l_j} i\sigma_{\alpha\beta} q^\beta (A_2^L P_L + A_2^R P_R) \right] u_j(p) \ , \tag{D.2}$$

in the limit of $q \to 0$ with q being the photon momentum. Here, e is the electric charge, ϵ the photon polarization vector, u_i the wave function for (anti-)leptons, and p the momentum of the particle l_j. Each coefficients in the above can be written as a sum of the two terms,

$$A_a^{L,R} \ = \ A_a^{(n)L,R} + A_a^{(c)L,R} \qquad (a = 1, 2) \ , \tag{D.3}$$

where $A_a^{(n)L,R}$ and $A_a^{(c)L,R}$ stand for the contributions from the neutralino loops and

chargino loops respectively. They are calculated in [64], and the neutralino contributions are given by

$$\begin{aligned} A_1^{(n)L} &= \frac{1}{576\pi^2} N_{iAX}^{R(l)} N_{jAX}^{R(l)*} \frac{1}{m_{\tilde{l}_X}^2} \frac{1}{(1-x_{AX})^4} \\ &\quad \times (2 - 9x_{AX} + 18x_{AX}^2 - 11x_{AX}^3 + 6x_{AX}^3 \ln x_{AX}) \ , \qquad \text{(D.4)} \\ A_2^{(n)L} &= \frac{1}{32\pi^2} \frac{1}{m_{\tilde{l}_X}^2} \left[N_{iAX}^{L(l)} N_{jAX}^{L(l)*} \frac{1}{6(1-x_{AX})^4} \right. \\ &\quad \times (1 - 6x_{AX} + 3x_{AX}^2 + 2x_{AX}^3 - 6x_{AX}^2 \ln x_{AX}) \\ &\quad \left. + N_{iAX}^{L(l)} N_{jAX}^{R(l)*} \frac{M_{\tilde{\chi}_A^0}}{m_{l_j}} \frac{1}{(1-x_{AX})^3} (1 - x_{AX}^2 + 2x_{AX} \ln x_{AX}) \right] \ , \qquad \text{(D.5)} \\ A_a^{(n)R} &= A_a^{(n)L}|_{L \leftrightarrow R} \qquad (a = 1, 2) \ , \qquad \text{(D.6)} \end{aligned}$$

where $x_{AX} = M_{\tilde{\chi}_A^0}^2 / m_{\tilde{l}_X}^2$ is the ratio of the neutralino mass squared, $M_{\tilde{\chi}_A^0}^2$, to the charged slepton mass squared, $m_{\tilde{l}_X}^2$. (Summation over the indices A and X are assumed to be understood.)

The chargino contributions are

$$\begin{aligned} A_1^{(c)L} &= -\frac{1}{576\pi^2} C_{iAX}^{R(l)} C_{jAX}^{R(l)*} \frac{1}{m_{\tilde{\nu}_X}^2} \frac{1}{(1-x_{AX})^4} \\ &\quad \times \left\{ 16 - 45x_{AX} + 36x_{AX}^2 - 7x_{AX}^3 + 6(2 - 3x_{AX}) \ln x_{AX} \right\} \ , \qquad \text{(D.7)} \\ A_2^{(c)L} &= -\frac{1}{32\pi^2} \frac{1}{m_{\tilde{\nu}_X}^2} \left[C_{iAX}^{L(l)} C_{jAX}^{L(l)*} \frac{1}{6(1-x_{AX})^4} \right. \\ &\quad \times (2 + 3x_{AX} - 6x_{AX}^2 + x_{AX}^3 + 6x_{AX} \ln x_{AX}) \\ &\quad \left. + C_{iAX}^{L(l)} C_{jAX}^{R(l)*} \frac{M_{\tilde{\chi}_A^-}}{m_{l_j}} \frac{1}{(1-x_{AX})^3} (-3 + 4x_{AX} - x_{AX}^2 - 2 \ln x_{AX}) \right] \ , \qquad \text{(D.8)} \\ A_a^{(c)R} &= A_a^{(c)L}|_{L \leftrightarrow R} \qquad (a = 1, 2) \ . \qquad \text{(D.9)} \end{aligned}$$

Here, $x_{AX} = M_{\tilde{\chi}_A^-}^2 / m_{\tilde{\nu}_X}^2$, where $M_{\tilde{\chi}_A^-}$ and $m_{\tilde{\nu}_X}$ are the masses for the chargino $\tilde{\chi}_A^-$ and the sneutrino $\tilde{\nu}_X$, respectively. The coefficients are

$$\begin{aligned} C_{iAX}^{R(l)} &= -g_2 (O_R)_{A1} U_{X,i}^{\nu} \ , \\ C_{iAX}^{L(l)} &= g_2 \frac{m_{l_i}}{\sqrt{2} m_W \cos\beta} (O_L)_{A2} U_{X,i}^{\nu} \ , \qquad \text{(D.10)} \end{aligned}$$

and

$$N^{R(l)}_{iAX} = -\frac{g_2}{\sqrt{2}}\{[-(O_N)_{A2} - (O_N)_{A1}\tan\theta_W]U^l_{X,i} + \frac{m_{l_i}}{m_W\cos\beta}(O_N)_{A3}U^l_{X,i+3}\} ,$$
$$N^{L(l)}_{iAX} = -\frac{g_2}{\sqrt{2}}\{\frac{m_{l_i}}{m_W\cos\beta}(O_N)_{A3}U^l_{x,i} + 2(O_N)_{A1}\tan\theta_W U^l_{X,i+3}\} , \qquad \text{(D.11)}$$

where the O's are 2×2 real orthogonal matrices that diagonalise the chargino and neutralino mass matrices as follows. The mass matrix of the charginos is given by

$$-\mathcal{L}_m = \left(\overline{\tilde{W}^-_R}\ \overline{\tilde{H}^-_{2R}}\right)\begin{pmatrix} M_2 & \sqrt{2}m_W\cos\beta \\ \sqrt{2}m_W\sin\beta & \mu \end{pmatrix}\begin{pmatrix} \tilde{W}^-_L \\ \tilde{H}^-_{1L} \end{pmatrix} + h.c. . \qquad \text{(D.12)}$$

This matrix M_C is diagonalized by 2×2 real orthogonal matrices O_L and O_R as

$$O_R M_C O_L^{\mathsf{T}} = (\text{diagonal}) , \qquad \text{(D.13)}$$

which are defined by

$$\begin{pmatrix} \tilde{\chi}^-_{1L} \\ \tilde{\chi}^-_{2L} \end{pmatrix} = O_L \begin{pmatrix} \tilde{W}^-_L \\ \tilde{H}^-_{1L} \end{pmatrix} , \qquad \begin{pmatrix} \tilde{\chi}^-_{1R} \\ \tilde{\chi}^-_{2R} \end{pmatrix} = O_R \begin{pmatrix} \tilde{W}^-_R \\ \tilde{H}^-_{2R} \end{pmatrix} . \qquad \text{(D.14)}$$

Then

$$\tilde{\chi}^-_A = \tilde{\chi}^-_{AL} + \tilde{\chi}^-_{AR} \qquad (A = 1, 2) \qquad \text{(D.15)}$$

forms a Dirac fermion with mass $M_{\tilde{\chi}^-_A}$.

The mass matrix of the neutralino sector is given by

$$-\mathcal{L}_m = \frac{1}{2}\left(\tilde{B}_L\tilde{W}^0_L\tilde{H}^0_{1L}\tilde{H}^0_{2L}\right)M_N\begin{pmatrix} \tilde{B}_L \\ \tilde{W}^0_L \\ \tilde{H}^0_{1L} \\ \tilde{H}^0_{2L} \end{pmatrix} + h.c. , \qquad \text{(D.16)}$$

where

$$M_N = \begin{pmatrix} M_1 & 0 & -m_Z \sin\theta_W \cos\beta & m_Z \sin\theta_W \sin\beta \\ 0 & M_2 & m_Z \cos\theta_W \cos\beta & -m_Z \cos\theta_W \sin\beta \\ -m_Z \sin\theta_W \cos\beta & m_Z \cos\theta_W \cos\beta & 0 & -\mu \\ m_Z \sin\theta_W \sin\beta & -m_Z \cos\theta_W \sin\beta & -\mu & 0 \end{pmatrix} . \tag{D.17}$$

The diagonalization is done by a real orthogonal matrix O_N,

$$O_N M_N O_N^{\mathsf{T}} = \text{diagonal} . \tag{D.18}$$

The mass eigenstates are given by

$$\tilde{\chi}^0_{AL} = (O_N)_{AB} \tilde{X}^0_{BL} \qquad (A, B = 1, \ldots, 4) , \tag{D.19}$$

where

$$\tilde{X}^0_{AL} = (\tilde{B}_L, \tilde{W}^0_L, \tilde{H}^0_{1L}, \tilde{H}^0_{2L}) . \tag{D.20}$$

We have thus Majorana spinors

$$\tilde{\chi}^0_A = \tilde{\chi}^0_{AL} + \tilde{\chi}^0_{AR} \qquad (A = 1, \ldots, 4) \tag{D.21}$$

with mass $M_{\tilde{\chi}^0_A}$.

The U^l's are 6×6 real orthogonal matrices that diagonalise the selectron mass matrix via

$$U^l m^2_{\tilde{E}} U^{l\mathsf{T}} = (\text{diagonal}) , \tag{D.22}$$

and we denote its eigenvalues by $m^2_{\tilde{l}_X}$ $(X = 1, \ldots, 6)$. The mass eigenstate is then written as

$$\tilde{l}_X = U^l_{X,i} \tilde{l}_{Li} + U^l_{X,i+3} \tilde{l}_{Ri} \qquad (X = 1, \ldots, 6) . \tag{D.23}$$

Conversely, we have

$$\tilde{l}_{Li} \quad = U^{l\mathsf{T}}_{iX} \tilde{l}_X \quad = U^l_{Xi} \tilde{l}_X , \tag{D.24}$$

$$\tilde{l}_{Ri} \quad = U^{l\mathsf{T}}_{i+3,X} \tilde{l}_X \quad = U^l_{X,i+3} \tilde{l}_X . \tag{D.25}$$

Attention should be paid to the neutrinos since there is no right-handed sneutrino in the MSSM. Let $\tilde{\nu}_{Li}$ be the superpartner of the neutrino ν_i. The mass eigenstate $\tilde{\nu}_X$ $(X = 1, 2, 3)$ is related to $\tilde{\nu}_{Li}$ as

$$\tilde{\nu}_{Li} = U^{\nu}_{Xi}\tilde{\nu}_X \ . \tag{D.26}$$

Bibliography

[1] F. Halzen and A. D. Martin, *Quarks and Leptons*, London, UK: Wiley (1984).

[2] M. E. Peskin and D. V. Schroeder, *An Introduction to Quantum Field Theory*, Reading, USA: Addison-Wesley (1995).

[3] N. Cabibbo, Phys. Rev. Lett. **10** (1963) 531; M. Kobayashi and T. Maskawa, Prog. Theor. Phys. **49** (1973) 652.

[4] K. Hagiwara *et al.* [Particle Data Group Collaboration], Phys. Rev. D **66** (2002) 010001.

[5] S. L. Glashow, J. Iliopoulos and L. Maiani, Phys. Rev. D **2** (1970) 1285.

[6] Y. Fukuda *et al.*, Super-Kamiokande Collaboration, Phys. Lett. **B433**, 9 (1998); *ibid.* Phys. Lett. **B436**, 33 (1998); *ibid.* Phys. Rev. Lett. **81**, 1562 (1998).

[7] Q. R. Ahmad *et al.* [SNO Collaboration], Phys. Rev. Lett. **89** (2002) 011301 [arXiv:nucl-ex/0204008]; Q. R. Ahmad *et al.* [SNO Collaboration], Phys. Rev. Lett. **89** (2002) 011302 [arXiv:nucl-ex/0204009].

[8] H. E. Haber and G. L. Kane, Phys. Rept. **110**, (1984).

[9] D. Bailin and A. Love, *Supersymmetric Gauge Field Theory and String Theory*, Bristol, UK: IOP (1994) (Graduate Student Series in Physics)

[10] J. D. Lykken, 'Introduction to Supersymmetry' TASI-96 lectures [arXiv:hep-th/9612114].

[11] S. P. Martin, [arXiv:hep-ph/9709356].

[12] L. Girardello and M. T. Grisaru, Nucl. Phys. B **194** (1982) 65.

[13] L. E. Ibanez and G. G. Ross, Phys. Lett. B **110** (1982) 215.

[14] G. L. Fogli, E. Lisi, A. Marrone, D. Montanino, A. Palazzo and A. M. Rotunno, [arXiv:hep-ph/0212127]; P. C. de Holanda and A. Y. Smirnov, [arXiv:hep-ph/0212270]; V. Barger and D. Marfatia, Phys. Lett. B **555** (2003) 144 [arXiv:hep-ph/0212126]; A. Bandyopadhyay, S. Choubey, R. Gandhi, S. Goswami and D. P. Roy, arXiv:hep-ph/0212146; M. Maltoni, T. Schwetz and J. W. Valle, arXiv:hep-ph/0212129.

[15] M. Gell-Mann, P. Ramond and R. Slansky, Print-80-0576 (CERN); T. Yanagida, *In Proceedings of the Workshop on the Baryon Number of the Universe and Unified Theories, Tsukuba, Japan, 13-14 Feb 1979*,

[16] S. F. King, Phys. Lett. B **439** (1998) 350 [arXiv:hep-ph/9806440]; S. F. King, Nucl. Phys. B **562** (1999) 57 [arXiv:hep-ph/9904210]; S. F. King, Nucl. Phys. B **576** (2000) 85 [arXiv:hep-ph/9912492]; S. F. King, JHEP **0209** (2002) 011 [arXiv:hep-ph/0204360].

[17] C. D. Froggatt and H. B. Nielsen, Nucl. Phys. B **147** (1979) 277.

[18] A. Brignole, L. E. Ibanez and C. Munoz, [arXiv:hep-ph/9707209].

[19] G. F. Giudice and A. Masiero, Phys. Lett. B **206** (1988) 480.

[20] S. F. King and D. A. J. Rayner, [arXiv:hep-ph/0111333].

[21] S. Abel, S. Khalil and O. Lebedev, Phys. Rev. Lett. **89** (2002) 121601 [arXiv:hep-ph/0112260].

[22] L. E. Ibanez, C. Munoz and S. Rigolin, Nucl. Phys. B **553** (1999) 43 [arXiv:hep-ph/9812397].

[23] M. B. Green, J. H. Schwarz and E. Witten, 'Superstring Theory. Vol. 1: Introduction,' M. B. Green, J. H. Schwarz and E. Witten, 'Superstring Theory. Vol. 2: Loop Amplitudes, Anomalies and Phenomenology'.

[24] J. Polchinski, 'String theory. Vol. 1: An introduction to the bosonic string,' J. Polchinski, 'String theory. Vol. 2: Superstring theory and beyond'.

[25] M. B. Green and J. H. Schwarz, Phys. Lett. B **149** (1984) 117.

[26] D. J. Gross, J. A. Harvey, E. J. Martinec and R. Rohm, Nucl. Phys. B **256** (1985) 253.

[27] A. Font, L. E. Ibanez, D. Lust and F. Quevedo, Phys. Lett. B **249** (1990) 35; M. J. Duff and J. X. Lu, Nucl. Phys. B **357** (1991) 534; A. Sen, Int. J. Mod. Phys. A **9** (1994) 3707 [arXiv:hep-th/9402002].

[28] C. P. Bachas, 'Lectures on D-branes,' [arXiv:hep-th/9806199.]

[29] J. Polchinski,
'Lectures on D-branes,' [arXiv:hep-th/9611050.]

[30] C. V. Johnson,
'D-brane primer,' [arXiv:hep-th/0007170.]

[31] A. Sagnottiin Cargese 87, 'Strings on Orbifolds', Ed. G. Mack et al. (Pergamon Press, 1988) p. 521

[32] P. Horava, Phys. Lett. B **231** (1989) 251., Nucl. Phys. B **327** (1989) 461; J. Dai, R. G. Leigh and J. Polchinski, Mod. Phys. Lett. A **4** (1989) 2073; R. G. Leigh, Mod. Phys. Lett. A **4** (1989) 2767.

[33] G. Pradisi and A. Sagnotti, Phys. Lett. B **216** (1989) 59; M. Bianchi and A. Sagnotti, Phys. Lett. B **247** (1990) 517.

[34] E. G. Gimon and J. Polchinski, Phys. Rev. D **54** (1996) 1667 [arXiv:hep-th/9601038].

[35] A. Dabholkar and J. Park, Nucl. Phys. B **472** (1996) 207 [arXiv:hep-th/9602030].

[36] M. Berkooz and R. G. Leigh, Nucl. Phys. B **483** (1997) 187 [arXiv:hep-th/9605049].

[37] Z. Kakushadze, Nucl. Phys. B **512**, 221 (1998) [arXiv:hep-th/9704059]; Z. Kakushadze and G. Shiu, Phys. Rev. D **56**, 3686 (1997) [arXiv:hep-th/9705163]; Z. Kakushadze and G. Shiu, Nucl. Phys. B **520**, 75 (1998) [arXiv:hep-th/9706051].

[38] G. Zwart, Nucl. Phys. B **526**, 378 (1998) [arXiv:hep-th/9708040].

[39] D. O'Driscoll, [arXiv:hep-th/9801114].

[40] L. E. Ibanez, JHEP **9807**, 002 (1998) [arXiv:hep-th/9802103].

[41] G. Aldazabal, A. Font, L. E. Ibanez and G. Violero, Nucl. Phys. B **536**, 29 (1998) [arXiv:hep-th/9804026]; G. Aldazabal, D. Badagnani, L. E. Ibanez and A. M. Uranga, JHEP **9906**, 031 (1999) [arXiv:hep-th/9904071]; L. E. Ibanez,

R. Rabadan and A. M. Uranga, Nucl. Phys. B **576**, 285 (2000) [arXiv:hep-th/9905098].

[42] L. E. Ibanez, R. Rabadan and A. M. Uranga, Nucl. Phys. B **542**, 112 (1999) [arXiv:hep-th/9808139].

[43] Z. Kakushadze, Phys. Lett. B **434**, 269 (1998) [arXiv:hep-th/9804110]; [arXiv:hep-th/9806044].

[44] J. Lykken, E. Poppitz and S. P. Trivedi, Nucl. Phys. B **543**, 105 (1999) [arXiv:hep-th/9806080].

[45] L. J. Dixon, J. A. Harvey, C. Vafa and E. Witten, Nucl. Phys. B **261** (1985) 678; L. J. Dixon, J. A. Harvey, C. Vafa and E. Witten, Nucl. Phys. B **274** (1986) 285.

[46] L. E. Ibanez, Class. Quant. Grav. **17** (2000) 1117 [arXiv:hep-ph/9911499].

[47] I. Antoniadis and G. K. Leontaris, Phys. Lett. B **216** (1989) 333.

[48] J. C. Pati and A. Salam, Phys. Rev. D **10** (1974) 275.

[49] L. L. Everett, G. L. Kane, S. F. King, S. Rigolin and L. T. Wang, Phys. Lett. B **531** (2002) 263 [arXiv:hep-ph/0202100].

[50] G. Shiu and S. H. H. Tye, Phys. Rev. D **58**, 106007 (1998) [arXiv:hep-th/9805157].

[51] S. F. King, Phys. Lett. B **325** (1994) 129 [Erratum-ibid. B **325** (1994) 538]; B. C. Allanach and S. F. King, Nucl. Phys. B **456** (1995) 57 [arXiv:hep-ph/9502219]; B. C. Allanach and S. F. King, Nucl. Phys. B **459** (1996) 75 [arXiv:hep-ph/9509205]; B. C. Allanach, S. F. King, G. K. Leontaris and S. Lola, Phys. Rev. D **56** (1997) 2632 [arXiv:hep-ph/9610517]; S. F. King and M. Oliveira, Phys. Rev. D **63** (2001) 095004 [arXiv:hep-ph/0009287]

[52] T. Blazek, S. F. King and J. K. Parry, JHEP **0305** , 016 (2003) [arXiv:hep-ph/0303192].

[53] A. Brignole, L. E. Ibanez and C. Munoz, Nucl. Phys. B **422** (1994) 125 [Erratum-ibid. B **436** (1995) 747] [arXiv:hep-ph/9308271]; A. Brignole, L. E. Ibanez, C. Munoz and C. Scheich, Z. Phys. C **74** (1997) 157 [arXiv:hep-ph/9508258].

[54] S. F. King and I. N. R. Peddie, Nucl. Phys. B **678** (2004) 339 [arXiv:hep-ph/0307091].

[55] M. Nakahara, *Geometry, Topology and Physics*, Bristol, England: IOP Publishing, Ltd (1990).

[56] G. L. Kane, S. F. King, I. N. R. Peddie and L. Velasco-Sevilla, [arXiv:hep-ph/0504038].

[57] V. Jain and R. Shrock, Phys. Lett. B **352** (1995) 83 [arXiv:hep-ph/9412367].

[58] S. F. King and M. Oliveira, Phys. Rev. D **63** (2001) 015010 [arXiv:hep-ph/0008183].

[59] B. C. Allanach, Comput. Phys. Commun. **143** (2002) 305 [arXiv:hep-ph/0104145].

[60] F. Borzumati and A. Masiero, Phys. Rev. Lett. **57** (1986) 961.

[61] F. Gabbiani, E. Gabrielli, A. Masiero and L. Silvestrini, Nucl. Phys. B **477** (1996) 321 [arXiv:hep-ph/9604387].

[62] D. J. H. Chung, L. L. Everett, G. L. Kane, S. F. King, J. Lykken and L. T. Wang, Phys. Rept. **407** (2005) 1 [arXiv:hep-ph/0312378].

[63] S. F. King, Rept. Prog. Phys. **67** (2004) 107 [arXiv:hep-ph/0310204].

[64] J. Hisano, T. Moroi, K. Tobe and M. Yamaguchi, Phys. Rev. D **53** (1996) 2442 [arXiv:hep-ph/9510309].

[65] S. F. King and M. Oliveira, Phys. Rev. D **60** (1999) 035003 [arXiv:hep-ph/9804283].

[66] T. Blazek and S. F. King, Nucl. Phys. B **662** (2003) 359 [arXiv:hep-ph/0211368].

[67] S. Davidson and A. Ibarra, JHEP **0109** (2001) 013; J. Hisano and D. Nomura, Phys. Rev. D **59** (1999) 116005; J. Hisano, arXiv:hep-ph/0204100; J. A. Casas and A. Ibarra, Nucl. Phys. B **618** (2001) 171; W. Buchmüller, D. Delepine and F. Vissani, Phys. Lett. B **459** (1999) 171; M. E. Gomez, G. K. Leontaris, S. Lola and J. D. Vergados, Phys. Rev. D **59** (1999) 116009; J. R. Ellis, M. E. Gomez, G. K. Leontaris, S. Lola and D. V. Nanopoulos, Eur. Phys. J. C **14** (2000) 319; W. Buchmüller, D. Delepine and L. T. Handoko, Nucl. Phys. B **576** (2000) 445; D. Carvalho, J. Ellis, M. Gomez and S. Lola, Phys. Lett. B **515** (2001) 323; F. Deppisch, H. Pas, A. Redelbach, R. Ruckl and Y. Shimizu, [arXiv:hep-ph/0206122]; J. Sato and K. Tobe, Phys. Rev. D **63** (2001) 116010; J. Hisano and K. Tobe, Phys. Lett. B **510** (2001) 197; J. R. Ellis, J. Hisano, M. Raidal and Y. Shimizu, Phys. Lett. B **528** (2002) 86, [arXiv:hep-ph/0111324]; J. R. Ellis, J. Hisano, S. Lola and M. Raidal, Nucl. Phys. B **621** (2002) 208, [arXiv:hep-ph/0109125]; J. Hisano, T. Moroi, K. Tobe and M. Yamaguchi, Phys. Lett. B 391 (1997) 341; [Erratum - *ibid.* **397**, 357 (1997)]; J. Hisano, D. Nomura, Y. Okada, Y. Shimizu and M. Tanaka, Phys. Rev. D **58** (1998) 116010; J. Hisano, D. Nomura and T. Yanagida, Phys. Lett. B **437** (1998) 351; S. Lavignac, I. Masina and C. A. Savoy, Phys. Lett. B **520** (2001) 269 [arXiv:hep-ph/0106245]; S. Lavignac, I. Masina and C. A. Savoy, Nucl. Phys. B **633** (2002) 139 [arXiv:hep-ph/0202086];

I. Masina and C. A. Savoy, [arXiv:hep-ph/0211283]; S. Pascoli, S. T. Petcov and C. E. Yaguna, Phys. Lett. B **564** (2003) 241 [arXiv:hep-ph/0301095]; S. Pascoli, S. T. Petcov and W. Rodejohann, [arXiv:hep-ph/0302054].

[68] P. H. Chankowski, O. Lebedev and S. Pokorski, Nucl. Phys. B **717** (2005) 190 [arXiv:hep-ph/0502076].

[69] S. A. Abel and G. Servant, Nucl. Phys. B **611** (2001) 43 [arXiv:hep-ph/0105262].

[70] G. G. Ross and O. Vives, Phys. Rev. D **67** (2003) 095013 [arXiv:hep-ph/0211279].

[71] S. F. King and I. N. R. Peddie, J. Korean Phys. Soc. **45** (2004) S443 [arXiv:hep-ph/0312235].

[72] G. L. Kane and S. F. King, Phys. Lett. B **451** (1999) 113 [arXiv:hep-ph/9810374].

[73] B. Aubert *et al.* [BABAR Collaboration], Phys. Rev. Lett. **95** (2005) 041802 [arXiv:hep-ex/0502032].